UNIVERSITÄT ZU LÜBECK

From the Institute of Endocrinology and Diabetes

of the University of Lübeck

Director: Prof. Dr. rer. nat. Jens Mittag

Metabolic and metagenomic impact of chronic cold exposure in humans

Dissertation

for Fulfillment of Requirements

for the Doctoral Degree

of the University of Lübeck

from the Department of Natural Sciences

Submitted by

Shirin Tabei

from Mashhad

Lübeck 2024

First referee: Prof. Dr. med. Sebastian Meyhöfer

Second referee: Prof. Dr. rer. nat. Jens Mittag

Datum of oral examination: 16. August 2024

Approved for printing: 19. August 2024, Lübeck

Table of Contents

Abbreviations ..... **V**

List of Figures ..... **VII**

List of Tables ..... **IX**

Summary ..... **X**

Zusammenfassung ..... **XII**

1 Introduction **1**

1.1 Obesity & metabolic syndrome *1*

1.2 Treatment of obesity *3*

1.3 Different colors of fat depots and their metabolic aspects *5*

1.3.1 White adipose tissue 6

1.3.2 Beige adipose tissue 7

1.3.3 Brown adipose tissue 8

1.4 Unique characteristics of brown adipose tissue in humans *9*

1.4.1 History and function of brown adipose tissue 9

1.4.2 Prevalence and detection of brown adipose tissue 11

1.4.3 Different activators of brown adipose tissue 13

1.5 Metabolic effect of cold-activated brown adipose tissue *15*

1.5.1 Cold-activated brown fat and stress hormones 15

1.5.2 Cold-activated brown fat and energy metabolism 15

1.5.3 Cold-activated brown fat and lipid metabolism 16

1.5.4 Cold-activated brown fat and glucose metabolism 16

1.6 Glucose homeostasis *18*

1.7 Cold and gut microbiota *20*

1.8 Hypothesis & Aims *24*

Hypothesis I: Metabolic impact of chronic cold exposure in humans *25*

Hypothesis II: Metagenomic impact of chronic cold exposure in humans *25*

2 Materials and Methods 26

Hypothesis I: Metabolic analyses 26

2.1 General study design 26

2.2 Study cohort and criteria 27

2.3 Novel cooling protocol under free-living conditions 28

2.4 Assessment of environmental effect 30

2.5 Assessment of physical activity and sleep duration 30

2.6 Overview of the experimental day 31

2.7 Assessment of body composition 33

2.8 Assessment of well-being and subjective appetite feelings 33

2.9 Assessment of brown adipose tissue activity 34

2.10 Sampling of the subcutaneous adipocyte 35

2.11 Assessment of hedonic hunger 36

2.12 Assessment of heart rate variability 36

2.13 Assessment of β-cell function and insulin sensitivity 37

2.14 Biological assays 41

Hypothesis II: Shotgun metagenomic analyses 42

2.15 Microbiota analyses 42

2.16 Cohort and stool sampling 42

2.17 DNA isolation and sequencing 42

2.18 Shotgun metagenomic analyses 43

2.19 Statistical analyses 44

3 Results 45

Hypothesis I: Metabolic analyses 45

3.1 Participants characteristics 45

3.2 No difference in outside temperature prior to experimental sessions 46

3.3 No differences in environmental parameters across experimental sessions 47

3.4 No differences in sleep duration and physical activity prior to experimental sessions..... 48

3.5 Body composition remained unchanged after sub-chronic cold exposure 49

3.6 Brown adipose tissue activity remained unchanged after sub-chronic cold exposure, whereas the supraclavicular temperature decreased..... 50

3.7 Glucose metabolism changed after sub-chronic cold exposure..... 51

3.8 Sympathetic and parasympathetic regulation remained unchanged after sub-chronic cold exposure 57

3.9 Heart rate variability remained unchanged after sub-chronic cold exposure 60

3.10 Subjective feelings of appetite increased significantly after sub-chronic cold exposure 61

3.11 Physical and mental competence remained unchanged after sub-chronic cold exposure .. 62

3.12 Motivation and pleasure for food remained unchanged after sub-chronic cold exposure.. 62

3.13 Subjective feeling of cold sensation and perception..... 63

Hypothesis II: Shotgun metagenomic analyses 64

3.14 Characteristics of the sub-cohort..... 64

3.15 Gut microbiota composition changed after sub-chronic cold exposure 65

3.15.1 Abundance of microbiota at the phylum level changed after sub-chronic cold exposure 65

3.15.2 Abundance of *Bacteroides uniformis* increased after sub-chronic cold exposure..... 67

3.15.3 Abundance of butyrate-producing species increased after sub-chronic cold exposure. 68

3.15.4 Abundance of glucose metabolism-related functional profiling changed after sub-chronic cold exposure 69

3.16 Metagenomic results correlate with metabolic outcomes related to glucose metabolism..71

4 Discussion 73

Hypothesis I: Metabolic analyses 73

4.1 No evidence of the impact of possible confounding factors on outcomes 73

4.2 Indirect assessment of brown adipose tissue activity measured the decreased skin temperature 75

4.3 Chronic cold exposure did not impact the hormonal stress axis and heart rate variability..77

4.4 Chronic cold exposure did not impact the body composition, despite increased appetite .. 79

4.5 Chronic cold exposure did not impact food preferences but stimulated the subjective feeling of appetite 79

4.6 Chronic cold exposure improved β-cell function, whereas insulin sensitivity remained unchanged 81

Hypothesis II: Metagenomic analyses 87

4.7 Metabolic and metagenomic outcomes related to glucose metabolism are associated..... 87

4.8 Importance of using standard cooling protocol and methods to assess metabolic impact and BAT activity in future studies 91

5 Limitations 93

6 Conclusion 95

7 Outlook 96

8 References 97

List of Appendix Tables 112

Acknowledgments 118

Curriculum Vitae 120

Abbreviations

[^{18}F]-FDG	^{18}F-fluorodeoxyglucose
ACTH	Adrenocorticotropic hormone
ADP	Air displacement plethysmography
ATP	Adenosine triphosphate
AUC	Area under the curve
BAs	Bile acids
BAT	Brown adipose tissue
BD	Body density
BeAT	Beige adipose tissue
BL	Baseline
BM	Body mass
BMI	Body mass index
BV	Body volume
cAMP	Cyclic adenosine monophosphate
CE	Cold exposure
CI	Confidence interval
Clr	Centered $\log_2$ ratio
CNS	Central nervous system
CREB	cAMP response element-binding protein
df	Degree of freedom
DWD	Deutscher Wetterdienst
ECG	Electrocardiogram
EMG	Electromyography
FFA	Free fatty acid
FFM	Fat-free mass
FGF21	Fibroblast growth factor 21
FM	Fat mass
FPIR	First phase insulin response
GIP-R	Gastric inhibitory polypeptide-receptor
GIR	Glucose infusion rate
GLP-1	Glucagon-like-peptide-1
GLUT	Glucose transporter
H&E	Hematoxylin and eosin
HOMA-IR	Homeostasis Model Assessment-Insulin Resistance
HOMA-Beta	Homeostasis Model Assessment-Beta Cell Function
HbA1c	Hemoglobin A1c
HF	High frequency
HRV	Heart rate variability
HPA	Hypothalamic-Ptuitary-Adrenal Axis

IL-6	Interleukin-6
IRT	Infrared thermography
IVGTT	Intravenous glucose tolerance test
iWAT	Inguinal WAT
LD	Lipid droplet
MCTQ	The Munich ChronoType Questionnaire
MCU	Metabolic Core Unit
NiAc	Nicotinic acid
NST	Non-shivering thermogenesis
OFTT	Oral fat tolerance test
OGTT	Oral glucose tolerance test
P2RX5	P2X purinoceptor 5
PAT2	Proton-coupled amino acid receptor 2
PET-CT	Positron emission tomography-computed tomography
PgC1-α	Proliferator-activated receptor gamma co-activator
PKA	Protein kinase A
PPAR	Peroxisome proliferator-activated receptor
PRISMA	Preferred Reporting Items for Systematic Reviews and Meta-Analysis
RCT	Randomized controlled trial
Rmcorr	Repeated measures correlation
ROI	Region of interest
ScAT	Subcutaneous adipose tissue
SCFAs	Short-chain fatty acids
SCV	Supraclavicular
SD	Standard deviation
SF-36	Short Form 36 Health Survey
SMD	Standardized mean difference
SNS	Sympathetic nervous system
SOP	Standard operating procedure
T2D	Type 2 diabetes
T3	Triiodothyronine
T4	Thyroxine
TSH	Thyroid-stimulating hormone
TG	Triglyceride
TMK	Average daily temperature
TN	Thermoneutrality
UCP1	Uncoupling protein 1
VAS	Visual analog scale
VAT	Visceral adipose tissue
WAT	White adipose tissue
WHO	World health organization
β-ARs	Beta-adrenergic receptors

List of Figures

Figure 1. Overview of the obesity pandemic in Germany. 2
Figure 2. Representative microscopy images of human fat sections. 6
Figure 3. Process of browning in white adipocytes. 7
Figure 4. Schematic characterizations and morphology of different adipocytes. 8
Figure 5. Schematic overview of cold-activated brown adipocyte. 10
Figure 6. Schematic interaction of cold and microbiota. 21
Figure 7. Schematic representation illustrating the impact of butyrate on glucose homeostasis. 22
Figure 8. Scheme of the study design of the eCooling study. 26
Figure 9. Representative image of the 3D technology incorporated in the cooling vest. 29
Figure 10. Design of an experimental day. 32
Figure 11. The anatomical points of the region of interest. 34
Figure 12. Overview of Botnia clamp system. 37
Figure 13. Illustration of IVGTT protocol. 38
Figure 14. Illustration of the HEC protocol. 39
Figure 15. Outside temperature over experimental sessions. 46
Figure 16. Environmental parameters across experimental sessions. 47
Figure 17. Sleep and physical activity prior to the experimental sessions. 48
Figure 18. Body composition over the experimental sessions. 49
Figure 19. Indirect assessment of brown adipose tissue activity over the experimental sessions. 50
Figure 20. Glucose metabolism parameters during IVGTT over experimental sessions. 52
Figure 21. AUC of glucose metabolism-related parameters during IVGTT. 53
Figure 22. GIR and C-peptide concentration during the steady state of HEC over experimental sessions. 55
Figure 23. Insulin sensitivity and β-cell function over experimental sessions. 56
Figure 24. Insulin resistance and β-cell function over experimental sessions. 57
Figure 25. Stress hormone levels during IVGTT across experimental sessions. 58
Figure 26. Stress hormone level during steady state across experimental sessions. 59
Figure 27. HRV across the experimental sessions. 60

Figure 28. Subjective feeling of appetite across experimental sessions. 61
Figure 29. Physical and mental components over experimental sessions. 62
Figure 30. Schematic overview of the self-reported perception of cooling protocols. 63
Figure 31. Glucose metabolism of sub-cohort with stool samples across the experimental sessions. 65
Figure 32. Gut microbiota composition at phylum level over experimental sessions. 66
Figure 33. Abundance of Bacteroides uniformis over experimental sessions. 68
Figure 34. Abundance of butyrate producers over experimental sessions. 68
Figure 35. Glycolysis pathways over experimental sessions. 69
Figure 36. Abundance of present species in Glycolysis pathways over experimental sessions. 70
Figure 37. Correlation between metagenomic and metabolic outcomes regarding glucose metabolism. 71
Figure 38. Correlation between metabolic and metagenomic outcomes related to glucose metabolism. 72

List of Tables

Table 1. Characteristics of the cohort at baseline..... 45
Table 2. Fasting glucose and hormone levels over the experimental sessions..... 51
Table 3. Food desire over the experimental sessions. 63
Table 4. Characteristics of sub-cohort of metagenomic analysis..... 64
Table 5. Overview of the changes at the species level across experimental sessions. 67

Summary

Cold exposure (CE) impacts the whole-body metabolism in different ways. One process is called thermogenesis. There is strong evidence that exposure to cold activates brown adipose tissue and leads to enhanced glucose homeostasis [2]. Our previous lab work highlighted improved insulin sensitivity and BAT activity in lean individuals and enhanced glucose tolerance in those with obesity after two hours of controlled mild CE in the lab unit [1].
Additionally, others have reported the metagenomic impact of chronic CE on microbiota composition associated with improved glucose hemostasis in mice [3,4]. Gut microbiota by producing metabolites such as butyrate can trigger glucagon-like peptide cells in the colon to stimulate β-cells and secret insulin [5]. However, the effects of chronic CE on whole-body metabolism in humans are still not well investigated.

The current study investigated the metabolic and metagenomic impacts of chronic daily CE by using a novel cooling protocol under free-living conditions in humans. We hypothesized that four weeks of chronic CE/10 hours a day improves glucose and energy metabolism, increases BAT activity, and leads to significant changes in gut microbiota composition at phylum and species levels as well as at functional profiling pathways related to glucose metabolism.
Eighteen individuals (body mass index: 25-35 kg/m^2) were involved in a cross-over randomized balanced study. Subjects arrived in the lab unit after 12 hours of fasting. The following parameters were assessed at baseline (BL) and after sub-chronic CE: body composition by air displacement plethysmography, β-cell function and insulin sensitivity by Botnia clamp procedure, BAT activity indirectly by using infrared thermography, and microbiota composition by Shotgun metagenomic analysis.
Following chronic CE compared to BL, first phase insulin response (FPIR) (p = 0.01), C-peptide concentration (p = 0.01), and Disposition index (p = 0.03) significantly increased. Alongside an improved glucose tolerance (p = 0.056) and increased HOMA-Beta (p = 0.06) were observed, although they failed to reach the level of significance. These findings reflect the improved pancreatic function following chronic CE in humans. However, insulin sensitivity (M-value) remained unchanged between conditions (p = 0.99). Furthermore, the assessment of BAT activity showed that the IRT technique only measured the 0.2°C decreased supraclavicular skin temperature and revealed the absence of BAT activity in individuals with overweight and

mild obesity. Concomitantly, in the previous study improved glucose tolerance and the absence of insulin sensitivity as well as BAT activity were reported in the sub-cohort with obesity. In this scenario, our findings alongside our previous study suggest that insulin sensitivity and glucose tolerance have separate mechanisms.

To investigate the mechanism behind improved β-cell function following chronic CE, we conducted Shotgun metagenomic analyses to investigate the role of microbiota on observed glucose metabolism.

Interestingly, our metagenomic analysis supported the metabolic outcomes. An increase in the abundance of Glycolysis I ($p = 0.045$) pathways and the microbiota at the species level that influences glucose metabolism, *Bacteroides uniformis* ($p = 0.02$), and a negative correlation between AUC of plasma glucose during intravenous glucose tolerance test and Glycolysis I pathway ($R^2 = 0.39$; $p = 0.03$) have been observed. Moreover, a positive correlation between the Disposition index and FPIR with butyrate producers underscores the potential influence of gut microbiota on glucose hemostasis.

Collectively, the findings of this doctoral study substantiate the interaction between gut microbiota and glucose metabolism. Our results demonstrate that chronic CE under free-living conditions improves β-cell function in individuals with overweight and mild obesity, which might be triggered by the changes in microbiota composition following chronic CE.

These findings introduce a novel non-pharmacological approach that shows promise in bolstering insulin secretion among individuals with overweight and obesity and those diagnosed with diabetes.

In pursuit of comprehending the underlying mechanism of this discovery and exploring the potential impact of microbiota metabolites, notably short-chain fatty acids (SCFAs) like butyrate, in enhancing insulin secretion, we aim to measure SCFAs. This endeavor aims to uncover a deeper understanding of the interplay among metabolite, metabolic, and metagenomic outcomes in our upcoming investigations.

Moreover, building on our prior study that demonstrated enhanced insulin sensitivity and BAT activity exclusively within the sub-cohort of lean individuals, it is recommended to explore the metabolic and metagenomic implications of applied prolonged CE specifically in a lean healthy cohort for our forthcoming clinical investigation.

Zusammenfassung

Kälteexposition (CE) beeinflusst den Gesamtstoffwechsel auf unterschiedliche Weise. Ein Prozess wird dabei als Thermogenese bezeichnet. In diesem Zusammenhang liegt starke Evidenz vor, dass die Exposition gegenüber Kälte braunes Fettgewebe aktiviert und zu einer verbesserten Glukosehomöostase führt [2]. Arbeiten aus unserer Arbeitsgruppe konnten bereits zeigen, dass eine verbesserte Insulinsensitivität und BAT-Aktivität bei schlanken Personen sowie eine verbesserte Glukosetoleranz bei Personen mit Adipositas nach zwei Stunden kontrollierter, milder CE unter Laborbedingungen zu sehen war [1]. Zusätzlich berichteten Arbeitsgruppen einen metagenomischen Einfluss chronischer CE auf die Mikrobiota-Zusammensetzung, die mit einer verbesserten Glukosehomöostase bei Mäusen verbunden ist [3,4]. Die Darmmikrobiota kann durch die Produktion von Metaboliten wie Butyrat Zellen des Glukagon-ähnlichen Peptid (GLP-1) im Kolon stimulieren, die β-Zellen anzuregen und Insulin zu sezernieren [5]. Über die Auswirkungen chronischer CE auf den Gesamtstoffwechsel beim Menschen ist hingegen wenig bekannt.

Die vorliegende Studie untersuchte daher die metabolischen und metagenomischen Auswirkungen täglicher chronischer CE unter Alltagsbedingungen beim Menschen mithilfe eines neuartigen Kühlprotokolls und folgende Hypothese wurde geprüft: „Vier Wochen chronischer CE/10 Stunden pro Tag verbessert den Glukose- und Energiestoffwechsel, erhöht die BAT-Aktivität und führt zu signifikanten Veränderungen in der Zusammensetzung der Darmmikrobiota, die mit dem Glukosestoffwechsel zusammenhängen“.

Achtzehn Personen (Body-Mass-Index: 25-35 kg/m^2) nahmen an einer randomisierten, balanzierten Cross-over-Studie teil. Folgende Parameter wurden zu Baseline (BL) und nach chronischer CE morgens nach mindestens 12 Stunden fasten gemessen: Körperzusammensetzung mittels Luftverdrängungsplethysmographie, β-Zell-Funktion und Insulinsensitivität mittels Botnia-Clamp-Verfahren, BAT-Aktivität indirekt mittels Infrarot-Thermographie (IRT) und Mikrobiotazusammensetzung mittels Shotgun-Metagenomanalyse.

Nach chronischer CE im Vergleich zu BL stiegen die erste Phase der Insulinreaktion (FPIR) ($p = 0,01$), die C-Peptid-Konzentration ($p = 0,01$) und der Disposition-Index ($p = 0,03$) signifikant an. Zusätzlich wurde die Tendenz einer verbesserten Glukosetoleranz ($p = 0,056$) und eines erhöhten HOMA-Beta ($p = 0,06$) beobachtet, wobei das Signifikanzniveau nicht

erreicht wurde. Diese Ergebnisse spiegeln eine verbesserte Funktion der β-Zellen nach chronischer CE beim Menschen wider. Allerdings blieb die Insulinsensitivität (*M*-value) zwischen den Bedingungen unverändert (p = 0,99). Darüber hinaus zeigte die Auswertung der IRT-Bilder keine BAT-Aktivität.

Zur Untersuchung des Mechanismus dieser verbesserten β-Zell-Funktion nach chronischer CE führten wir Shotgun-Metagenomanalysen durch, um die Rolle der Mikrobiota im Glukosestoffwechsel zu klären. Es zeigte sich, dass unsere metagenomische Analyse die metabolischen Ergebnisse stützen. Es wurde eine Zunahme der Abundanz vom Glykolyse I (p = 0,045) Signalweg und der Mikrobiota auf der Spezies-Ebene, die den Glukosestoffwechsel beeinflussen, wie *Bacteroides uniformis* (p = 0,02), und eine negative Korrelation zwischen der AUC des Plasmaglukosespiegels während des intravenösen Glukosetoleranztests und dem Glykolyseweg I (R^2 = 0,39; p = 0,03) beobachtet. Darüber hinaus unterstreicht eine positive Korrelation zwischen dem Disposition-Index und FPIR mit Butyratproduzenten den potenziellen Einfluss der Darmmikrobiota auf die Glukosehomöostase.
Insgesamt bestätigen die Ergebnisse dieser Doktorarbeit die Interaktion zwischen Darmmikrobiota und Glukosestoffwechsel. Unsere Ergebnisse zeigen, dass chronische CE unter Alltagsbedingungen die β-Zell-Funktion bei Personen mit Übergewicht und beginnender Adipositas verbessert, was durch die Veränderungen in der Mikrobiota-Zusammensetzung nach chronischer CE ausgelöst werden könnte.
Diese Erkenntnisse stellen einen neuen, vielversprechenden nicht-pharmakologischen Ansatz dar, die Insulinsekretion bei Personen mit Übergewicht und Adipositas sowie bei Personen mit Diabetes zu stärken. Um den zugrunde liegenden Mechanismus dieser Ergebnisse zu aufzuklären und den potenziellen Einfluss von Mikrobiota-Metaboliten, insbesondere kurzkettigen Fettsäuren (SCFAs) wie Butyrat, auf die Verbesserung der Insulinsekretion zu erforschen, ist ein nächster Schritt die SCFAs zu messen. Dieses Bestreben zielt darauf ab, ein tieferes Verständnis für das Zusammenspiel von Metaboliten-, metabolischen und metagenomischen Ergebnissen in unseren bevorstehenden Untersuchungen zu gewinnen. Die Ergebnisse unserer vorigen Studie, die eine verbesserte Insulinsensitivität und BAT-Aktivität ausschließlich bei schlanken Personen zeigen, legt nahe, die metabolischen und metagenomischen Auswirkungen einer chronischen CE speziell in einer gesunden Kohorte mit Normalgewicht zu erfassen.

1 Introduction

1.1 Obesity & metabolic syndrome

Obesity has become one of the biggest health problems worldwide and has its incidence almost tripled since 1975 and continues to rise [6]. In addition to industrialized countries, developing countries are also increasingly affected, so the term "obesity pandemic" is justified. Based on the laws of thermodynamics, the imbalance between energy intake and energy expenditure has been recognized as a crucial factor contributing to the development of obesity [7,8].

The World Health Organization (WHO) classifies overweight and obesity using the body mass index (BMI) [6], which is defined as body weight in kilograms divided by height in meters squared (kg/m²). A BMI between 18.5 kg/m^2 and < 25 kg/m^2 is defined as normal weight, from 25 kg/m^2 to < 30 kg/m² as overweight, and from ≥ 30 kg/m² as obesity. A further distinction is made between three degrees of obesity: a BMI between 30 and < 35 kg/m² is referred to as obesity grade I, a BMI between 35 and < 40 kg/m² is obesity grade II, and a BMI measuring ≥ 40 kg/m² is considered obesity grade III. However, BMI does not provide direct information on body fat content as it, for example, does not differentiate body composition into fat and muscle mass. Nonetheless, research has shown that BMI usually correlates with direct measurements of body fat mass (FM) [9]. BMI serves as an important characteristic that describes the health status of a population. It increases with age in both women and men [10,11], and a greatly increased BMI is often associated with secondary diseases such as type 2 diabetes (T2D) or increased blood pressure [12]. Thus, along with tobacco consumption, alcohol abuse, and cardiological diseases, an increased BMI counts as the main cause of premature deaths [6]. In 2016, 39% of adults aged 18 years and older (39% of men and 40% of women) worldwide were overweight. Of these, about 11% of men and 15% of women were obese [6]. In Germany, according to the evaluation of the study "Gesundheit in Deutschland Aktuell" (GEDA) of the Robert Koch Institute from 2019/2020, 53.5% of adults are overweight, and the percentage is higher in men than women. When looking at the prevalence of overweight and obesity in Schleswig-Holstein, it is 55.8% and 19.6%, respectively (Figure 1).

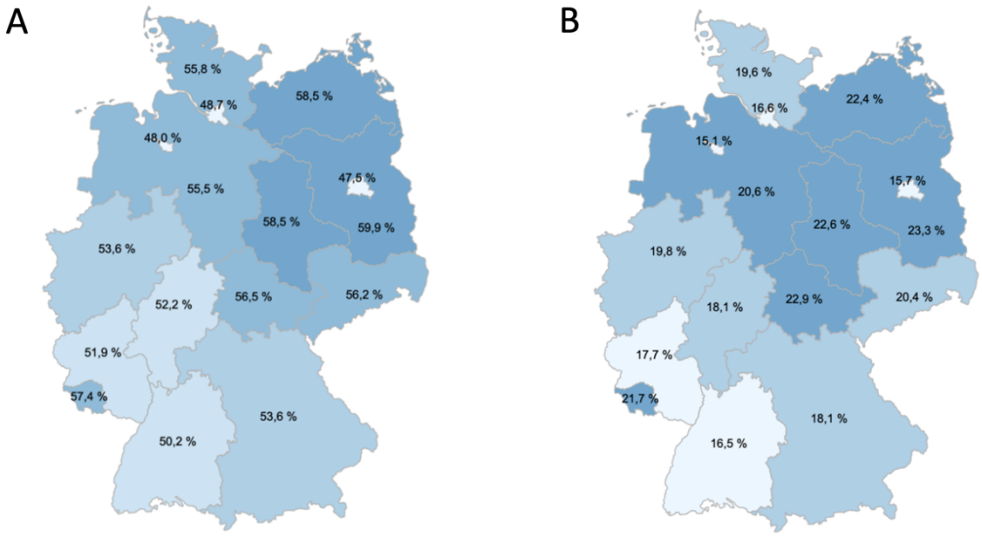

Figure 1. Overview of the obesity pandemic in Germany.
A) The left panel shows the prevalence of overweight; B) the right panel shows the prevalence of obesity in Germany. Data from the cross-sectional GEDA study in 2019/2020, which included 23.000 individuals. The image belongs to the GADA study, Robert Koch Institute.[1]
Abbreviation: Gesundheit in Deutschland Aktuell (GEDA).

This high prevalence and the associated short- and long-term complications underscore the need for effective prevention and treatment of obesity and research on the underlying causes. However, it is important to notice that not all patients with obesity suffer from associated comorbidities. In general, 25% of patients with grade II and III obesity are described as metabolically healthy obesity, as they exhibit no metabolic disorders, including T2D, dyslipidemia, and hypertension [13].

The causes for the development of the "obesity pandemic" are diverse, as obesity is a multifactorial disease. Genetic predispositions, environmental conditions, social environment, and lifestyle, among others, play an important role in the development of obesity [14]. Obesity can be explained by a single mutation in specific genes only in 5% of cases, e.g., mutations in leptin [15,16]. Gene-environment interactions are pivotal factors contributing to the development of obesity and T2D. In this scenario, a clinical study conducted a comparative analysis of two distinct Pima groups in America: one group had embraced “1”, and resided in modernized Arizona, while the other group, based in Mexico, remained isolated and adhered to their “traditional lifestyle and diets”, serving as the control group. The results revealed a

[1] Figures downloaded 01.11.2023
https://public.tableau.com/app/profile/robert.koch.institut/viz/Gesundheit_in_Deutschland_aktuell/GEDA_20192020-EHIS

significant rise in T2D and insulin resistance rates in the Arizona group, with an increase from 6% to 47% in men and from 11% to 54% in women. This study furnishes compelling evidence of the profound impact of environmental and lifestyle factors on these health conditions [17,18].

It is important to mention that the prevalence of T2D is closely related to the rise in obesity. According to WHO, the number of people with T2D has increased from 108 million in 1980 to over 422 million in 2014 worldwide [6,19]. This underscores the imperative need for the development of novel approaches to prevent and combat obesity and T2D to enhance metabolic health worldwide.

1.2 Treatment of obesity

Obesity treatment can be generally classified into three categories: lifestyle intervention, medical therapy, and bariatric surgery [20]. In the following paragraphs, these categories are briefly described.

Lifestyle interventions, such as a healthy diet and increased physical activity are preventive against complications associated with obesity, such as elevated blood pressure or insulin resistance and T2D, but not sufficient in most cases. Importantly, exercise and physical activity are consequential in maintaining metabolic and mental health [21–23]. According to the American Heart Association's Diet and Lifestyle, adequate moderate-intensity physical activity of at least 150 minutes of moderate-intensity or 75 minutes of vigorous aerobic activity per week protects against cardiovascular disease [24].

Additionally, one of the most important causes of obesity is the global increase in a high-calorie "Western diet" of cheap, energy-dense, low-fiber foods, combined with decreased physical activity [25,26]. By comparing different diets and their effects on weight loss so far "Mediterranean diet", with rich consumption of vegetables, fruits, whole grains, legumes, fish, nuts, and olive oil, proves to be the healthiest diet with leads to weight loss and shows beneficial effect on lipids and glucose level and cardiovascular diseases [27,28]. Generally, it is important to mention that the Mediterranean diet's influence on body metabolism does not primarily stem from calorie restriction. Instead, it hinges on its association with healthier food choices and lifestyle habits. These factors contribute to potential enhancements, including increased physical activity, elevated energy expenditure, and improved body metabolism. This

collective effect aids individuals striving for weight loss by helping them maintain a healthier body weight [29].

Recently, intermittent fasting has gained substantial attention in discussions about “metabolic switching”, associated with improved insulin sensitivity, increased fat oxidation, preservation of lean body mass (BM), and better cardiometabolic health. This involves cycles of regular versus restricted calorie intake, like daily fasting for 16 hours with an 8-hour eating window, fasting for 24 hours on alternate days, or periodic fasting for one or two nonconsecutive days per week, among various other patterns [30,31].

However, generally, diets do not yield sustainable long-term weight loss, often leading to the observed 'yo-yo' effect. This effect typically involves an initial phase of weight loss followed by subsequent weight regain [32,33].

Anti-obesity medications primarily focus on decreasing food intake. Nevertheless, they have demonstrated modest effectiveness while often presenting a range of adverse side effects [34]. Metformin, the most important and first-line antidiabetic medication [35], has demonstrated only a weight-neutral effect or in some cases, 5% weight reduction over four years, primarily attributed to its influence on the hypothalamic appetite regulatory center [36]. Consequently, it is not employed as a treatment for obesity [37]. The development of a new generation of anti-diabetic drugs has ushered in a new era in the treatment of obesity, and weight management. One of the most effective anti-diabetic medications is an incretin hormone or glucagon-like peptide (GLP-1)-receptor agonist. GLP-1 is a peptide hormone mainly produced in the L-cells in the ileum and colon, in response to high carbohydrate and fatty foods [38]. GLP-1 receptors are found on various tissues and cells for instance on the surface of β-cells, the central nerve system (CNS), and the peripheral nervous system. Upon release, GLP-1 binds to these receptors, serving a pivotal role in appetite regulation and increased feelings of fullness, plasma glucose reduction, hypothalamic satiety enhancement, deceleration of gastrointestinal motility, and the stimulation of insulin secretion in the pancreas [39,40]. In 2010 Liraglutide, in 2014 Dulaglutide, and later in 2017 Semaglutide were three GLP-1 receptor agonists approved by the Food and Drug Administration as anti-diabetic drugs. Surprisingly, this medication showed significant weight loss in some individuals after only 8-12 weeks in comparison to the placebo [41–43] and since 2021 these medications become one of the most frequently prescribed drugs [44]. Notably, the gastric inhibitory polypeptide receptor(GIP-R)/GLP1-receptor co-agonist Tirzepatide recently got approval for

T2D treatment, delivering an impressive average weight loss of 22% in individuals with obesity [45]. This brings hope regarding the treatment of obesity and T2D. However, anti-diabetic medications also often show some side effects such as nausea, vomiting, and diarrhea in severe cases high risk for heart attack, breast cancer, and death [46,47].

For obese patients with a BMI > 40 kg/m^2, who do not respond to traditional weight loss therapies or a 35 > BMI > 40 kg/m^2 with comorbidities such as heart and/or kidney diseases, high blood pressure, T2D, and severe sleep apnea, so far bariatric surgery is the most effective therapy approach that leads to significant weight loss and remission of obesity-related diseases such as T2D and insulin resistance [48,49]. However, the invasiveness of this method, along with different side effects such as hypoglycemia, malnutrition, chronic nausea, and vomiting make it a high-risk choice as the best recommendation to combat obesity and T2D [50,51].

As mentioned earlier, obesity is a key risk factor for the development of secondary diseases such as T2D, hypertriglyceridemia, cardiovascular comorbid disorders, elevated blood pressure, various types of cancer (e.g., colorectal cancer), and stroke [52,53]. Considering the abovementioned points, it is urgent and critical to find new strategies to mitigate the growing pandemic of obesity and to combat the related metabolic disorders.

In recent years, there has been a surge of interest in brown adipose tissue (BAT) as an emerging focal point for enhancing metabolic well-being and addressing obesity and T2D. This growing attention follows the re-discovery of BAT in humans and ongoing research continues to unveil its multifaceted physiological and therapeutic significance. Chapter 1.4 provides an exhaustive exposition of this distinct adipose tissue and its intricate functionality.

1.3 Different colors of fat depots and their metabolic aspects

In lean healthy humans, about 20-25% of total body weight consists of adipose tissue [54]. Fat depots are distributed throughout the body and vary considerably in their accumulation and position. In mammals, including humans, it is well accepted that there are three types of adipose tissue: white fat (WAT), beige or brite or brown within white fat (BeAT), and BAT [55,56]. Morphologically and characteristics of different fat depots are not the same and have different origins and impacts on our health status. All fat depots have a high plasticity origin but with different functions [57]. Figure 2 illustrates the microscopy images of two human adipose tissue sections, WAT and BAT, which I meticulously prepared as part of my Master's

thesis project. The different fat depots are distinguishable based on their color and the size of adipocytes. This study focuses primarily on examining the metabolic effects of chronic CE, with a particular emphasis on its influence on BAT activity. Subsequently, for a comprehensive understanding of BAT and its functions, the subsequent sections briefly outline the main types of fat depots.

A B

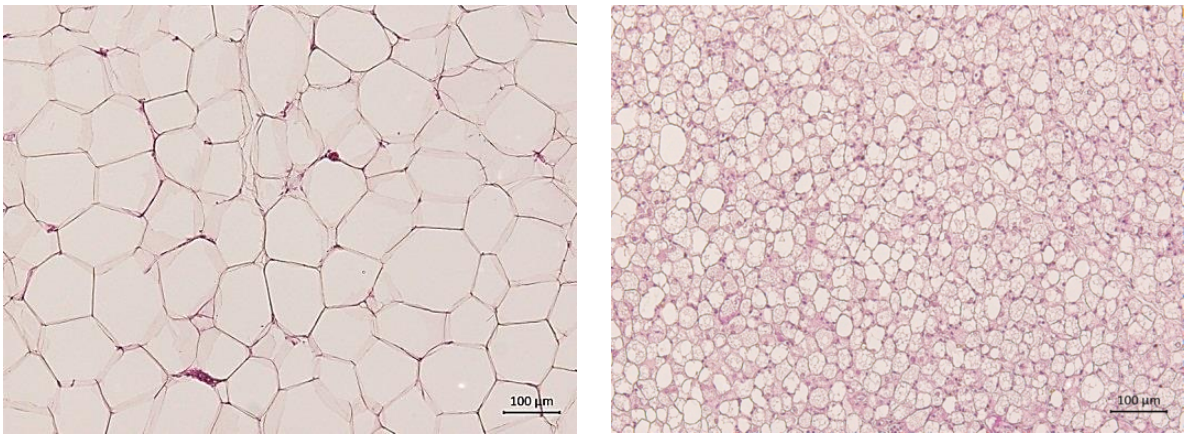

Figure 2. Representative microscopy images of human fat sections.
Microscopy images of H&E staining from A) WAT section and B) BAT section of individuals with obesity. The different tissues are distinguishable based on their color and the size of adipocytes. The image belongs to [58].
Abbreviations: Hematoxylin & eosin (H&E); white adipose tissue (WAT); brown adipose tissue (BAT).

1.3.1 White adipose tissue

Most of the human adipose tissue is located in WAT, which in turn is generally divided into subcutaneous and visceral adipose tissue, ScAT and VAT, respectively.

The basic building blocks of these depots are preadipocytes and immune cells. White adipocytes are unilocular ring-shaped and thus form the largest component of adipose tissue. ScAT is located under the entire skin of the body surface [59,60] and is generally referred to as the "good" adipose tissue depot. Under an imbalance between energy uptake and energy expenditure conditions, when the storage capacity of ScAT is exceeded, its inherent plasticity leads to the development of ectopic fat accumulations. This imbalance eventually results in hypertrophy and hyperplasia [61], which develops VAT and ultimately contributes to the progression of obesity [62]. VAT belongs to the intra-abdominal adipose tissue group and is located around hollowed or solid organs like the colon, pancreas, kidney, and liver [63]. In obesity, VAT is closely associated with metabolic complications such as insulin resistance, T2D, and cardiovascular risk. Therefore, it is often referred to as the "bad" fat depot [64,65].

Notably, white adipose tissue is not only specialized in the storage of lipids and release of free fatty acid (FFA) to meet body metabolic requirements but also is an important endocrine organ [61]. Its cells, especially adipocytes, secrete a variety of hormones so-called adipokines such as e.g., leptin, adiponectin, fibroblast growth factor 1 (FGF21), and interleukin-6 (IL-6) [66], which play an important role in regulating the biological processes of adipose tissue, communication of fat depots with other tissues as well as organ systems, appetite and modulation of energy homeostasis of systemic energy balance [67].

1.3.2 Beige adipose tissue

Lately, BeAT, a novel depot exhibiting robust expression of *uncoupling protein 1* (*UCP1*) and sharing morphological, molecular, and functional similarities with the "conventional" BAT, has garnered recognition [68,69]. UCP1 is a hallmark protein in brown adipocytes, which play the main role in thermogenesis and producing heat (see Chapter 1.4). BeAT mainly develops in ScAT and increases the thermogenesis capacity of this fat depot, which has been termed “browning” [70,71]. Different stimuli induce *UCP1* expression during adipogenesis in ScAT, for example, cold exposure (CE), capsinoids, peroxisome proliferator-activated receptor (PPAR) gamma and alpha, β-adrenergic receptors (β-ARs) agonists, and FGF21 [57,72–75]. Beige adipocytes exhibit thermogenic capabilities, elevating energy expenditure, due to increased *UPC1* expression (Figure 3), which makes this fat tissue a significant focal point within the realm of anti-obesity research.

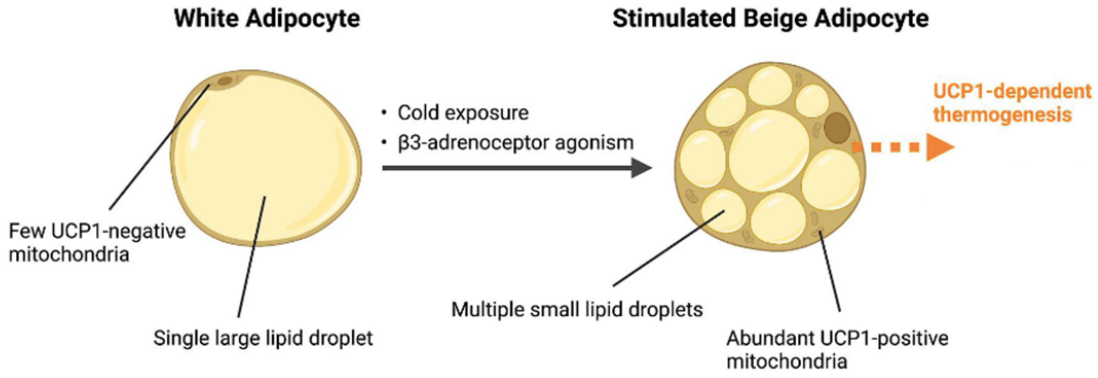

Figure 3. Process of browning in white adipocytes.
The image belongs to [76].
Different activators such as CE can stimulate browning in white adipocytes. This leads to changes in the morphology and function of adipocytes due to increased UCP1 expression.
Abbreviations: Cold exposure (CE); uncoupling protein1 (UCP1).

1.3.3 Brown adipose tissue

BAT is exclusively found in mammals. Brown adipocytes are multilocular cells with multiple cytoplasmatic lipid droplets and a high number of mitochondria and UCP1, which defines their brownish color and function to expand the stored energy via lipolysis to produce heat by the process of "non-shivering thermogenesis" (NST) [77]. Furthermore, within our bodies, muscles also serve as thermogenic tissue, generating heat through contractions in response to cold conditions, a process known as "shivering" [78]. Brown adipocytes originate from the Myf5+ myogenic lineage and share a common precursor with skeletal muscle cells, rather than white adipocytes [79–81]. This initially surprising lineage clarifies the fundamental contrast between WAT and BAT in their respective roles of thermogenesis and fat storage in the body. Figure 4 compares the morphology and function of different adipocytes.

In recent years, browning and BAT have shown different metabolic improvements and become novel research approaches to combat T2D and obesity. One of the aims of this study is to assess the impact of chronic CE on BAT activity, therefore the subsequent Chapter will delve into various aspects of this tissue, thoroughly exploring its characteristics and functions.

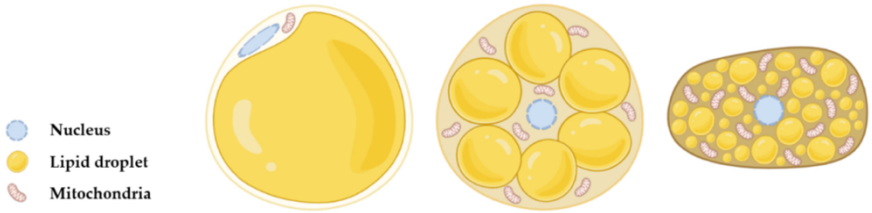

	White adipocyte	Beige adipocyte	Brown adipocyte
UCP1 expression	Negative	Positive	Positive
Mitochondria density	Low	Medium	High
LD morphology	One large lipid droplet	Small multiple droplets	Small multiple droplets
Function	Store excess energy as fat	Heat generation	Heat generation

Figure 4. Schematic characterizations and morphology of different adipocytes.
The image belongs to [57].
White, beige, and brown adipocytes have different functions and morphology.
Abbreviations: Uncoupling protein1 (UCP1); lipid droplet (LD).

1.4 Unique characteristics of brown adipose tissue in humans

The adipose tissue under consideration in this study is the unique BAT. This uniqueness is particularly relevant in the context of thermoregulation, maintaining the core body temperature, and improvement of energy, glucose, and lipid metabolism when activated [82–84].

1.4.1 History and function of brown adipose tissue

The discovery of BAT can be traced back to the early 16th century when the Swiss anatomist Konrad Gesner first observed it in groundhogs. He described it as “neither fat nor meat, it was something in between” [85]. Four centuries later, in 1963, Smith and Hock studied the mechanism of thermoregulation during hibernation. They uncovered a unique type of tissue known as a “hibernation gland”. This marked the first instance of identifying tissue with thermoregulatory capabilities [86], playing a pivotal role in protecting mammals during the winter seasons and hibernation period. In 1993, the effect of BAT on metabolism and the regulation of body weight was identified for the first time in rodents [87]. For a long time, it has been thought that BAT in humans exists only in newborns and serves to generate heat in the body and avoid hypothermia. It has been evidenced that this tissue plays an important functional role in the early years after birth, but this tissue degrades rapidly postnatal [88,89]. Interestingly, 2009 represents a turning point in research regarding BAT studies in adult humans. First, Cypess and colleagues [82] and subsequently, different investigators [90,91] separately identified regions of the body that demonstrated high metabolic activity via increased ^{18}F-fluorodeoxyglucose (^{18}F-FDG) uptake in specific depots in the supraclavicular (SCV) region of the body during positron emission tomography-computed tomography (PET-CT) after acute mild CE. At that time, these findings led to the re-discovery of BAT in adults and sparked renewed interest in studying the role of BAT in regulating metabolism in humans.

The hallmark of BAT is the UCP1 protein, which plays the main role in heat generation as well as lipid oxidation [92,93]. Different activators can stimulate BAT, for instance, CE (see Chapter 1.4.3). Cold activates the sympathetic nervous system (SNS), resulting in the release of norepinephrine. Norepinephrine subsequently binds to ß-ARs, located on the surface of brown adipocytes [94]. This initiates an intracellular signaling cascade that activates the cyclic

adenosine monophosphate (cAMP)-dependent mechanism, ultimately leading to the activation of protein kinase A (PKA) [95].

Activated PKA, in turn, upregulates *UCP1* genes through the activation of the cAMP response element-binding protein (CREB) and triggers proliferator-activated receptor gamma co-activator (PgC1-α). Additionally, PKA facilitates the breakdown of Triglyceride (TG) into FFA. These FFA molecules enter the mitochondria, where they serve as a fuel for β-oxidation, further promoting the activation of UCP1 on the inner mitochondrial membrane. Figure 5 schematically illustrates the cold-activated BAT thermogenic function.

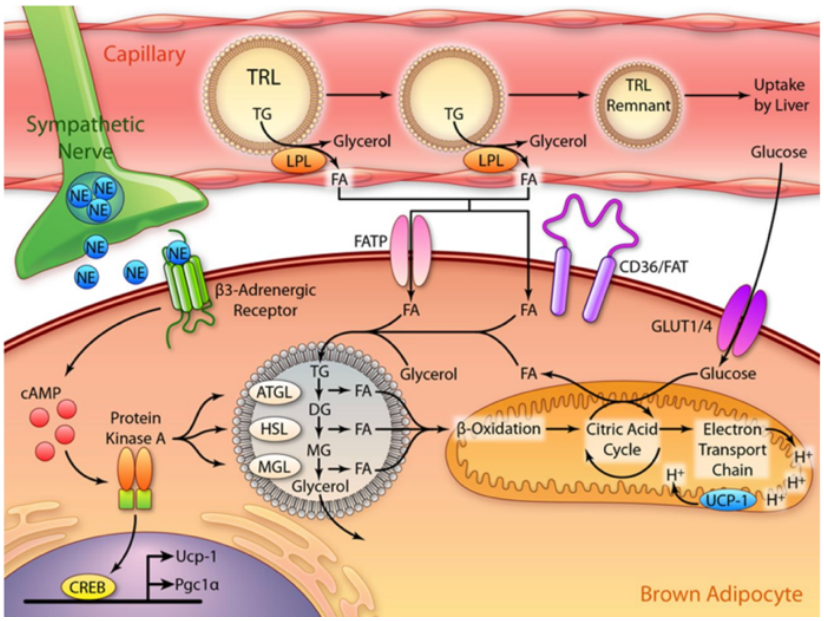

Figure 5. Schematic overview of cold-activated brown adipocyte.
The image belongs to [95].
Released norepinephrine from the nervous system due to CE, binds to ß-ARs on the surface of brown adipocyte and leads to activation of a complex cascade. At the end of this cascade and due to the activation of UCP1, heat will be produced. This function is called NST.
Abbreviations: Cold exposure (CE); norepinephrine (NE); toll-like receptor (TLR); triglyceride (TG); lipoprotein lipase (LPL); fatty acid (FA); fatty acid transport protein (FATP); cyclic adenosine monophosphate (cAMP); adipocyte-triglyceride-lipase (ATGL); hormone-sensitive-lipase (HSL); monoglyceride lipase (MGL); uncoupling protein-1 (UCP-1); prolifetor-activated receptor-gamma co-activator (PgC1-α); cAMP response element-binding protein (CREB); cluster of differentiation/FAT (CD36)/FAT; glucose transporter (GLUT); diglyceride (DG); monoglyceride (MG); non-shivering thermogenesis (NST).

Upon UCP1 activation, this protein forms channels that permit the free flow of protons across the inner mitochondrial membrane, thereby uncoupling the process of oxidative phosphorylation and releasing the energy in the form of heat, resulting in NST [96]. The presence of glucose transporters (GLUT)1/4 on the surface of brown adipocytes not only facilitates the efficient transport of glucose from the bloodstream into the fat cell but also plays a pivotal role in stimulating the citric acid cycle, ultimately converting glucose to FFA, a critical process for energy storage and thermogenesis in brown adipose tissue [95].

Some evidence suggests that BAT also has a secretory function as an endocrine organ, just like WAT, and produces batokines including IL-6, which induces increased *FGF21* expression [97]. The endocrine function of BAT has been more detectable after cold BAT transplantation. After transplantation of BAT into ob/ob mice, improved energy expenditure, glucose hemostasis, and insulin sensitivity were reported [98]. In summary, the thermogenic function of BAT identifies it as a promising and prospective target for enhancing metabolism [99,100].

1.4.2 Prevalence and detection of brown adipose tissue

To investigate and study the positive metabolic effect of activated BAT, the precise determination and assessment of BAT mass and activity serves as a starting point in the field of research. Generally, the detection of BAT activity can be categorized into two main methods: direct and indirect. The direct and reliable method involves collecting BAT samples and quantifying genes and the expression of protein levels of BAT markers, such as *UCP1*, proton-coupled amino acid receptor 2 (*PAT2*), and P2X purinoceptor 5 (*P2RX5*) [93,101]. While this approach is widely used in animal studies, its application in human research is limited due to its invasiveness and difficulties in reaching the anatomical area.

PET/CT is the gold standard for indirectly detecting BAT and assessing its activity due to ^{18}F-FDG accumulation [102]. The terms "BAT+" and "BAT-" denote the presence of active BAT and minimal or undetectable active BAT, respectively [103]. This distinction is pivotal for clinical studies, as it helps stratify the cohort based on BAT activity prior to further investigations. This method aids research into BAT activity; however, it has drawbacks, such as invasiveness, radiation exposure, cost, time consumption, and variability in results due to a lack of standardization and environmental factors.

In recent years, infrared thermography (IRT) has been used as an alternative method in research to detect and assess BAT activity in rodents and humans [104]. Activated BAT generates heat, and an IRT camera detects infrared radiation emitted directly from the skin and indirectly from BAT and converts it to thermal images. In 2018, James Law and colleagues after two hours of CE compared the SCV region showing increased ^{18}F-FDG uptake in PET/CT images with the region displaying elevated skin temperature in IRT images. Their analysis demonstrated a positive correlation between these datasets in both techniques and underscored the accuracy of the IRT technique [105]. Furthermore, this method offers the advantages of being an economical, easy-to-use, and non-invasive method in comparison to PET/CT [104]. Additional insights into this approach can be found in Chapter 2.9.

The findings of the studies have yielded promising results on the presence and physiology of BAT in humans. As a critical thermoregulator, BAT is present abundantly in infants and children to shield them from the cold. In humans, the quantity of brown fat depot is heterogeneous [82,88]. Additionally, its distribution in various parts of the body, makes it challenging to accurately quantify its exact mass. The exact distribution and prevalence of BAT depend on various factors such as outdoor temperature and seasonal effect, BMI, diabetes status, gender, and age. It is widely recognized that BAT prevalence is higher during winter compared to summer [106,107]. Different studies have shown evidence that activated BAT due to CE is higher in lean compared to patients with obesity. In other words, the quantity of BAT exhibits a negative correlation with BMI [90,108,109]. Moreover, individuals with impaired glucose metabolism, and insulin resistance, or patients with T2D exhibit disturbed BAT metabolism and BAT whitening [2,110]. These findings emphasize the potential significance of BAT in both the pathogenesis and therapeutic strategies for addressing T2D and obesity. Remarkably, women exhibit higher BAT prevalence than men, suggesting a role for sex steroids in BAT thermogenesis regulation in healthy adults [111]. Additionally, aging leads to BAT regression into WAT, diminishing its positive metabolic impact, with a noticeable decline starting around ages 30-35 [112]. Nevertheless, research has uncovered promising stimuli for activating and recruiting more BAT in adulthood. The upcoming chapter will delve into these activators of BAT and their significance.

1.4.3 Different activators of brown adipose tissue

To gain a deeper understanding of the BAT function, the next step in the study of BAT is to activate it. In this chapter, the most effective activators of BAT will be briefly described.

Norepinephrine: One of the earliest, extensively studied, and most significant activators of BAT is norepinephrine. In rodents, norepinephrine triggers thermogenesis through β-ARs [113] and leads to the activation of BAT and NST. Moreover, the parasympathetic nervous system activation in mice broadly influences insulin and glucose regulation, β-cell secretion, and enhances glucose uptake and BAT thermogenesis [114,115].

β-adrenergic receptors agonist*:* Activation of β3-ARs has long been considered an attractive approach to stimulate BAT, leading to increased energy expenditure and NST in rodents [116]. However, translating this method from rodent experiments to human applications has proven to be a complex and challenging endeavor. Mirabegron, a β3-ARs agonist used for overactive bladder, has become a leading option for BAT activation in humans. Recent research shows that a four-week regimen of 200 mg oral Mirabegron, significantly higher than the clinical dosage, notably enhances BAT activity in young women [117]. However, chronic use of β3-ARs agonists at these high dosages can put a strain on the cardiovascular system, limiting their applicability in obesity management [118]. Nevertheless, evidence showed a pivotal discovery, revealing that the activation of BAT in humans is primarily mediated by β2-ARs, rather than β3-ARs. Consequently, lower doses of Mirabegron fail to produce a significant effect, therefore Mirabegron in clinical dosage is not an effective BAT activator for humans [119].

Diet & macronutrients: Diet and macronutrients play a pivotal role in BAT activation, as supported by studies in both rodents and humans studies [120,121]. This impact is known as diet-induced thermogenesis or “thermic effect of food” [122]. For instance, a high-caloric meal serves as a potent stimulant for BAT activation and increased ^{18}F-FGD Uptake in BAT [123]. Important to note that diet-induced thermogenesis was not observed in *UCP1* ablated mice and only in wild-type [124]. Experimental data has revealed the influence of specific micronutrients, such as capsaicin derived from chili peppers, on enhancing thermogenesis and increased energy expenditure [125,126]. Besides, strong evidence supports the thermogenic

effects of caffeine, as it stimulates BAT, increases resting energy expenditure, and triggers lipolysis in both humans and rodents [127,128]. As a result, it is imperative to refrain from caffeine consumption for 1-2 days before conducting BAT studies.

Exercise: The effect of exercise and physical activity on BAT activity has been controversial thus far. Exercise leads to the secretion of a specific protein from skeletal muscles named irisin, which has a significant effect on the browning of WAT in mice [129]. This showed improved glucose tolerance as well as significant weight loss in mice [130]. Other circulating parameters such as IL-6, FGF21, and catecholamine may also play a role in BAT activity due to exercise. In humans, moderate exercise for patients with T2D and obesity showed an increased BAT activity [131]. However, longer endurance training seems to have the opposite and adaption effect [132].

Thyroid hormones*:* Thyroid hormones play a pivotal role in maintaining body temperature as well as regulation of BAT activity [133,134]. Specifically, triiodothyronine (T3) and thyroxine (T4), two key thyroid hormones, exert an important influence on BAT function by regulation of *UCP1* expression [135]. Furthermore, thyroid hormones enhance lipolysis and therefore increase the FFA as fuel for thermogenesis [136]. An imbalance in thyroid hormone levels can lead to an alteration in BAT activity, potentially impacting thermoregulation and energy metabolism [137].

Cold exposure*:* So far, acute CE is regarded as the most effective stimulus to activate BAT in both rodents and humans [1,82,90,91,138]. Human cooling protocols exhibit significant diversity, with or without shivering, encompassing both acute and chronic CE. Acute exposure usually lasts a few hours followed by metabolic experiments and BAT assessment. Chronic CE, on the other hand, extends beyond a few hours in a single session [83]. This protocol variability complicates the comparison and discussion of the impact of CE on whole-body metabolism and cold-activated BAT within human and rodent studies. Chapter 4.8 of this thesis delved into the significance of the implemented cooling protocol.

1.5 Metabolic effect of cold-activated brown adipose tissue

The following chapters describe the different metabolic effects of cold-activated BAT.

1.5.1 Cold-activated brown fat and stress hormones

Typically, exposure to cold temperatures is considered a stressor for the body. Consequently, the body responds by generating heat and implementing protective mechanisms to maintain its core temperature within the normal range [135]. Glucocorticoids stress hormones, such as adrenaline, norepinephrine, cortisol, and adrenocorticotropic hormone (ACTH), trigger different reactions to increase the body temperature, for instance by increasing the heartbeat per minute and activating BAT [139]. Additionally, the release of ACTH leads to increased energy expenditure and maintains the core temperature [140]. Evidence suggests that acute CE leads to an increase in the circulatory hormone cortisol. Adaption to four-week chronic CE at 4°C for 24 hours per day showed an increase in BAT weight but no changes in cortisol concentration in mice [141]. As an example, in a clinical study, a group of healthy individuals participated in a winter swimming study in water between 0-2°C three times a week for 12 weeks. After analysis of the blood samples, a decrease in ACTH and cortisol was observed in weeks 4-12 in comparison to BL, which suggests habituation due to prolonged cold [142]. In summary, adaption to cold is an important aspect that should be considered while analyzing and interpreting the data of chronic cold studies.

1.5.2 Cold-activated brown fat and energy metabolism

In recent years, there has been a growing focus on harnessing the potential of BAT to combat obesity and related metabolic disorders, driven by its substantial role in adaptive thermogenesis and energy expenditure. In obese mice, transplanting cold-activated BAT led to significant weight loss [143], whereas mice without BAT developed obesity, emphasizing the importance of this tissue [87].

In humans, increased BAT activity following CE can enhance resting metabolic rate [92,144,145]. According to Virtanen and colleagues, approximately 63 grams of cold-activated BAT contribute to 5% of the total energy expenditure [91].

Additionally, 24 hours post-CE (16°C) compared to BL in healthy male individuals the total energy expenditure increased; however, no changes in body weight have been observed

[146]. Yoneshiro and his team conducted a four-week study involving five healthy men who underwent 10 hours of overnight CE at 19°C. The results showed increased energy expenditure and BAT volume, while body weight and FM remained unchanged [109]. In summary, in humans, despite the improved energy expenditure after cold, it falls short of achieving substantial clinical weight loss, i.e., more than 5% over 6-12 months [147], necessitating the development of new cooling protocols and longer cold acclimation to explore their effects on body composition and weight changes.

1.5.3 Cold-activated brown fat and lipid metabolism

As already discussed, circulatory TG and FFA are involved in the NST of BAT activity. In mice, strong evidence established that BAT can effectively dissipate a significant amount of stored lipids following CE [148]. Short-term CE for two hours accelerated the clearance of plasma TG in obese mice with hyperlipidemia, primarily due to increased uptake by cold-activated BAT [149]. Human studies have yielded varied results, with some showing no changes in TG levels [150–152], and others demonstrating increased TG following CE [153]. In contrast, FFA concentrations have consistently shown an increase after acute CE which provides a positive correlation between FFA and BAT activity as well as increased energy expenditure after cold [1]. Taken together, these data suggest that activated BAT plays a crucial role in lipid metabolism.

1.5.4 Cold-activated brown fat and glucose metabolism

Generally, the positive effect of cold-induced BAT on glucose metabolism is a result of increased expression of genes and proteins that are involved in glucose and insulin signaling [154]. Additionally, substantial quantities of glucose are stored in the form of glycogen and undergo anaerobic glycolysis to be converted into lactate [155].

It is well established that BAT is an insulin-sensitive tissue and has a high capacity to handle circulating glucose, due to the identification of GLUT1 and GLUT4 at murine brown adipocytes, which indicates the insulin-dependent and independent uptake of glucose [156]. In humans, increased insulin-mediated ^{18}F-FDG uptake in BAT confirmed the presence of GLUT4 transporter in brown adipocytes as well [92,98].

In rodents, transplantation of cold BAT improved the glucose uptake in BAT and also led to increased browning in WAT which additionally increased glucose disposal [98]. In humans at

the fasting level, only one study demonstrated a decreased glucose level in healthy obese participants after cold [2].

In addition to glucose, two other parameters, insulin, and C-peptide, are crucial metabolites that play a significant role in regulating glucose metabolism (see Chapter 1.6). Hence, examining their changes following CE is of utmost importance. CE stimulates norepinephrine and can have both stimulatory and inhibitory effects on various components of insulin signaling.

My colleagues in our lab reported that after two hours of acute moderate CE at 18°C in healthy young lean men, insulin sensitivity increased significantly in comparison to thermoneutrality (TN) at 22°C. However, fasting plasma glucose remained unchanged [1]. Along with this finding, increased BAT volume and activity after 10 days of CE (14-15°C) has been observed in patients with T2D by 43% increased peripheral insulin sensitivity [2].

Taken together, it has been extensively proven that acute CE activates BAT and improves glucose metabolism. However, the impact of chronic cold in humans is still not well established and requires further investigation, using gold-standard methods to assess glucose metabolism.

1.6 Glucose homeostasis

Glucose metabolism is intended to be explored as one of the primary objectives of the present study. This chapter provides a concise overview of this topic.

Glucose homeostasis is the intricate and ever-changing mechanism by which the human body controls plasma glucose concentration, preserving it within a tightly regulated range of euglycemic plateau [157]. Insulin resistance and disrupted glucose homeostasis are frequently observed outcomes of being overweight and obese [158]. The main organs involved in regulating plasma glucose levels are the pancreas, liver, kidneys, muscles, adipose tissues, hormones, and brain [159].

In healthy non-diabetic individuals, the liver is mainly responsible for approximately 95% of gluconeogenesis, while the kidneys contribute about 5%. This balanced glucose production, which precisely matches the whole-body glucose utilization, leads to the maintenance of the euglycemic plateau [160]. The basal plasma glucose level depends on a controlled balance between gluconeogenesis and glucose utilization [159]. Pancreatic β-cells play an important role in glucose metabolism by producing two main hormones: glucagon and proinsulin. Glucagon elevates plasma glucose concertation, while proinsulin exerts an opposing influence. Proinsulin is composed of two components: C-peptide and insulin [161]. C-peptide is a small peptide and is secreted in equal molar quantities with insulin during insulin production. C-peptide cannot promote glucose uptake into cells and most importantly, counts as an indicator of endogenous insulin secretion and to evaluate β-cell function. Insulin and C-peptide have very different half-lives of four vs. 30 minutes, respectively [162]. Peripheral insulin concentration does not reflect the exact insulin concentration, as half of secreted insulin undergoes the first phase of hepatic removal and therefore doesn't reach the periphery [162].

It is important to note that glucose homeostasis and diabetes status are influenced not only by genetics but also by environmental factors, forming an intricate "Enviro-Genetic" effect. Unhealthy lifestyle choices, such as obesity, lack of physical activity, sleep deprivation, and constant exposure to an unhealthy diet, can directly impact insulin secretion [163–165]. When the body experiences constant high insulin levels due to these factors, cells and insulin receptors become less sensitive to insulin, leading to insulin resistance. Without improvement

in lifestyle choices and as individuals age, this insulin resistance over time can progress, ultimately culminating in the manifestation of T2D.

In this context, assessment of β-cell function and insulin sensitivity by using different methods for early diagnosis of insulin resistance and T2D is of paramount importance to combat obesity-related comorbidities. Generally, there are various methods to monitor plasma glucose concentration and assess glucose homeostasis:

Short-term plasma glucose concentration: According to WHO, normoglycemia refers to a plasma glucose level in the fasting state that falls within the range of 70-99 mg/dL. Relying only on fasting blood glucose level as an indicator to investigate diabetes status may not provide a reliable assessment, thus this parameter can be easily influenced by factors such as recent food intake and/or physical activity [166,167].

Long-term plasma glucose concentration: In the clinic, the first step to evaluate diabetes status is initially by measuring the long-term plasma glucose level of glycated hemoglobin or hemoglobin A1c (HbA1c). Red blood cells, with a 120-day lifespan, accumulate glycated hemoglobin over this period, offering a valuable view of the individual's health for the previous two to three months [168]. This value in healthy individuals without T2D is defined as less than 5.7% [169].

Botnia clamp: Gold standard to assess insulin secretion and insulin sensitivity [170]. It is a combination of an intravenous glucose tolerance test (IVGTT) and a hyperinsulinemic euglycemic clamp (HEC). The physiology behind this technique is to perturb the glucose hemostasis with a high and constant insulin infusion and to keep the glucose plasma concentration at a euglycemic plateau, with a variable exogenous glucose infusion rate (GIR) [171]. In other words, elevated insulin levels effectively inhibit liver gluconeogenesis, potentially leading to hypoglycemia. To avoid this, an exogenous glucose infusion is administered, facilitating the assessment of whole-body glucose utilization. Within the clamp procedure, under the influence of elevated insulin levels, approximately 80% of plasma glucose is actively absorbed by skeletal muscles, with an additional 10% taken up by adipose tissue [170]. Chapter 2.13 of this work provides a comprehensive detail of this technique.

1.7 Cold and gut microbiota

The composition of gut microbiota and its association with glucose homeostasis is intended to be explored as one of the primary objectives of the present study. This chapter provides a concise overview of this topic.

The gastrointestinal tract acts as a host to a complex microbiota ecosystem, which holds importance due to its pivotal role in both human health and disease [172]. Microbiota colonization begins shortly after birth, with the initial pattern based on sex and ethnicity, which is heavily influenced by factors like delivery mode and early feeding choices [173]. By the age of one, the intestinal microbiota establishes itself [174]. Gut microbiota is a key regulator of xenobiotic and drug metabolism, the preservation of the structural integrity of the gut mucosal barrier, immunomodulation, and defense against pathogens [175]. Most importantly, microbiota regulates the digestion system by synthesis and absorption of nutrients, vitamins, lipids and producing metabolites such as short-chain fatty acids (SCFAs) and bile acids (BAs) [176].

Generally, gut microbiota consists of bacteria, yeast, and viruses. Bacteria are the most abundant domain in the human gut microbiota and are categorized taxonomically into various hierarchical levels, which are phyla, classes, orders, families, genera, species, and strains [177]. Under normal physiological conditions, around 90% of gut microbiota composition belongs to the phyla Firmicutes (64%) and phyla Bacteroidetes (23%). However, the phylum abundance does not provide clear information regarding the intricacies of a healthy microbiota, and therefore deeper metagenomic analysis at genus, species, and strain levels is required. One of the current state-of-the-art methods in this field, which provides the mentioned information, is Shotgun metagenomic analysis [178].

Disruptions in the balanced composition of the microbiota, commonly referred to as “dysbiosis”, are strongly associated with a range of conditions, including inflammation [179], cardiovascular diseases [180], obesity [181], other metabolic diseases such as T2D [182], and even disorders affecting mental well-being [183,184]. Different parameters, notably dietary habits, stress, exercise, sleep, antibiotics, medication, and environmental temperature continue to shape the composition and dynamics of the intestinal microbiota [185].

To examine the effect of microbiota on thermoregulation, germ-free mice using antibiotics and housed acutely (48 hours) at 4°C showed an impaired thermogenic capacity of BAT and reduced browning in WAT, although the control mice could sustain their body temperature

[186]. Additionally, four weeks of daily cold at 4°C affected microbiota diversity, increased gut size, and absorptive capacity, and improved insulin sensitivity in mice [3] (Figure 6).

In humans, it is well investigated that patients with T2D have a different microbiota composition in comparison to healthy individuals [187]. In patients with T2D, depleted bacteria at the genera level e.g., *Ruminococus,* and at the species level e.g., *Bacteroides uniformis, Roseburia intestinalis, Roseburia insulinivorans, Eubacterium rectale and Eubacterium ventriosum* is reported [188–191].

Evidence in this regard stems from the experiments on mice fed with a high-fat diet (HFD), and supplementation of wild-type mice for seven weeks with *Bacteroides uniformis* showed a significantly reduced body weight and plasma glucose concentration in comparison with control mice only under HFD and without this specific species gavage [192].

Additionally, some species such as *Bacteroides thetaiotaomicron* as a glutamate-fermenting species have an anti-obesity impact [193].

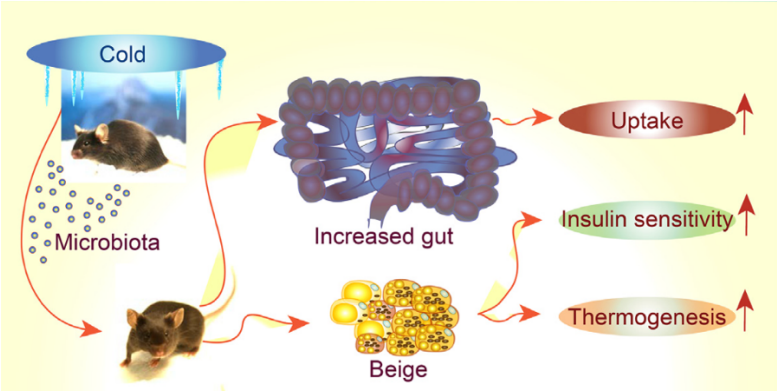

Figure 6. Schematic interaction of cold and microbiota.
The image belongs to [3].
Chronic cold for four weeks changes microbiota composition and increases insulin sensitivity as well as thermogenesis in mice.

The exact mechanism behind the association of the microbiota and improved glucose metabolism or thermoregulation is still not well investigated. One factor that defines a healthy microbiota is the genes encoding glycosaminoglycan degradation and production of SCFAs, such as butyrate, acetate, and propionate, which affect glucose homeostasis significantly. Butyrate, a bacterial metabolite, plays a crucial role in maintaining the integrity and thickness of the entire mucosal barrier [194].

These butyrate-producing species increase the production of the abovementioned metabolites in the large intestine [177] and can bind G-protein coupled receptors (GPCRs) on

endothelial L-cells in the intestine, leading to GLP-1 secretion and peptide YY. These hormones enter the circulation, which stimulates β-cell function and insulin secretion as well as increases energy expenditure [177,195] (Figure 7).

In 2016, Perry and colleagues reported that SCFAs can activate the parasympathetic nervous system, which leads to increased appetite and "glucose-stimulated insulin secretion" [196]. Moreover, a deficiency of SCFAs is associated with T2D [197]. Therefore, a fiber-rich diet, which is known to change the diversity of microbiota toward a higher abundance of butyrate-produced species, can help patients with T2D to reduce plasma glucose by increasing GLP-1 secretion [198].

Figure 7. Schematic representation illustrating the impact of butyrate on glucose homeostasis. SCFAs initiate a cascade by activating GPRs, prompting the release of GLP-1 from L-cells located in the colon. This release, in turn, triggers the activation of β-cells, subsequently stimulating insulin secretion and regulating glucose metabolism.

Abbreviations: Short-chain fatty acids (SCFAs); G protein-coupled receptors (GPRs); glucagon-like peptide-1(GLP-1).

SCFAs also have been demonstrated to enhance glucose uptake by increasing *GLUT4* expression in muscles [199]. A recent study showed that butyrate can activate BAT via gut-brain crosstalk [200,201]. To examine the direct effect of butyrate on BAT activity and thermoregulation, both control and germ-free mice were administered butyrate for days at room temperature, showing an increased body temperature in germ-free mice [186].

In summary, the microbiota offers a promising avenue for addressing metabolic disturbances, such as obesity and T2D. However, it is imperative to conduct additional research on human subjects to comprehensively assess the impact of CE on this intricate interplay. Moreover, elucidating the specific mechanisms by which gut microbiota alterations mediate cold-induced changes in glucose homeostasis is essential for developing promising therapeutic interventions. Further investigations in this area hold great potential for improving our understanding of metabolic health and the potential role of the gut microbiota and its crosstalk with other organs.

The present study builds upon previous investigations within our lab, which centered on the metabolic effects of acute exposure to cold in lean individuals and with obesity under controlled experimental visits using a whole-body cooling garment in the lab unit [1]. Throughout my doctoral research the so-called “eCooling study”, I aimed to delve into a deeper understanding of the metabolic and metagenomic implications of chronic daily exposure to cold on humans.

According to our current comprehension, this study for the first time investigated the metabolic and metagenomic effects of chronic daily mild cold exposure in individuals with overweight and mild obesity, without any comorbidities, under free-living conditions utilizing an innovative local cooling protocol.
To achieve this, we initiated a controlled randomized clinical trial. Diverse metabolic experiments were conducted to comprehensively characterize the impact of chronic cold, four weeks/10 hours a day, and assess its influence on the gut microbiome composition [3].

Hence, this doctoral thesis consists of two parts structured around two primary focal points, exploring the metabolic impact induced by chronic daily cold (hypothesis I) as well as investigating its potential metagenomics impact related to glucose homeostasis in humans as compared to baseline (BL) conditions (hypothesis II).

1.8 Hypothesis & Aims

Cold impacts the whole-body metabolism in different ways. As previously described, CE counts so far as one of the most important activators of BAT. The mechanism of cold-induced BAT activation is very complex. Extensive research in rodents has elucidated the underlying general mechanisms of cold-induced BAT through various cooling experiments using intense cold temperatures and revealed how acute and chronic exposure to cold improves energy expenditure, glucose homeostasis, and lipid metabolism [98,149,202].

The re-discovery of BAT in humans, despite a growing body of research over the last decade [82,90,91], continues to unveil novel aspects yet to be fully understood. This dynamic field holds the promise of uncovering fresh insights into the importance of cold-activated BAT in whole-body metabolism. In the previous study in our lab, my colleagues reported an improved glucose tolerance in the sub-cohort with obesity and an improved insulin sensitivity in the sub-cohort of lean individuals after only two hours of moderate CE (18°C) compared to TN (22°C) by wearing a whole-body cooling garment in the lab unit [1]. Additionally, they reported increased BAT activity in only three of the 15 lean participants, whereas in individuals with obesity, no evidence of BAT activity was reported. Their findings have illuminated a path of hope for improved glucose tolerance and homeostasis due to acute CE as a therapeutic target for individuals with obesity and T2D.

Additionally, cold influences the body's metabolism by altering the composition of the gut microbiota [203]. In mice, chronic CE altered microbiota composition, which was associated with improved glucose hemostasis [3].

In humans, many aspects of chronic CE are still not fully understood. In this doctoral research project, I aim to deepen our understanding of the metabolic and metagenomic impacts of chronic CE, four weeks/10 hours per day, of individuals who are overweight or with mild obesity. This study represents a pioneering approach, utilizing a unique local cooling vest as a novel cooling protocol under free-living conditions.

The objective of this research is to evaluate the impact of chronic CE on various facets including glucose metabolism, body composition, BAT activity, the stress hormonal axis, subjective appetite, and the composition of gut microbiota related to glucose metabolism, comparing it to BL conditions. The rationale behind this approach is to integrate daily CE within lifestyle interventions, potentially offering improvements in metabolic health for individuals dealing with obesity and T2D.

Hypothesis I: Metabolic impact of chronic cold exposure in humans

Chronic daily CE for four weeks/10 hours a day improves glucose and energy homeostasis and activates BAT in individuals with overweight and mild obesity.

To prove this hypothesis, the following aims comparing chronic CE vs. BL were investigated:

Aim 1: Assessment of body composition.
Aim 2: Assessment of BAT activity.
Aim 3: Analyzing different metabolites and hormones such as glucose, insulin, C-peptide, ACTH, and cortisol in plasma at the fasting level.
Aim 4: Analyzing glucose metabolism.
Aim 5: Assessment of the sympathetic and parasympathetic nervous system and stress axis.
Aim 6: Assessment of subjective feelings of appetite and well-being.

Hypothesis II: Metagenomic impact of chronic cold exposure in humans

Chronic daily CE for four weeks/10 hours a day impacts microbiota diversity, which correlates with metabolic outcomes related to glucose homeostasis in individuals with overweight and mild obesity.

To prove this hypothesis, the following aims comparing chronic CE vs. BL were investigated:

Aim 1: Quantifying the gut microbiome at phyla and genus level.
Aim 2: Predicting metabolic functional profiling.
Aim 3: Correlation of gut microbiome with clinical and metabolic parameters related to glucose metabolism.

2 Materials and Methods

In this part, the process of the experimental study consisting of metabolic and Shotgun metagenomic analyses is explained. The list of materials utilized in this study is provided in the Appendix (Table S1 1).

Hypothesis I: Metabolic analyses

2.1 General study design

The study was carried out at the Institute of Endocrinology and Diabetes, University of Lübeck, within the Center of Brain, Behavior, and Metabolism (CBBM). The project received funding from the "Deutsche Forschungsgemeinschaft" (DFG) as part of the "Graduiertenkolleg" (GRK) 1957 Adipocyte-Brain Crosstalk program.

To examine the hypotheses, a cross-over, randomized clinical trial (RCT), within-subjects balanced study was designed. The schematic design is depicted in Figure 8.

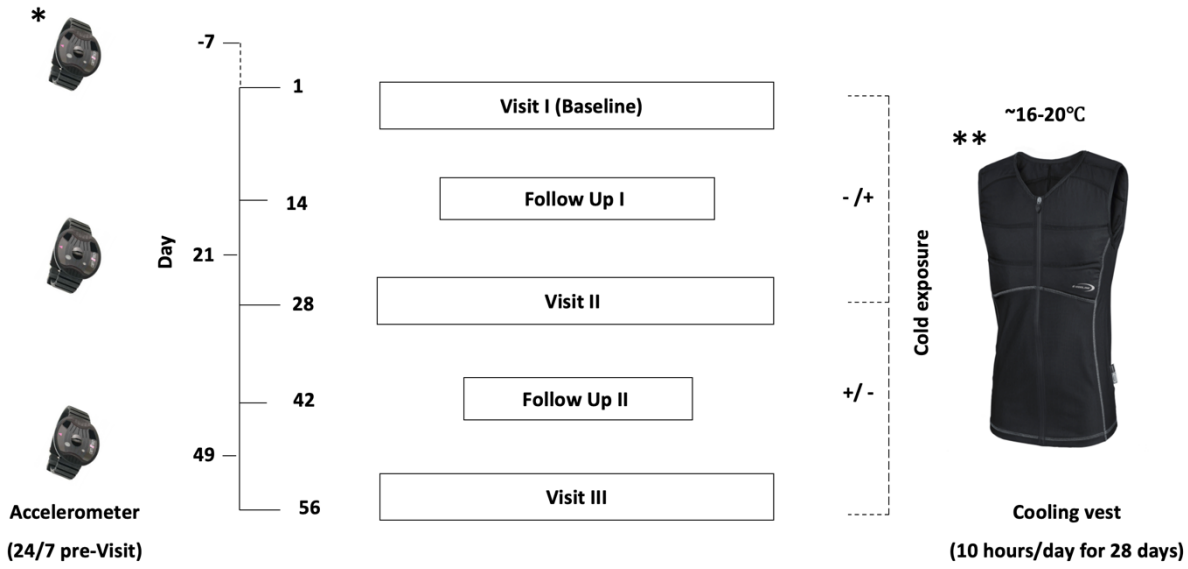

Figure 8. Scheme of the study design of the eCooling study.
The design consisted of a cross-over, randomized, balanced study with three experimental days and two subsequent follow-up periods, allowing for the comparison of interventions with each other.[2]

[2] *Image downloaded 12.10.2023 https://www.camntech.com/motionwatch-8/

The study spanned eight weeks and encompassed three measurement points: BL, post-CE, and post-TN, each separated by a four-week interval. In the BL experimental session, participants underwent different measurements without any intervention. Subsequently, the experimental session was conducted post-CE and post-TN. Two weeks after each main visit, a follow-up appointment took place. The order of wearing vests with CE in the entire cohort was previously established using a computerized randomization process. Half of the cohort commenced by wearing the vest under CE condition, i.e., wearing the activated vest, while the remaining half started wearing the vest under TN condition, i.e., wearing the non-activated vest for the first four weeks, after which they switched and continued to the other condition from the fifth to end of the eighth week.

2.2 Study cohort and criteria

Commencing in March 2020, the project unfortunately encountered delays attributable to the adverse effects of the COVID-19 pandemic and subsequent lockdowns in Germany. After the lifting of restrictions, the recruitment was initiated through a dual approach, involving the distribution of flyers throughout the city of Lübeck and its suburbs and the dissemination of emails to University of Lübeck students.

Recruitment commenced with a telephone screening, during which I provided a brief overview of the study, discussed potential risks, addressed queries, and clarified crucial points related to the study's inclusion and exclusion criteria. If the individual expressed interest and met the criteria, I forwarded the study details via email or post. Following the screening call, within one to three days, I reconnected with the interested potential participants. Upon verification of sustained interest, invitations for screening visits were forwarded.
All participants provided informed written consent, adhering to the principles outlined in the Declaration of Helsinki. The study received approval from the local Human Ethics Committee of the University of Lübeck (AZ 19-140). On a screening day, all subjects again were informed about the procedure of the study and experimental days and provided informed written consent, signed by all the participants before being included in the study. During the screening visit, height was measured using a stadiometer (Seca, Hamburg, Germany). Subsequently, weight by using a digital scale (Seca, Hamburg, Germany) and waist circumference were

**Image downloaded 12.10.2023 https://shop.e-cooline.de/en/powercool-sx3-shirt-vest_204_1190

obtained. BMI was calculated as weight in kilograms divided by height in meters squared (kg/m^2). A routine physical examination from the study doctor was performed, and an overnight fasted blood sample was collected. Additionally, a questionnaire about sleep schedules and the circadian clock, "The Munich ChronoType Questionnaire" (MCTQ) [204], was provided. Based on this questionnaire, individuals with night shift and/or sleep deprivation were excluded.

To ensure cohort homogeneity to the greatest extent possible, further stringent criteria were established. The exclusion criteria were the following: acute or chronic internal diseases, neurological diseases such as Morbus Parkinson and Epilepsy, current medication of any kind, anxiety disorders, alcohol, smoking or drug abuse, active competitive sports, or strenuous physical activity of more than five hours per week, special psychological and physical stressful situations. In addition, three months before and during the trials the participants may not be donated blood. Besides, three months prior to the start of the trial and during the study, the individuals were not allowed to participate in any drug trials, not to change their eating behavior, or start a new diet. Any other strict dietary regimen was an exclusion criterion of the study. Only men and women with an age between 18-50 years and a BMI between 25-35 kg/m^2 who met all the aforementioned criteria were enrolled in this study. Generally, the subjects were asked to maintain their diet and a normal day/night rhythm during the eight weeks of study.

2.3 Novel cooling protocol under free-living conditions

In this study, the Powercool SX3 ShirtVest - cooling vest (E-COOLINE, Ulm, Germany) has been utilized. These vests, provided by E-COOLINE cooling textile company, offer numerous advantages.

It is crucial to note that the aforementioned company played no role in influencing the scientific or clinical aspects of this project, including study design, participant recruitment, data analysis, and forthcoming publications.

The cooling vest is lightweight, easy to wear for everyday use, and can deliver 660 watts of cooling power. The upper section of the vest covers the chest and features 25 pads that can be activated by only using tap water. The lower portion, situated beneath the chest and over the kidney and intestine areas, is made of transparent netting fabric to remain dry during use.

Participants were directed to adhere to a cooling protocol: briefly immerse the padded part of the vest in tap water for a maximum of 1-2 seconds, gently press and roll the vest on a towel to remove excess moisture, allow it to air dry for a few seconds, wear a thin T-shirt underneath, and then don the vest for a continuous 10-hour period each day, commencing each morning upon waking.

The participants were then free to layer any clothing items such as a jacket, T-shirt, or other garments on top of the vest as they preferred. While participating in the study, they were encouraged to maintain their regular daily routines, which could include work, school, gym activities, and both indoor and outdoor leisure.

How does the cooling effect work? The padded section incorporates a specialized 3D-COOL material designed to absorb water molecules within its fibers. When exposed to body heat, the water gradually evaporates (Figure 9) leading to a temperature drop in the vest, cooling it down to approximately 16-18°C, and maintaining this refreshing effect for up to 20 hours.

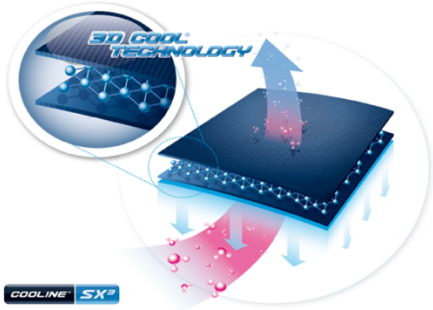

Figure 9. Representative image of the 3D technology incorporated in the cooling vest.
Water molecules adhere to the three-dimensional fibers within the insulated upper portion of the vest, subsequently evaporating as they absorb body heat, effectively lowering the skin temperature.[3]

Assessment of cold sensation and perception: To assess the effectiveness of the newly implemented cooling protocol within this study, I developed a self-reporting questionnaire regarding cold sensation and cooling perception of individuals. Participants were asked to answer the questions at the end of the final experiment for their response. The scale ranged

[3] Image downloaded 12.10.2023 https://shop.e-cooline.de/en/powercool-sx3-shirt-vest_204_119

from zero, denoting generally no sensation of cold, to 10, indicating an extreme sensation of old, as well as while wearing the vest no perception of cold to 10 extreme perceptions of cold. Subsequently, these questionnaires were evaluated.

In addition, participants were provided with a pre-prepared chart to monitor their consistent use of the vest. In the event of any circumstances preventing vest usage on a particular day, participants were requested to make a corresponding notation.

2.4 Assessment of environmental effect

To establish a control parameter for this study, the outside temperature was assessed. Outside temperature information was retrieved from the Blankensee station, accessible through the Deutscher Wetterdienst (DWD)[4]. The Blankensee station, being the closest one to Lübeck, consistently records hourly outside temperatures. This dataset included various weather-related metrics, including the daily average temperature (Tagesmittel der Temperatur; TMK). Throughout this study, it was imperative for the participants to predominantly remain in Lübeck without any planned travel to other countries, continents, or differing climate environments. In line with this, we downloaded outside temperature data for the seven days preceding each experimental day and calculated the mean temperature for those seven days. Subsequently, the average temperature between the different visits was compared.

2.5 Assessment of physical activity and sleep duration

Before each experimental day, participants received Motionwatch accelerometers to track their physical activity and sleep duration [205]. These wrist-worn devices monitored movement during daily activities. Participants were instructed to wear the device continuously on their non-dominant arms for seven consecutive days before the experimental session.

The device captured various parameters, including total physical activity and vigorous activity in 30-second intervals. Vigorous physical activity was defined as activities such as running, swimming, or carrying heavy loads, characterized by increased heart rate and rapid breathing [205]. The Motionwatch software (CamNtech, Fenstanton, UK) analyzed the intensity of

[4] https://www.dwd.de/DE/Home/home_node.html

physical activity based on predefined protocols: vigorous = 1000, moderate = 500, and low activity = 50 counts per minute. For this study, the average of total and vigorous activity was calculated over six days preceding the measurements, with this study setting a threshold of less than five hours per week. Sleep quality was assessed by calculating both actual and assumed sleep. Actual sleep denotes the total time spent in sleep according to the epoch-by-epoch wake/sleep categorization, while assumed sleep involves the total elapsed time between the "Fell Asleep" and "Woke Up" times.[5] The average duration of actual and estimated sleep was computed over seven nights preceding each experimental visit for subsequent statistical analysis.

2.6 Overview of the experimental day

24 hours before the experimental day, participants were instructed to abstain from engaging in any strenuous physical activity, consuming alcohol, caffeine, and chili (capsaicin) spicery. They were encouraged to prioritize restful sleep, aiming to retire to bed by 10:00 p.m.

All visits took place at the Metabolic Core Unit (MCU) of CBBM at the University of Lübeck. On the experimental days, riding a bike to the lab unit was not allowed and the participants were asked to take a bus or drive a car. Subjects arrived at the lab unit at 07:50 a.m., after 12 hours of fasting with the last meal before 08:00 p.m. of the previous night.

Upon the arrival of participants at the laboratory unit, their sleep duration and daily physical activity data were downloaded, exported to an Excel table (Microsoft Office 2018) using a 13.3" laptop (Lenovo, Beijing, China), and analyzed. If no indications of sleep deprivation or significant changes in sleep duration and physical activity were identified, the planned experiments proceeded as scheduled. In rare cases, where such indications were present, the participant was advised to return home, and a new appointment was arranged. An overview of the experimental days is illustrated in Figure 10.

[5] https://www.camntech.com/motionware-software/

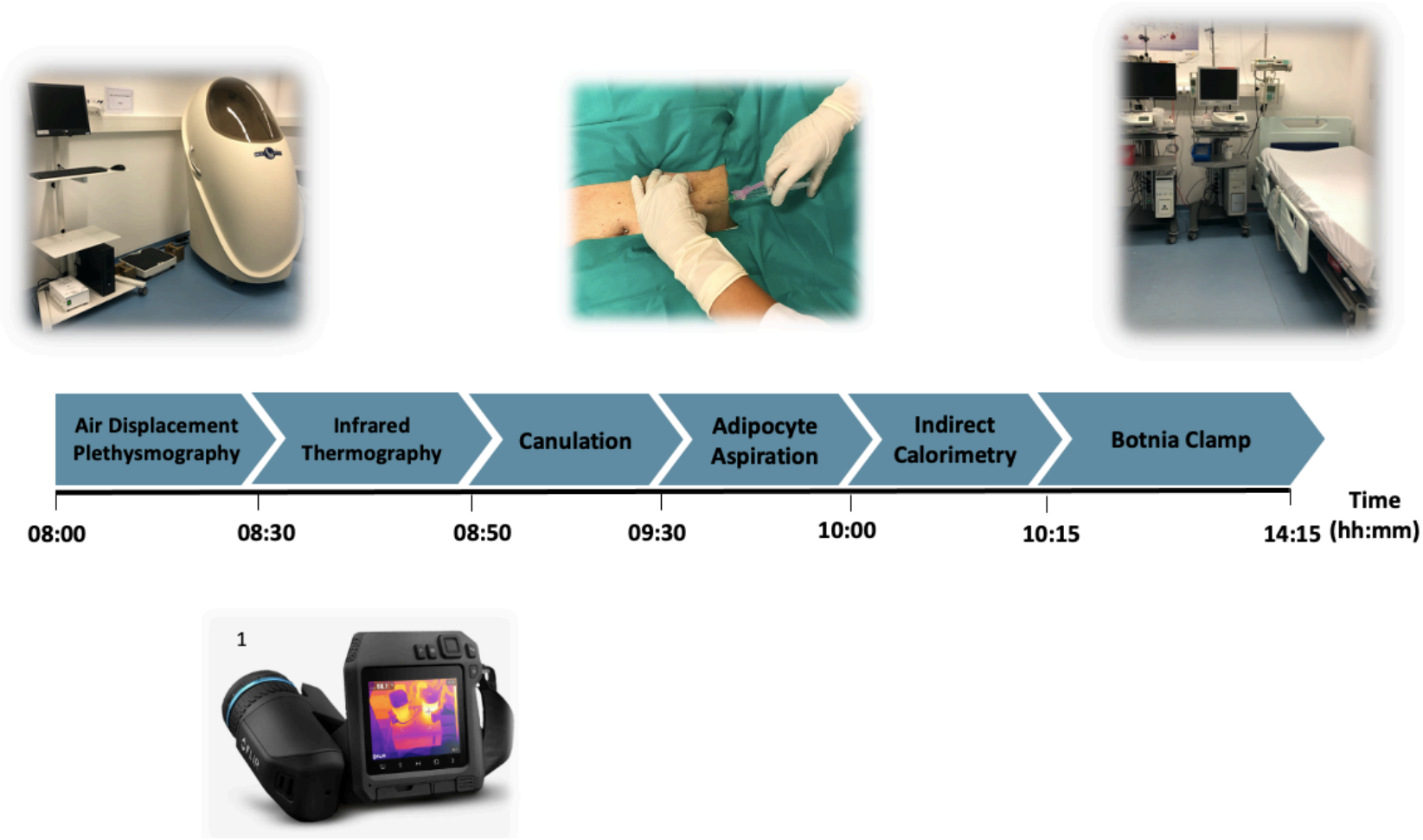

Figure 10. Design of an experimental day.

Individuals arrived after 12 hours of fasting at the lab unit. An experimental day took between seven to eight hours based on the length of observation time, which varied from one participant to another. Because of the COVID-19 hygiene restriction at the beginning of the study in 2020 and later in 2021, indirect calorimetry had to be excluded from the experimental protocol. [1] image downloaded October.2023 www.Flir.de.

Abbreviations: Air displacement plethysmography (ADP); infrared thermography (IRT).

2.7 Assessment of body composition

At 8:00 a.m., body composition was assessed using Air Displacement Plethysmography (ADP, BOD POD® device, COSMED, Werneck, Germany). ADP is a non-invasive, rapid, and repeatable method, that serves as a gold standard for measuring FM and fat-free mass (FFM) [206]. The process involves an airtight chamber equipped with sensors, where an individual's body volume (BV) is determined. The initial BM is measured, and then the subject, wearing minimal clothing (underwear/swimwear/bikini) to reduce interference, sits comfortably in the plethysmograph chamber. The measurement begins as the movable partition shifts to alter the chamber's volume and compress the air within. By measuring pressure changes resulting from air displacement, the individual's BV is calculated following Boyle's law (P1 x V1 = P1 x V1). Subsequently, body density (BD) was determined automatically based on weight and volume:

$$BD = BM / BV$$

BD is used to estimate FM and FFM. Based on Siri's equation, the percentage of FM has been automatically calculated:

$$\%FM = \left[\left(\frac{4.95}{BD}\right) - 4.50\right] \text{x } 100$$

After the body composition assessment, participants were given standard clothing (cotton pants and T-shirts, with the option to keep their socks). They sat in the experimental room for 20 minutes to acclimate, during which they filled out questionnaires before starting the next measurement. Notably, separate sets of standard clothing were provided for males and females and were laundered at 90°C after use.

2.8 Assessment of well-being and subjective appetite feelings

During the acclimation time, the participants received different questionnaires. The Short Form 36 Health Survey (SF-36) is a self-report questionnaire to assess a broad range of physical and mental health aspects with eight health concepts, including physical functioning, pain,

overall health, social functioning, and mental health [207]. For the present study, the questionnaire with the report of the previous four weeks has been chosen.

Additionally, a digital Visual Analog Scale (VAS) questionnaire on a 15.6” laptop (Fujitsu, Tokyo, Japan) was provided to answer. VAS is a tool for quantifying subjective traits or attitudes and is also used in research in the field of nutrition to assess the desire to eat, for instance, before and after an intervention in controlled studies. In this study, a computerized task with 38 items was employed to assess subjective feelings related to hunger and satiety, utilizing a 100-millimeter horizontal line ranging from 'not at all' to 'extremely' for respondents to express their agreement or the intensity of these sensations.

2.9 Assessment of brown adipose tissue activity

The subsequent step involved assessing BAT activity through the IRT technique. As explained in Chapter 1.4.2, activated BAT generates heat, which theoretically results in an elevation of skin temperature in the SCV region [208].

Preparation of the participant: Core body temperature was indirectly measured with an ear thermometer (Braun ThermoScan type 6014 Braun GmbH, Kronberg, Germany). Subsequently, the correct anatomical region of interest (ROI) was identified, a crucial step in assessing BAT activity. Following an established standard operating procedure (SOP), five anatomical points were marked using double-sided tapes and aluminum foil: the left and right superolateral apices, left and right acromioclavicular apices, sternal apex, and reference point below (Figure 11).

1: Superolateral apices

2: Acromioclavicular apices

3: Sternal apex

4: Reference point

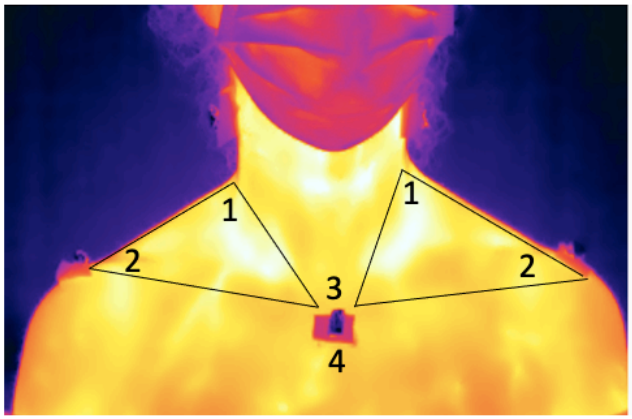

Figure 11. The anatomical points of the region of interest.
An example of the IRT image with marked anatomical points of a participant.
Abbreviations: Infrared thermography (IRT).

IRT imaging acquisitions*:* To facilitate thermal imaging acquisitions, participants were instructed to sit upright on a standard chair. The SCV regions needed to be free of, for instance, necklaces, hair, or clothes. Simultaneously, the camera FLIR T530 (FLIR Systems, Oregon, USA) was positioned perpendicularly to the participant's body. This setup maintained the camera lens at a consistent distance of one meter from the larynx while capturing both shoulders within its field of view on the screen. To achieve this, the camera's height was individually adjusted. The camera was calibrated, and the room temperature, humidity, and reflected temperature were documented and entered the camera. The skin emissivity was set constant at $\varepsilon = 0.98$. Imaging was taken for 10 minutes at 20-second intervals. During this procedure, the participants were asked to face the camera directly, breathe normally, and not move. Analysis of the thermal images succeeded using the software developed at the University of Nottingham (Nottingham, England) [105]. The marked anatomical points were used to draw and define the ROI by using a polygon function. Afterward, the mean and 95th percentile of SCV temperature of the ROI left and right as well as the reference point of 30 images for each experimental day were entered into an Excel table (Microsoft Office, 2018) for further analysis and comparing BL vs. post chronic CE.

2.10 Sampling of the subcutaneous adipocyte

In the next stage, participants reclined in a hospital bed, prepared for adipocyte aspiration. They were positioned at a 45°C upper body elevation with bent legs to relax the abdominal wall. Caudally and laterally, folio drapes were applied, and the abdominal skin was thoroughly disinfected. Local anesthesia Scandicain 2% (Aspen Pharmcarem, Durban, South Africa) was administered by the study doctor in a 2 x 4 cm area within Sherren's triangle. After a two-minute wait, adipocyte aspiration was initiated using a 14-gauge needle, extracting approximately 2 mL of subcutaneous adipocytes. I assisted the doctor during the procedure. The fat samples were washed with a 0.9% sodium chloride solution and subsequently were transferred in ribonucleic acid (RNA) protect, Tissue Reagent (Qiagen, Hilden, Germany) stored for five hours at 4°C and then moved to -80°C.

The participant then wore a compression bandage and lay recumbent for 30 minutes with a sand sack weight on the abdominal area. These samples are not analyzed in this doctoral project.

2.11 Assessment of hedonic hunger

The potential influence of cold-induced BAT activation on hedonic appetite control was examined through computer-based 'liking-wanting' tests [209], which assess food preferences. Liking refers to the subjective satisfaction derived from a rewarding experience while wanting signifies the craving for something pleasurable [210].

The test featured 42 food images categorized by calorie content (high vs. low) and taste (sweet vs. savory). Ratings for general liking and current wanting for each food item were collected on a scale from one (not at all) to five (very much). The order of these questions was randomized for each participant, and the test was administered in MATLAB R2019b (MathWorks, Massachusetts, USA) installed on a 15,6" laptop (Fujitsu, Tokyo, Japan), while participants were in bed, recovering from adipocyte aspiration. Data analysis focused on changes in liking and wanting for high-calorie-sweet, high-calorie-savory, and low-calorie foods post-intervention compared to BL.

2.12 Assessment of heart rate variability

Heart rate variability (HRV) was assessed during each experimental visit using a mobile heart rate monitor (Actiheart, Camntech, Fenstanton, UK), which was adhered to the participant's chest. After finishing the adipocyte aspiration, two standard electrocardiogram (ECG) pads were applied at the fourth intercostal space, facilitating easy attachment of the device. The first electrode was positioned at V1 and V2, while the second electrode was situated 10 cm away on the left side at V3 and V4 of the sternum and then the Actiheart was located and recorded at one-minute intervals (one-minute epochs) to investigate potential HRV changes following CE.

The HRV assessment explores the impact of CE on sympathetic and parasympathetic stimulation and regulation of the sinoatrial node [211]. In this assessment, the variance of intervals between heartbeats, heartbeat per minute low frequency (LF), and high frequency (HF), is measured. The raw data were extracted using software, and the mean of the aforementioned was calculated from a 10-minute timeframe during the steady state of HEC following chronic CE compared to BL. Generally, HF is indicative of parasympathetic nervous system activity, while LF represents SNS activity. The cut-off for these parameters is the following: $0.04 < LF < 0.15$ Hz and $0.15 < HF < 0.4$ Hz. An informative result concerning a healthy cardiovascular status is provided by a lower LF/HF ratio [212].

2.13 Assessment of β-cell function and insulin sensitivity

The subsequent procedure involved executing the Botnia clamp technique, following a standardized SOP. The initial step was cannulation, wherein the study doctor or nurse inserted two 18-gauge venous catheters (Vasofix Braunüle, B. Braun, Melsungen, Germany) into the antecubital fossa veins of both arms. On one hand, frequent blood sampling took place, and on the other, glucose and insulin infusions were administered. In instances of cannulation complications, a substitution involved the insertion of two 20-gauge venous catheters. However, this circumstance rendered the HEC technique unfeasible, restricting the procedure solely to IVGTT. Maintaining the patency of both intravenous lines is essential for the successful execution of the Botnia clamp procedure.

Generally, the Botnia clamp system comprises a glucose pump (Infusion pump fms, B. BRUAN, Melsungen, Germany), an insulin pump (Infusion pump fm, B. BRUAN, Melsungen, Germany), a Clamp-EKF diagnostic software (EKF Diagnostic, Barleben, Germany), and blood glucose analyzer (Biosen C-line, EKF Diagnostic, Barleben, Germany) (Figure 12).

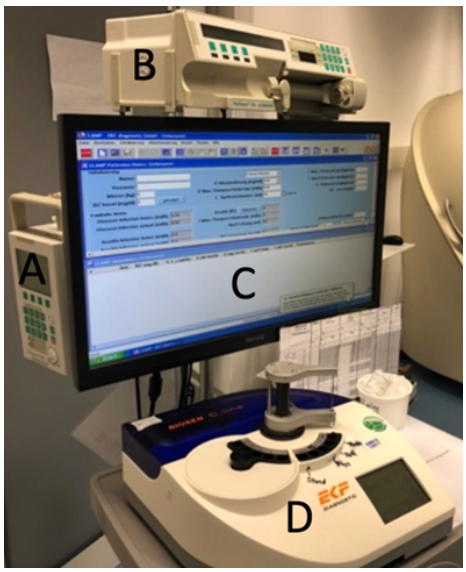

Figure 12. Overview of Botnia clamp system.
The Botnia clamp system consists of A) a glucose pump, B) an insulin pump, C) an installed software on a computer to calculate the insulin and glucose infusion rate during the measurement to maintain the plasma glucose concentration at the euglycemic level and D) a frequent blood glucose analyzer.
This system was used at MCU, Institute of Endocrinology and Diabetes, University of Lübeck.
Abbreviation: Metabolic Core Unit (MCU).

Participants were placed in bed in a comfortable spin condition, dressed the standardized clothing, and covered with a blanket to avoid shivering during the experiment at room temperature (21-22°C). Throughout the procedure, participants were regularly monitored, and they were asked at intervals whether they experienced any sensations of shivering. As previously mentioned, the Botnia clamp technique is a combination of IVGTT and HEC.

Intravenous glucose tolerance: Exactly seven minutes following the fasting blood draw and measuring the plasma glucose level, IVGTT began with the administration of an intravenous injection of 20% glucose solution (G20) bolus over three minutes from one catheter. The G20 volume was calculated regarding the individual's body weight (0.3 g/kg body weight). The blood drawing occurred at a two-minute interval till minute 10, afterward every 10 minutes till minute 60 (Figure 13).

The glucose concentrations from the first two samples were recorded in a pre-established Excel table (Microsoft Office, 2018), and their mean was calculated. If the SD between these two samples exceeded four plasma glucose units, a third blood sample was taken for analysis. The participant was allowed to use the restroom at the 50th minute of the IVGTT. Following the final blood sample collection at the 60th minute, the IVGTT was successfully completed, paving the way for the subsequent step, the HEC technique.

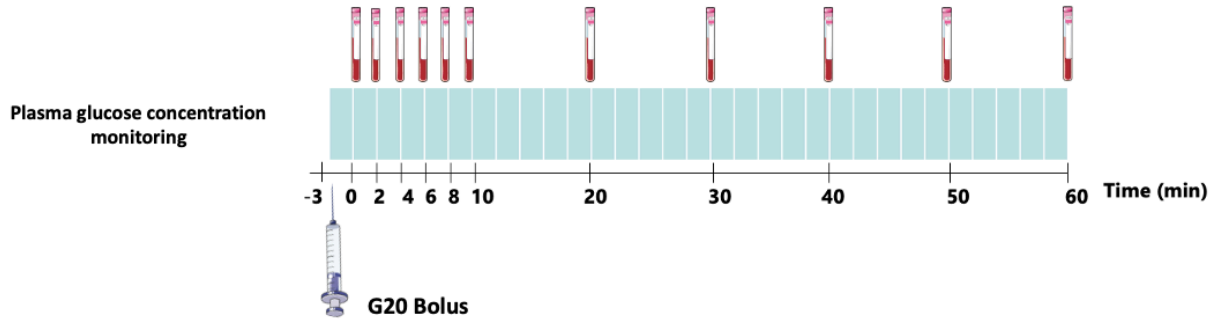

Figure 13. Illustration of IVGTT protocol.
Glucose bolus injection was administrated within the three-minute timeframe, followed by blood drawings based on the established protocol for 60 minutes.
Abbreviations: Intravenous glucose tolerance test (IVGTT); 20% glucose solutionl (G20).

Hyperinsulinemic euglycemic clamp: This part was started with a continuous and high insulin infusion rate (1.0 IU/kg body weight). The insulin stock was prepared from short-acting human insulin (Insuman Rapid, 100 I.E., SANOFI, Frankfurt am Main, Germany). To prevent hypoglycemia, the exogenous G20 pump was also activated. To maintain the plasma glucose level at an euglycemic level (85-95 mg/dl) a frequent assessment of plasma glucose concentration at an interval of five minutes and a variable GIR for two hours was required (Figure 14).

The mean of two blood samples was calculated and entered into the clamp system. If required, a third sample was also measured and entered in the Excel table (Microsoft Office, 2018). The software, based on the previously entered information and the plasma glucose level at that time, semi-automatically calculated the required GIR at that time point to maintain the plasma glucose at an euglycemic level. The entire procedure required meticulous control and oversight by the operator, who, in this case, was me.

Throughout the test, the participants were periodically queried about their well-being, and their status was continuously monitored.

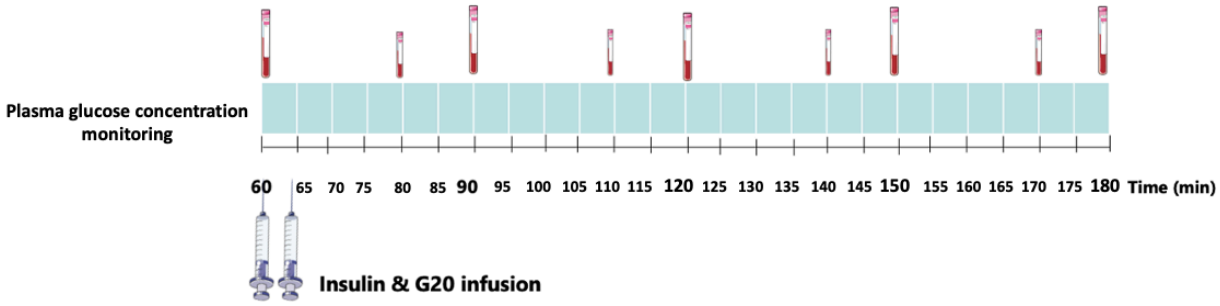

Figure 14. Illustration of the HEC protocol.
Insulin infusion starts at minute 60 and continuously continues for two hours. Collecting blood samples and assessing plasma glucose concentration at five-minute intervals. Variable glucose infusion maintains plasma glucose at the euglycemic level.
Abbreviations: Hyperinsulinemic euglycemic clamp (HEC); 20% glucose solution (G20)

After the final blood draw at minute 180 and measuring the plasma glucose concentration, the insulin pump was deactivated, participants continued to receive a 30-minute G20 infusion alongside a high carbohydrate meal, marking the commencement of the observation period. Subsequently, blood glucose levels were monitored at 10-minute intervals, following the

standard protocol. If, after 30 minutes, the plasma glucose concentration exceeded 120 mg/dl, the glucose pump was also deactivated.

Afterward, participants were required to remain in the laboratory unit for a minimum of one hour, during which plasma glucose concentrations were assessed every 15 minutes. Once glucose concentration at the euglycemic level stabilized, participants were permitted to leave the laboratory unit.

It is crucial to note that plasma potassium concentration was measured both before and after the HEC technique at the central laboratory of the University Hospital of Schleswig-Holstein (UKSH, Lübeck, Germany). Insulin plays a role in regulating potassium levels in the body. High insulin concentration promotes the movement of potassium from the bloodstream into cells and leads to hypokalemia, which can pose several risks including arrhythmias, muscle weakness, and fatigue. In consultation with the study doctor and guided by laboratory results, participants were administered a KALINOR effervescent tablet (containing 1.56 gr of potassium and 2.5 gr of citrate) when necessary.

Afterward, participants were granted permission to exit the laboratory unit. They were advised to refrain from engaging in sports on that day and to have a high-protein and carbohydrate dinner.

Analyses of Botnia clamp

Drawing from the literature, the analysis effectively calculated the following parameters:

Homeostatic Model Assessment of Insulin Resistance and Beta*:* These two common mathematical models based on plasma fasting glucose and insulin are used in diabetes research and clinical practice to assess insulin resistance, Homeostatic Model Assessment of Insulin Resistance (HOMA-IR) and Homeostatic Model Assessment of Beta-Cell (HOMA-Beta). HOMA-IR reflects insulin resistance and HOMA-Beta reflects β-cell function [213].

$$HOMA - IR = \frac{Fasting\ Plasma\ Inuslin\ x\ Fasting\ Plasma\ Glucose}{22.5}$$

$$HOMA - \text{Beta} = \frac{20\ x\ Fasting\ Plasma\ Insulin}{Fasting\ Plasma\ Glucose - 3.5}$$

First phase insulin response: Characterized by a rapid secretion of insulin directly after entering the glucose into the bloodstream, for instance after a glucose bolus during IVGTT. First phase insulin response (FPIR) is calculated from the sum of plasma insulin concentration of minutes 2, 4, and 6. This phase plays a crucial role in immediately controlling the rise of plasma glucose level after food intake.

***M*-value:** The main result of Botnia clamp as a direct indicator of insulin sensitivity which is calculated from GIR during the steady state of HEC using the following formula [170]:

$$M - Value = \frac{GIR\ \left(\frac{ml}{h}\right).200\ (\frac{mg}{l})}{Weight\ (kg).60\ (\frac{min}{h})}$$

Disposition index: Another parameter that reflects the β-cell and pancreatic function and ist calculated from the multiplication of insulin sensitivity and insulin secretion parameters [170]:

$$DI = FPIR\ x\ M - value$$

2.14 Biological assays

The laboratory analyses at the screening were determined at the external service laboratory facility LADR (LADR GmbH, Lübeck, Germany).

Serum insulin, C-peptide, cortisol, and ACTH in plasma were measured using IMMULITE 2000 ELISA System (Siemens Healthcare, Erlangen, Germany) in CBBM.

The assay's mean detection limits and coefficients of variation were for insulin 2.0 µUI/ml and ≤ 3.8%; C-peptide 0.3 ng/ml and ≤ 3.3%; cortisol 0.2 µg/dl and ≤ 5.2; ACTH 9.0 pg/ml and ≤ 8.7, respectively.

Hypothesis II: Shotgun metagenomic analyses

2.15 Microbiota analyses

This part succeeded as my research stay abroad project at Prof. Mirko Trajkovsi's laboratory within the Department of Cell Physiology and Metabolism, Medical Faculty, University of Geneva, Geneva, Switzerland.

2.16 Cohort and stool sampling

From the main cohort (n=18), a sub-cohort of 11 participants (mean ± SEM; age = 31.4 ± 2.5 years; BMI = 28.3 ± 1.1 kg/m^2) collected fecal samples at both BL and post-CE.

Participants were provided with stool sampling tubes, sterile gloves, and a standardized protocol outlining the collection of one gram of fecal matter, incorporating measures to prevent cross-contamination.

Inclusion criteria for the fecal sampling stipulated a minimum of one year since the last antibiotic uptake, no regular probiotics consumption, and no changes in diet and eating habits, as previously described (see Chapter 2.2). Participants were instructed to gather samples within 24 hours before the experimental day and preserve them at 4°C, bringing them on the day of the experiment. Upon arrival, fecal samples were promptly stored at - 80°C, awaiting future analysis.

2.17 DNA isolation and sequencing

DNA extraction was performed using the QIAGEN QIAamp PowerFecal Pro DNA kits (Qiagen GmbH, Gilden, Germany). Every step of the standard protocol was followed to isolate DNA from the fecal samples. Briefly, 250 mg of stool samples were prepared in PowerBead Pro Tube (Qiagen GmbH, Gilden, Germany), mixed in solutions, and vortexed to get homogenized. In the next step, the lysis buffer was added to the homogenized sample and incubated following the protocol to release DNA, lysate was transferred to the provided columns and filtered to bind the DNA to the columns. The last step was washing the columns and DNA elution to release and collect the DNA from the columns and stored at -20°C.

Subsequently, the DNA samples were sent on dry ice to the Max Planck Institute in Plön, Germany for library preparation and Shotgun DNA sequencing.

2.18 Shotgun metagenomic analyses

The metagenomics sequencing analyses, including quality control (QC), read mapping, and the following statistical analyses, were done under the supervision of Prof. Mirko Trajkovski and a Ph.D. student, at the Institute of Cell Physiology and Metabolism, University of Geneva, Switzerland. The raw sequencing data were quality-controlled using the "QC" module of ATLAS [214]. Using tools from the BBmap suite v37.78 (ANACONDA, Python, Wilmington, USA). Reads were quality-trimmed, and contaminations from the human genome were filtered out. The abundances of bacterial taxa were estimated using MetaPhlAn v4.0.6 [215] with default parameters. Similarly, the pathways and abundances were obtained using HUMAnN v3.6 [216] with default parameters. Briefly, HUMAnN quantifies the abundance of the genes by tallying the number of reads on the map to each gene. This step provides information on the relative abundance of various microbial genes within the community. Using the identified genes and their abundances was the next step, which reconstructs the metabolic pathways. It connects the dots between genes to form pathways, interfering with the potential functional capabilities of the microbial community. Afterward, HUMAnN normalizes the data to account for differences in gene length and other factors. The normalization enables comparisons between different samples or databases. Finally, visualization of the reconstructed pathways occurs. However, the accuracy of the results depends on the quality of the initial sequencing data and the comprehensiveness of the reference databases.

2.19 Statistical analyses

Following cannulation complications observed in half of the cohort post-TN experimental session, those data had to be omitted from the analysis. Consequently, the current study centered on comparing data between the BL and post-chronic CE stages for comprehensive analysis.

Statistical analysis was conducted using IBM SPSS Statistics 22 (IBM, Chicago, USA) and RStudio (R Core Team, Massachusetts, USA) was used to calculate the repeated measured correlation (rmcorr). Figures were prepared using GraphPad Prism (GraphPad, La Jolla, USA) and RStudio (R Core Team, Massachusetts, USA). Values are presented as mean ± SEM unless otherwise stated.

Initially, normality for each parameter was assessed using the Kolmogorov-Smirnov test. For comparisons between post-chronic CE and BL conditions, a paired student's t-test was employed if the data demonstrated normal distribution ($p > 0.05$) unless specified otherwise. In cases where the data deviated from normality ($p < 0.05$), a logarithmic transformation ($\log_{10}$) was applied before conducting the paired t-test. If $\log_{10}$ calculation was not feasible for certain values, such as those involving zero (e.g., subjective appetite), a Wilcoxon paired test was conducted to compare BL vs. post-chronic CE.

For parameters measured during the Botnia clamp, the area under the curve (AUC) was calculated using the trapezoidal rule. In the case of repeated measurements, ANOVA (intervention * time) with factors “intervention” (CE vs. BL) and “time” (60 minutes of IVGTT or 60 minutes of steady state) were considered.

The metagenomic statistical analysis was conducted in Python (Python Software Foundation, Wilmington, Delaware, USA). Relative abundances of both taxa and pathways were transformed to centered $\log_2$ ratios (Clr) after the multiplicative replacement of the zero values. Comparisons were done using the student’s paired t-test and Wilcoxon paired t-test (as implemented in scipy.stats.ttest_rel) and followed by the Benjamini-Hochberg procedure for *p*-values correction.

3 Results

This chapter presents the outcomes of the doctoral study, encompassing both metabolic and subsequent Shotgun metagenomic analyses.

Hypothesis I: Metabolic analyses

3.1 Participants characteristics

Eighteen Caucasian young participants (73% men), who were overweight or obese (Range: age: 30-48 years; BMI: 24.7-34.8 kg/m^2) were enrolled in this study. The anthropometric and clinical characteristics of the individuals are provided in Table 1. The mean ± SEM of measured raw data parameters is provided in the Appendix (Table S1).

All individuals successfully underwent BL and sub-chronic CE experimental sessions and completed the study. However, it is important to note that in half of the participants, the Botnia clamp procedure could not be carried out post-TN due to complications during cannulation. As a result, for statistical analysis and to enhance the robustness of the study's findings, the post-TN condition was excluded and the comparison focused solely on the BL session and before implementing any interventions, as the control condition, in comparison to post-CE.

Table 1. Characteristics of the cohort at baseline.

Parameter	Value
Gender (f/m)	5/13
Age (years)	31.4 ± 1.9
Weight (kg)	88.3 ± 2.9
Fat mass (%)	31.1 ± 1.9
BMI (kg/m^2)	28.5 ± 0.8
HbA1c (%)	5.2 ± 1.0
TSH (µE/ml)	1.6 ± 0.2

N = 18; Data are given in mean ± SEM or absolute values.

Abbreviations: Body mass index (BMI); hemoglobin A1c (HbA1C); thyroid-stimulating hormone (TSH).

3.2 No difference in outside temperature prior to experimental sessions

The outside temperature was collected and analyzed as a control parameter to evaluate its impact on the results. When comparing the mean of outside temperature seven days before each experimental session, no difference wobserved before CE compared to BL (p = 0.16) (Figure 15).

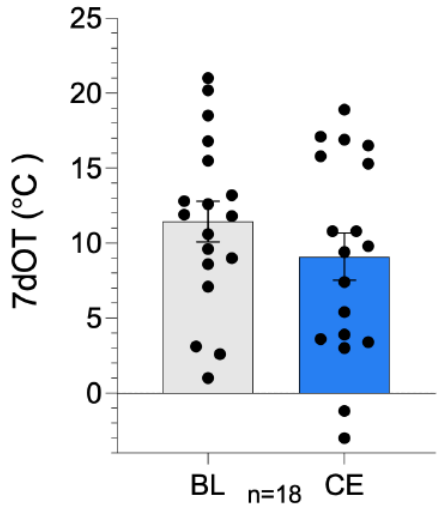

Figure 15. Outside temperature over experimental sessions.
The figure shows the average of outside temperature over seven days prior to measurements of CE compared to BL. Paired t-test.
Abbreviation: Mean of seven days outside temperature (7dOT); baseline (BL); cold exposure (CE).

3.3 No differences in environmental parameters across experimental sessions

As further control parameters, the temperature and humidity of the experimental room were recorded during the measurements. When comparing these two parameters between the CE and BL no differences were detected (p = 0.51; p = 0.29, respectively) (Figure 16A & B).

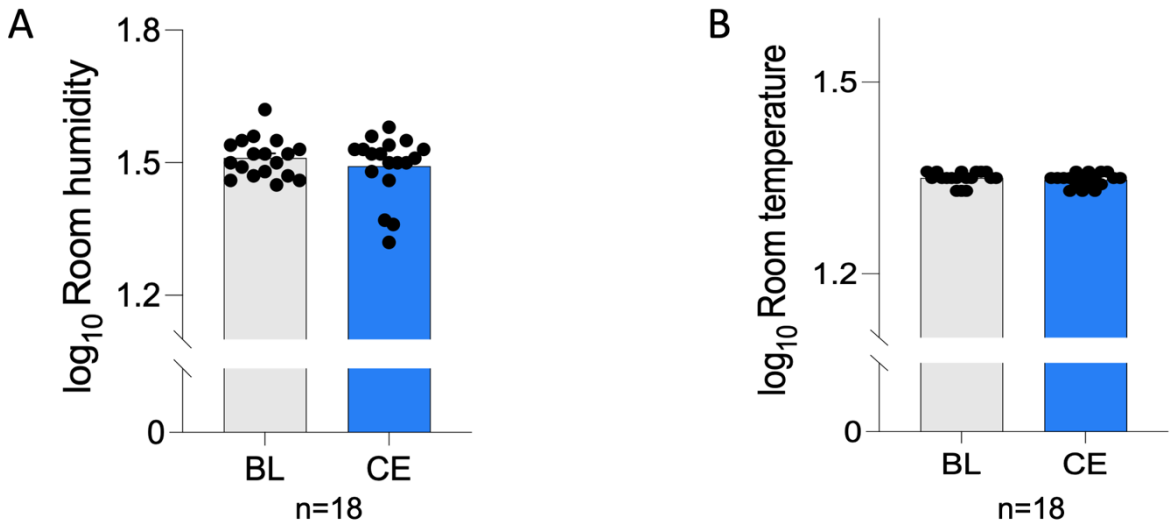

Figure 16. Environmental parameters across experimental sessions.
The figures show the average of A) $\log_{10}$ room temperature and B) $\log_{10}$ room humidity across the experimental sessions as after sub-chronic CE compared to BL. Paired t-test.
Abbreviations: Baseline (BL); cold exposure (CE).

3.4 No differences in sleep duration and physical activity prior to experimental sessions

In the investigation of two control variables, sleep duration, and physical activity means for these variables were calculated based on data collection seven and six days prior to each experimental session, respectively. Subsequently, a comparison between CE and BL conditions for both actual and log_{10} assumed sleep (p = 0.49; p = 0.89, respectively) (Figure 17A & B) as well as total and log_{10} vigorous physical activity (p = 0.51; p = 0.79, respectively) (Figure 17C & D), showed no differences between conditions.

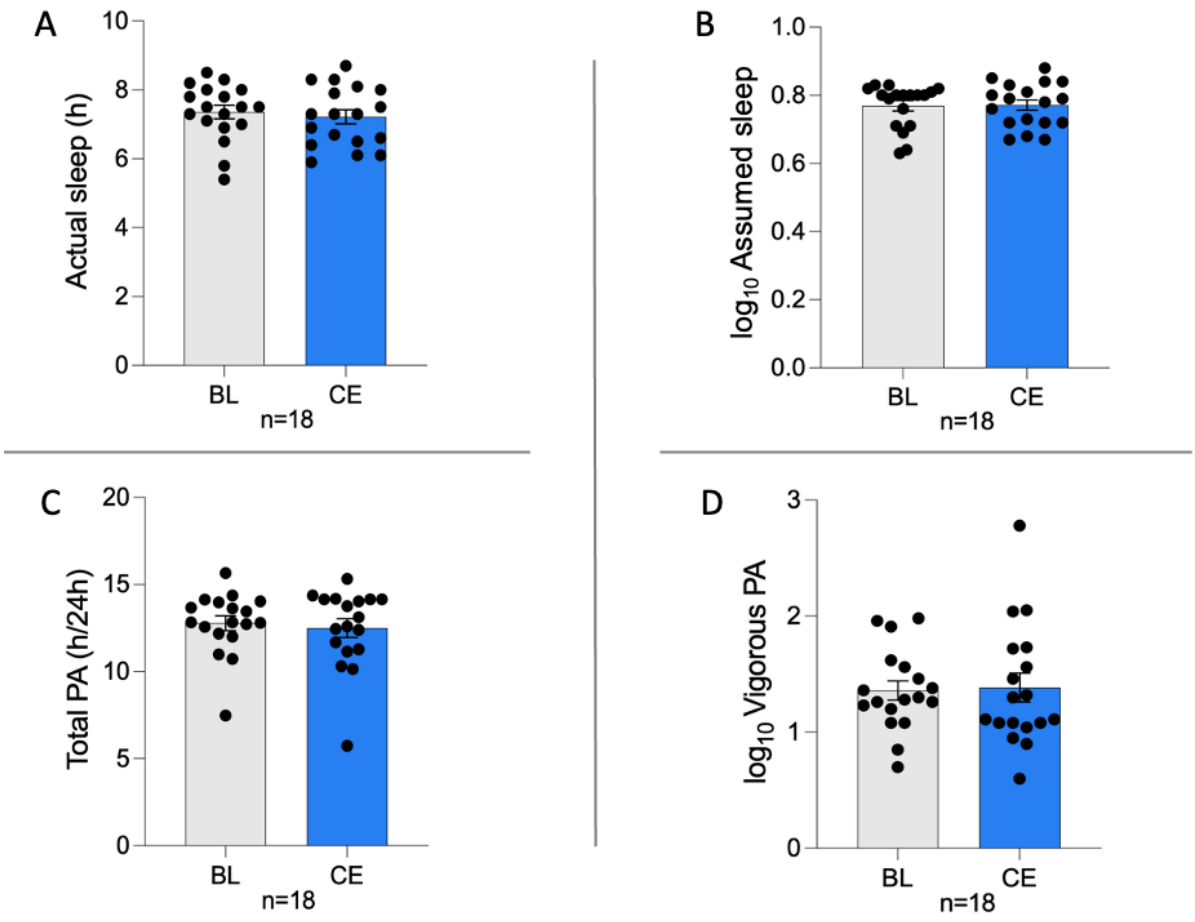

Figure 17. Sleep and physical activity prior to the experimental sessions.
The panels show A) average actual sleep duration; B) average log_{10} Assumed sleep; C) average total physical activity; and D) average log_{10} Vigorous physical activity post-chronic CE compared to BL. Paired t-test.
Abbreviations: Baseline (BL); cold exposure (CE).

3.5 Body composition remained unchanged after sub-chronic cold exposure

Following four weeks of daily CE compared to BL, the analysis of body composition parameters, encompassing body weight, relative FM, and log_{10} BMI, demonstrated no changes (p = 0.1; p = 0.34; p = 0.26, respectively) (Figure 18A & B & C).

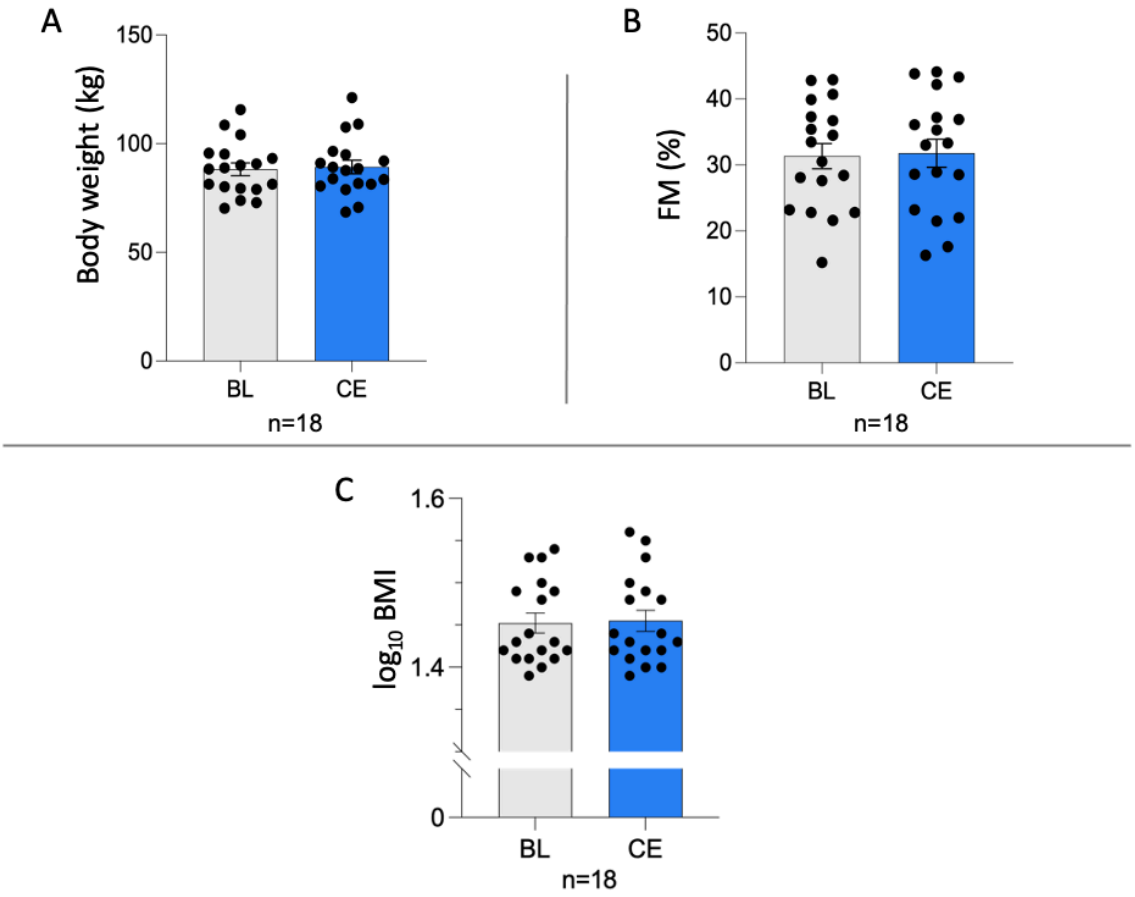

Figure 18. Body composition over the experimental sessions.
The panels show the body composition parameters, A) body weight; B) body FM; and C) log_{10} BMI after sub-chronic CE compared to BL. Paired t-test.
Abbreviation: Body mass index (BMI); fat mass (FM); baseline (BL); cold exposure (CE).

3.6 Brown adipose tissue activity remained unchanged after sub-chronic cold exposure, whereas the supraclavicular temperature decreased

Comparison of the mean and 95th percentile of the SCV skin temperature revealed a significant decrease of 0.2°C following CE compared to BL (p = 0.009; p = 0.003, respectively) (Figure 19A & B). However, body core temperature and reference skin temperature were measured as control parameters and found to remain unchanged between CE and BL (p = 0.24; p = 0.29, respectively) (Figure 19C & D).

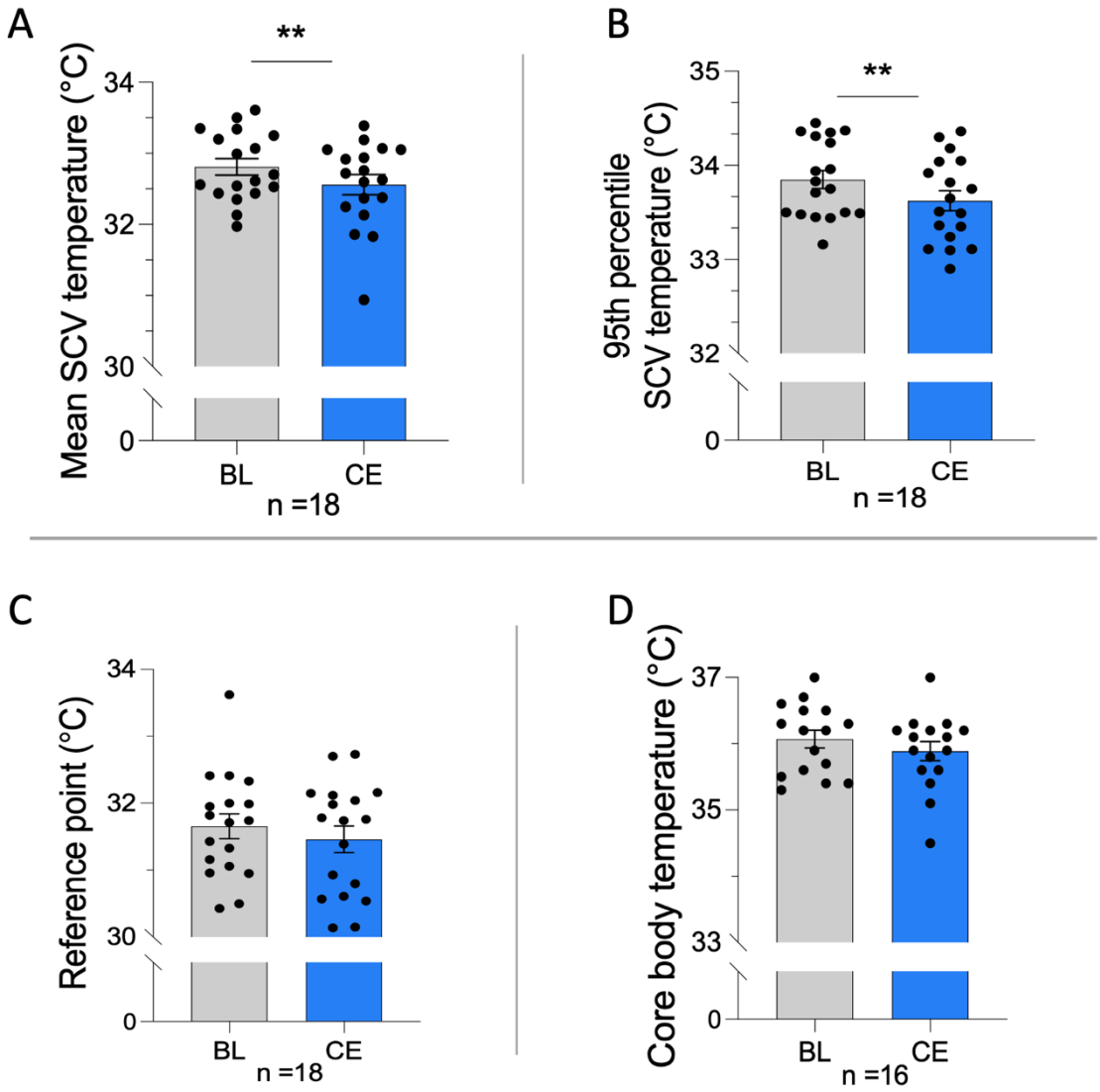

Figure 19. Indirect assessment of brown adipose tissue activity over the experimental sessions. Analysis of IRT images shows the mean of A) SCV temperature; B) 95th percentile SCV temperature; C) reference point skin temperature; and D) core body temperature post-chronic CE compared to BL (data of two participants are missing, therefore n =16). Paired t-test. **p < 0.01.

Abbreviations: Infrared thermography (IRT); Supraclavicular (SCV); baseline (BL); cold exposure (CE).

3.7 Glucose metabolism changed after sub-chronic cold exposure

At the basal level, the concentrations of plasma glucose, log_{10} Insulin, and log_{10} C-peptide were comparable between conditions (p = 0.31; p = 0.12; p = 0.43, respectively). The mean of the data is given in Table 2.

It is important to mention that the blood analysis of one subject had to be excluded due to error detection in serum samples, in which the value of insulin and C-peptide concentrations was lower than the biological range.

Table 2. Fasting glucose and hormone levels over the experimental sessions.

Parameter	n	BL	CE	p-Value
Glucose (mg/dl)	18	80.59 ± 1.15	80.07 ± 1.37	0.31
Log_{10} Insulin	17	0.62 ± 0.70	0.77 ± 0.94	0.12
Log_{10} C-peptide	17	0.13 ± 0.40	0.17 ± 0.43	0.43
Cortisol (µg/dl)	17	9.15 ± 0.94	9.68 ± 0.89	0.61
ACTH (pg/ml)	16	12.32 ± 1.67	13.36 ± 1.27	0.21

Data are given in mean ± SEM. The non-parametric data were transformed to log_{10}.
Abbreviations: Adrenocorticotropic hormone (ACTH); baseline (BL); cold exposure (CE).

Analysis of intravenous glucose tolerance test

Analysis of the plasma glucose during IVGTT showed a tendency towards decrease, although it failed to reach the level of significance and the log_{10} Insulin showed no changes (p = 0.08; p = 0.19, ANOVA intervention x time, respectively) (Figure 20A & B), while the log_{10} C-peptide increased (p = 0.01, ANONA intervention x time) (Figure 20C).

The concentration of plasma glucose over time decreased significantly (p < 0.001), while it remained unchanged between conditions (p = 0.42). The level of plasma log_{10} Insulin and log_{10} C-peptide increased over time (all p < 0.001). The concentration of log_{10} Insulin failed to reach the level of significance (p = 0.08), while the log_{10} C-peptide remained unchanged between conditions (p = 0.24).

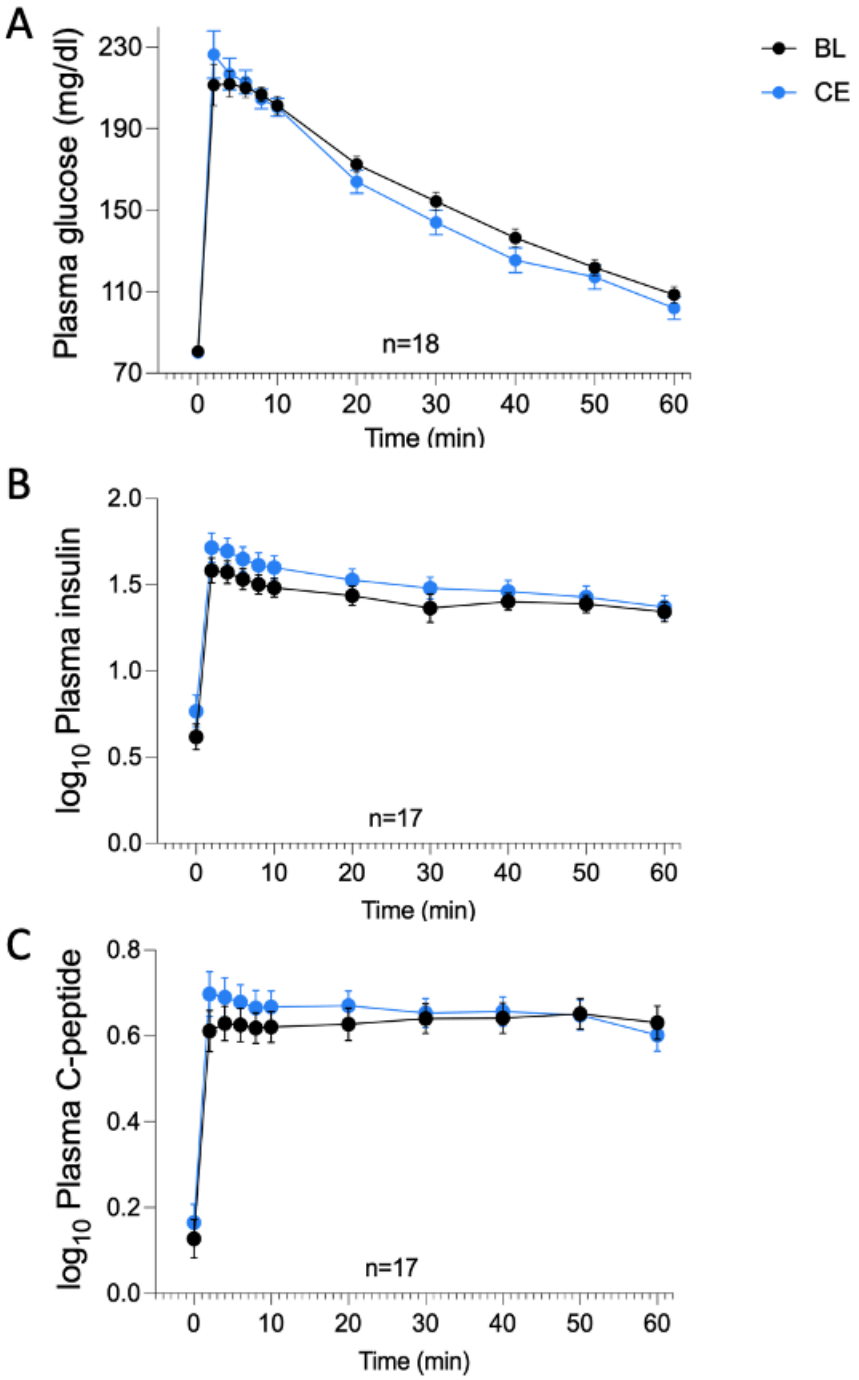

Figure 20. Glucose metabolism parameters during IVGTT over experimental sessions.
BL is indicated in black and post-chronic CE in blue. The figures show plasma A) glucose; B) $\log_{10}$ Insulin; and C) $\log_{10}$ C-peptide concentration over time during IVGTT after sub-chronic CE compared to BL. Repeated measures ANOVA (intervention x time).
Abbreviations: Intravenous glucose tolerance test (IVGTT); baseline (BL); cold exposure (CE).

The AUC for plasma glucose levels during IVGTT appeared lower when CE compared to the BL (9506.5 ± 221.3 vs. 9171.9 ± 277.7, respectively; $p = 0.059$), yet it failed to reach the level of statistical significance (Figure 21A). The AUC for $\log_{10}$ Insulin and $\log_{10}$ C-peptide during IVGTT remained unchanged between conditions ($p = 0.12$; $p = 0.39$, respectively) (Figure 21B & C).

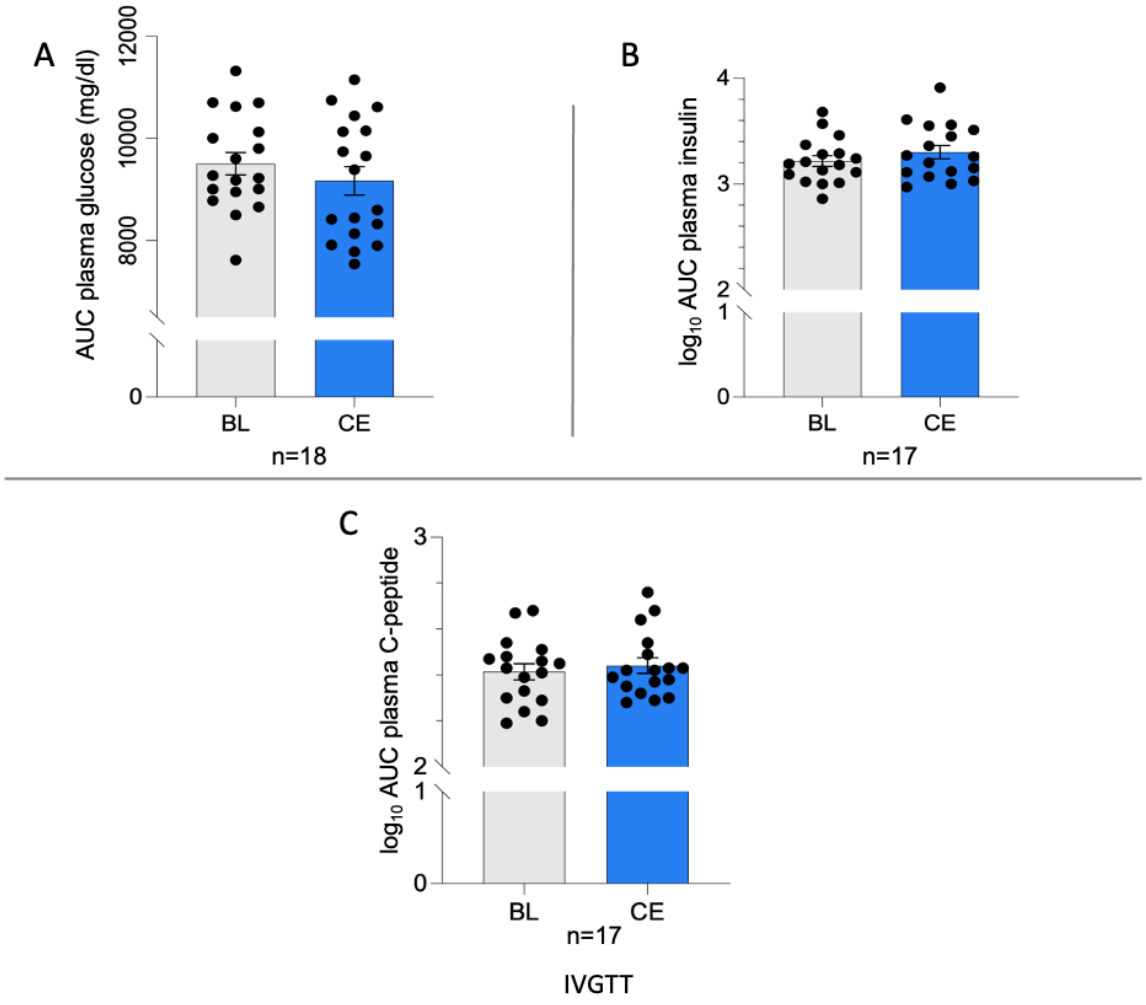

Figure 21. AUC of glucose metabolism-related parameters during IVGTT.
The panels show the AUC of plasma A) glucose; B) $\log_{10}$ Insulin; and C) $\log_{10}$ C-peptide during IVGTT after sub-chronic CE compared to BL. Paired t-test.
Abbreviations: Intravenous glucose tolerance test (IVGTT); area under the curve (AUC); baseline (BL); cold exposure (CE).

Analysis of hyperinsulinemic euglycemic clamp

Out of the 18 participants enrolled in this study, two participants could not complete HEC because of complications in cannulation. Furthermore, it was necessary to exclude one participant's insulin and C-peptide analyses due to a measurement error, resulting in a final number of n=15 included samples.

During the steady state of the HEC a significant change in GIR was noted (p = 0.014, ANOVA intervention x time) (Figure 22A). However, it is important to mention that this change did not display a consistent pattern. GIR was higher after CE at minutes 120, 160, and 170, while it was lower at minutes 140 and 180. The concentration of GIR changed over time ($p < 0.001$). Nevertheless, no changes between conditions were observed (p = 0.96) as CE was compared to BL.

During the steady state of HEC, the $\log_{10}$ plasma insulin didn't change (p = 0.50, ANOVA intervention x time). Its concentration failed to reach the level of significance over time and between conditions (p = 0.057; p = 0.058, respectively).

Furthermore, it was observed that the serum C-peptide concentration remained unchanged during the steady state (p = 0.47, ANOVA intervention x time) (Figure 22B). Although there was a significant increase in C-peptide levels over time (p = 0.005), there were no changes between the CE and BL conditions (p = 0.58).

Additionally, there were no changes in AUC for GIR and the $\log_{10}$ AUC of the C-peptide concentration when comparing CE to BL (p = 0.98; p = 0.73, respectively) (Figure 22C & D).

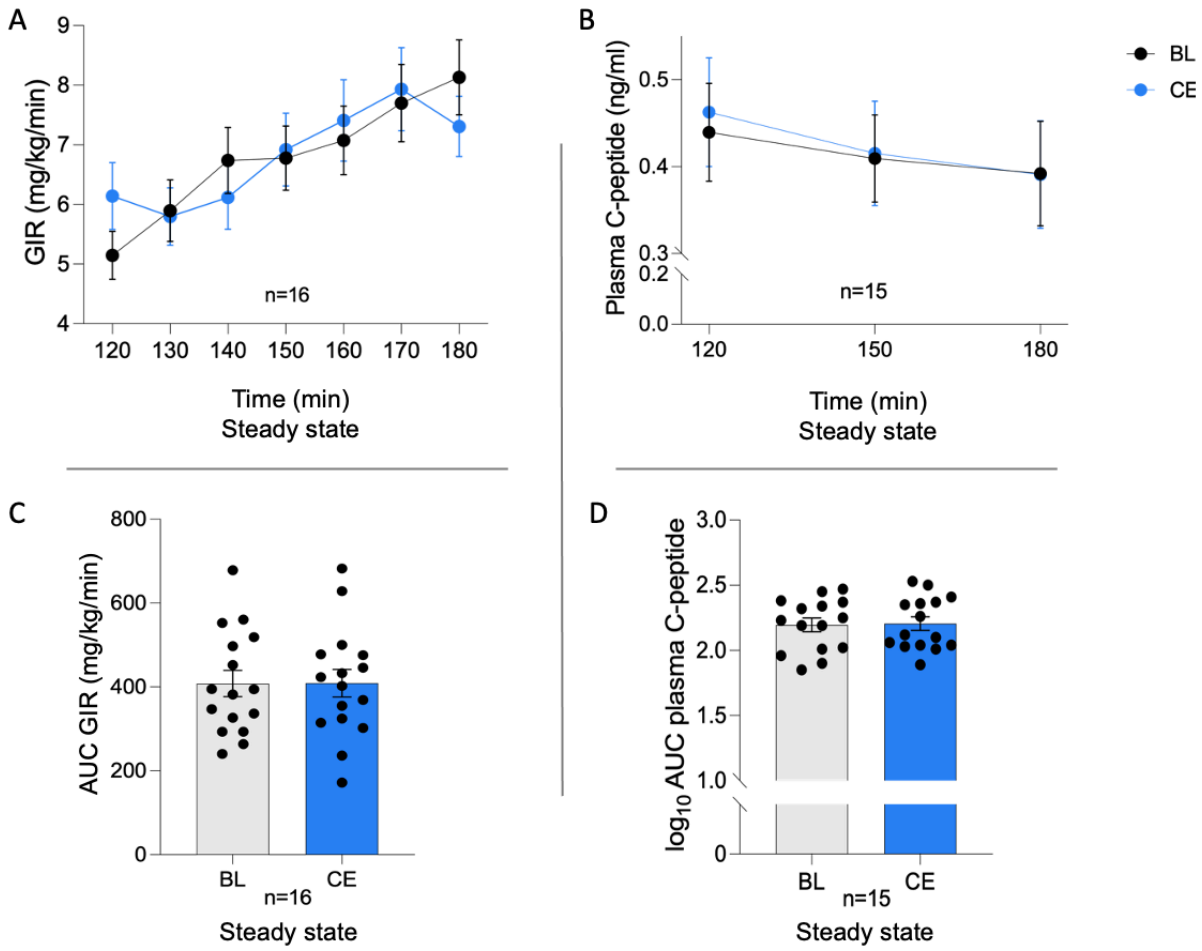

Figure 22. GIR and C-peptide concentration during the steady state of HEC over experimental sessions.

BL is indicated in black, and post-chronic CE in blue. The panels show A) GIR; and B) C-peptide concentration over the steady state of HEC post-CE compared to BL. Repeated ANOVA (intervention x time). Additionally, C) AUC of GIR; and D) $\log_{10}$ AUC of C-peptide during steady state post-CE compared to BL. Paired t-test.

Abbreviations: Glucose infusion rate (GIR); hyperinsulinemic euglycemic clamp (HEC); area under the curve (AUC); baseline (BL); cold exposure (CE).

No changes were observed when comparing the total GIR post-chronic CE to the BL ($p = 0.78$) (Figure 23A). Additionally, *M*-value remained unchanged between conditions ($p = 0.99$) (Figure 23B).

A significant increase of 45% in the $\log_{10}$ FPIR was observed after sub-chronic CE when compared to the BL ($p = 0.01$) (Figure 23C).

Furthermore, the Disposition index revealed a statistically significant increase after sub-chronic CE vs. BL ($p = 0.03$) (Figure 23D).

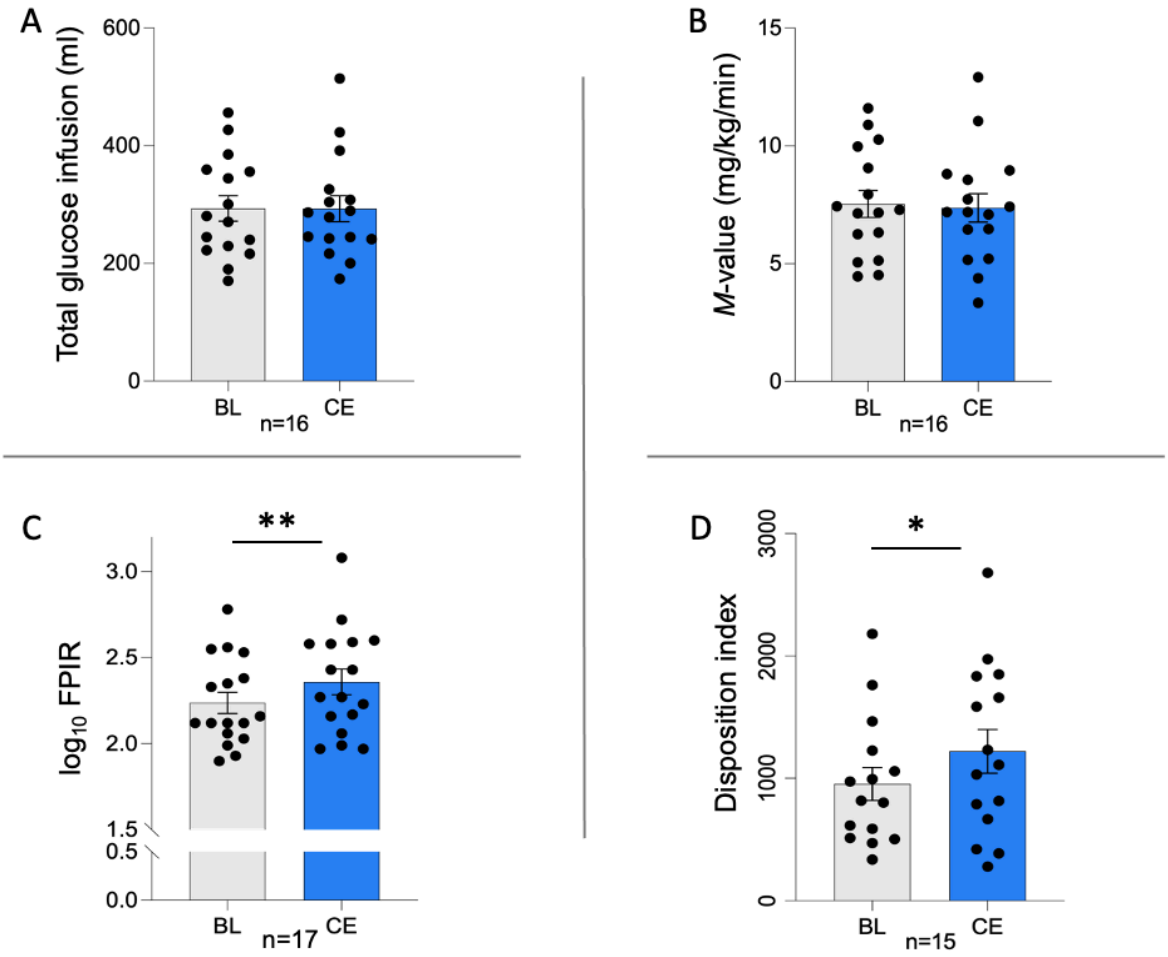

Figure 23. Insulin sensitivity and β-cell function over experimental sessions.
The panels show A) the total glucose infusion HEC; B) the *M*-value during steady state; C) the FPIR during IVGTT; and D) the Disposition index after sub-chronic CE compared to BL. Paired t-test. *$p < 0.05$; **$p < 0.01$.

Abbreviations: Hyperinsulinemic euglycemic clamp (HEC); First phase insulin response (FPIR); intravenous glucose tolerance test (IVGTT); baseline (BL); cold exposure (CE).

Log_{10} HOMA-IR was not different between conditions (p = 0.31) (Figure 24A). However, log_{10} HOMA-Beta (p = 0.06) showed an 8.7% tendency towards increase, yet it failed to reach the level of significance after sub-chronic CE vs. BL (Figure 24B).

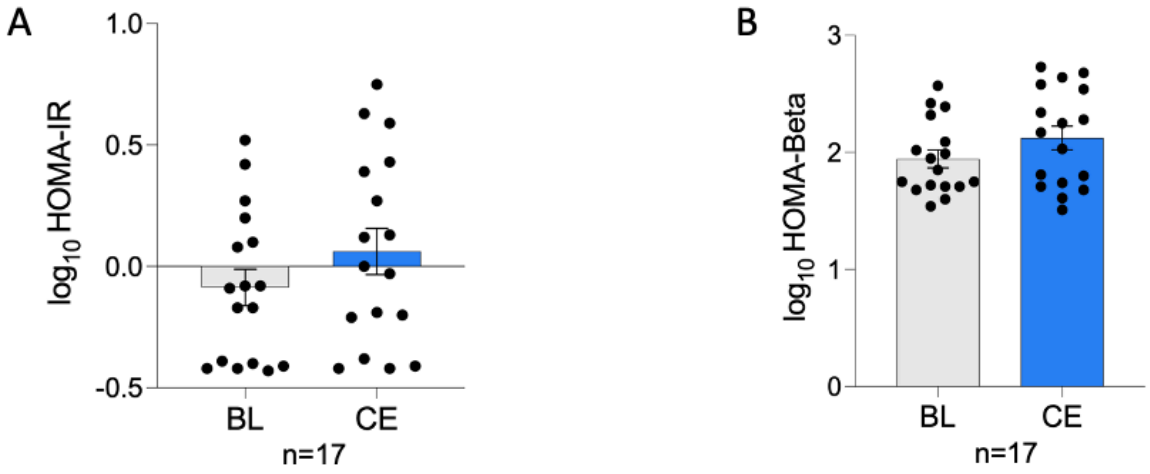

Figure 24. Insulin resistance and β-cell function over experimental sessions.
The figures show A) log_{10} HOMA-IR; and B) log_{10} HOMA-Beta after sub-chronic CE compared to BL. Paired t-test.
Abbreviations: Homeostasis Model Assessment-Insulin Resistance (HOMA-IR); Homeostasis Model Assessment-Beta Cell Function (HOMA-Beta); baseline (BL); cold exposure (CE).

3.8 Sympathetic and parasympathetic regulation remained unchanged after sub-chronic cold exposure

The initial examination of stress hormone concentrations at the basal level revealed no changes in cortisol and ACTH levels after sub-chronic CE when compared to BL (p = 0.68; p = 0.43, respectively) (Table 2). It should be noted that data from one participant for cortisol analysis and data from two participants for ACTH analysis had to be excluded due to measurement errors, therefore the final number of included samples was n=17 and n=16, respectively.

Analyses of Intravenous Glucose Tolerance Test

Cortisol and ACTH concentration during IVGTT showed no changes (p = 0.18; p = 0.78, ANOVA intervention x time, respectively) (Figure 25A & B).

Moreover, the concentration of these hormones over time (p = 0.21; p = 0.28, respectively), and between conditions (p = 0.45; p = 0.21, respectively) remained unchanged.

The AUC of cortisol and ACTH showed no changes between conditions (p = 0.40; p = 0.41, respectively) (Figure 25C & D).

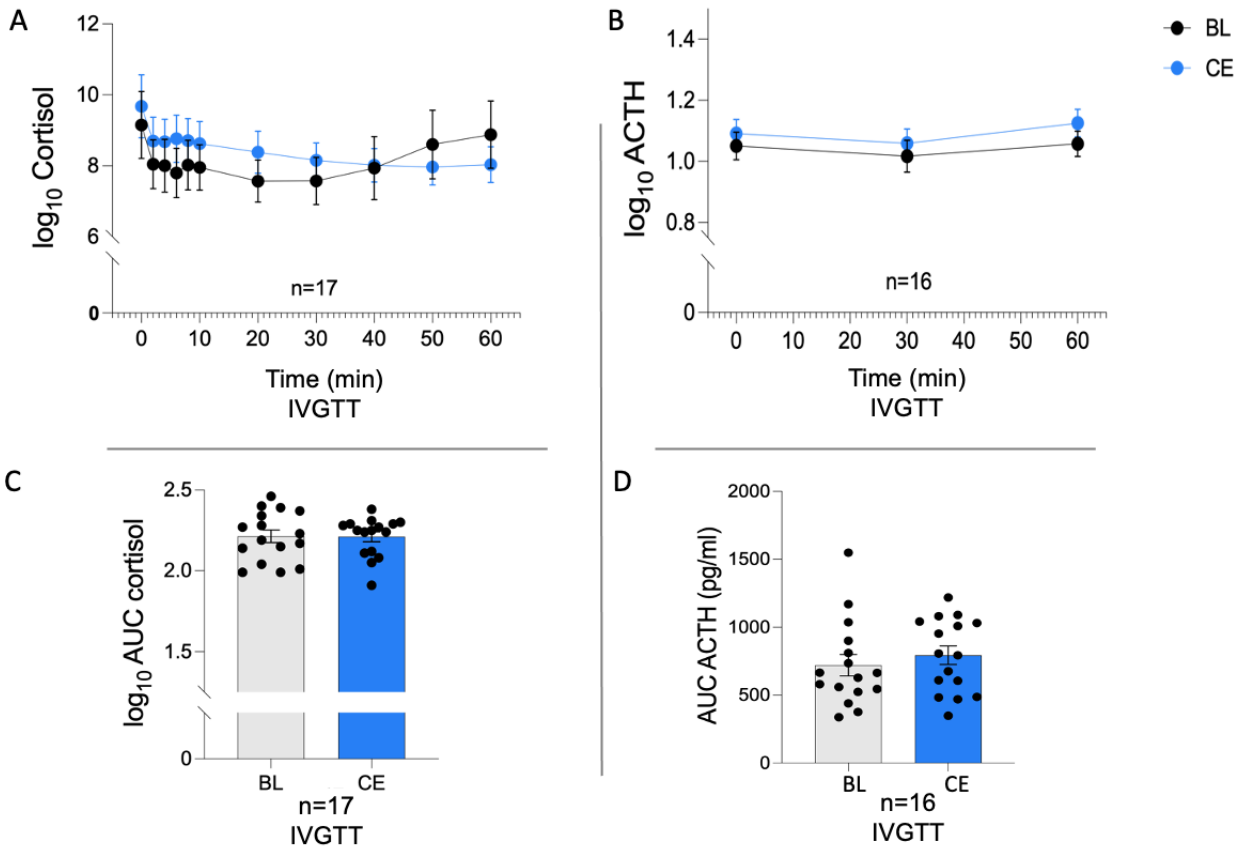

Figure 25. Stress hormone levels during IVGTT across experimental sessions.
BL is indicated in black, and post-chronic CE in blue. The panels show the concentration of A) log_{10} Cortisol; and B) log_{10} ACTH during IVGTT after sub-chronic CE compared to BL. Repeated measures ANOVA (intervention x time).
Additionally, the rest of the figures show C) log_{10} AUC cortisol; and D) AUC ACTH during IVGTT as post sub-chronic CE compared to BL. Paired t-test.
Abbreviations: Intravenous glucose tolerance test (IVGTT); adrenocorticotropic hormone (ACTH); area under the curve (AUC); baseline (BL); cold exposure (CE).

Analysis of hyperinsulinemic euglycemic clamp

From 16 participants who completed HEC, the blood analyses of one cortisol and two ACTH had to be excluded due to a measurement error.

The concentration of log_{10} Cortisol and ACTH during steady state did not show any changes (p = 0.26; p = 0.39, ANOVA intervention x time, respectively) (Figure 26A & B). Moreover, the concentration of cortisol and ACTH over time (p = 0.24; p = 0.14, respectively) and between conditions (p = 0.12; p = 0.48, respectively) remained unchanged.

Upon examining the AUC of the abovementioned parameters during a steady state, the concentration of cortisol and ACTH did not change between conditions (p = 0.13; p = 0.45, respectively) (Figure 26C & D).

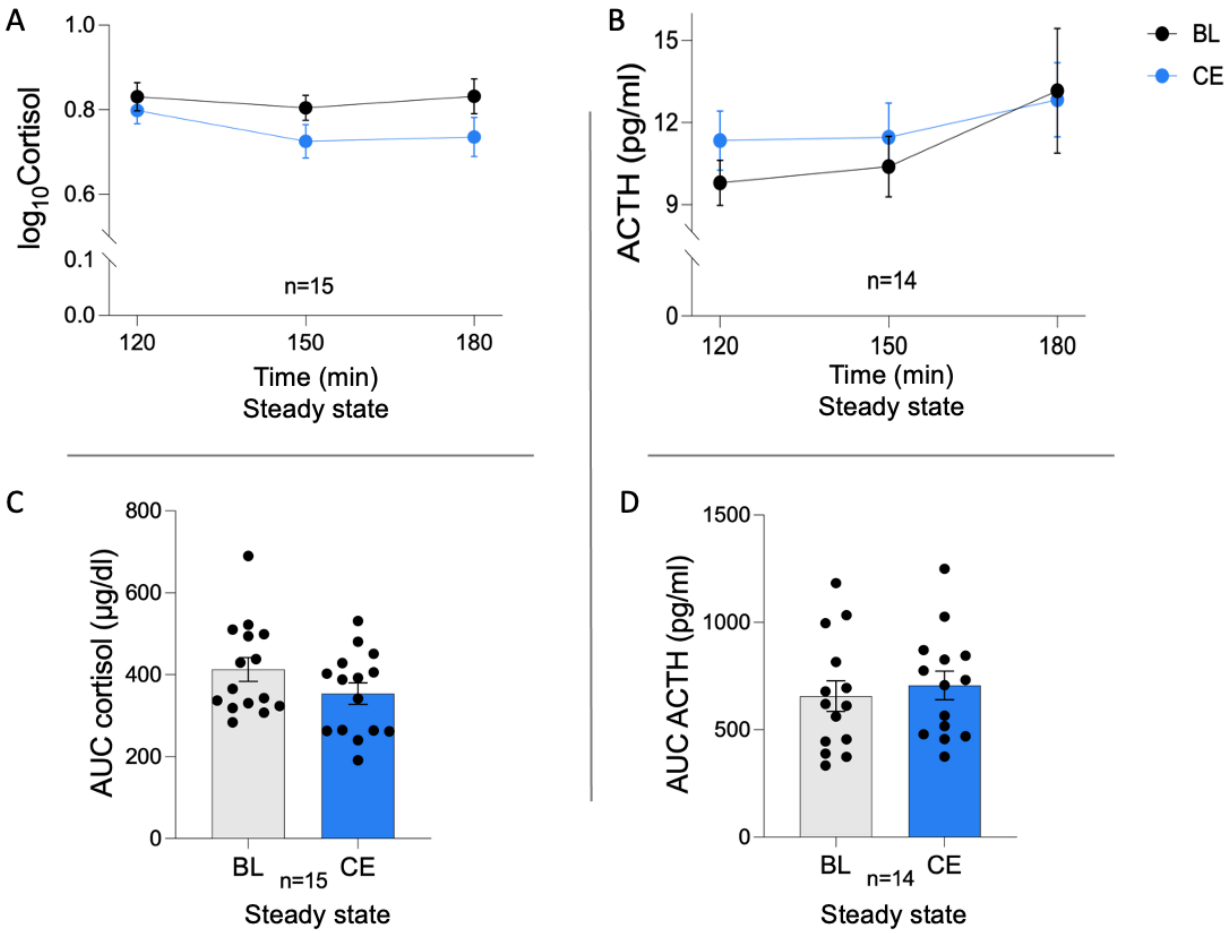

Figure 26. Stress hormone level during steady state across experimental sessions.
BL is indicated in black, and post-chronic CE in blue. The panels show the concentration of A) log_{10} Cortisol; and B) ACTH over time during steady state of HEC as post sub-chronic CE compared to BL. Repeated measures ANOVA (intervention x time). Furthermore, the figures show the AUC of C) cortisol level; and D) ACTH concentration during steady state between the conditions. Paired t-test.

Abbreviations: Adrenocorticotropic hormone (ACTH); hyperinsulinemic euglycemic clamp (HEC); area under the curve (AUC); baseline (BL); cold exposure (CE)

3.9 Heart rate variability remained unchanged after sub-chronic cold exposure

To investigate the impact of chronic mild CE as a stress factor on the SNS and parasympathetic nervous system, HRV parameters were analyzed during the steady state of HEC. No changes were observed in average heart rate, interbeat intervals, or LF/HF ratio (p = 0.51; p = 0.49; p = 0.94, respectively) (Figure 27A & B & C).

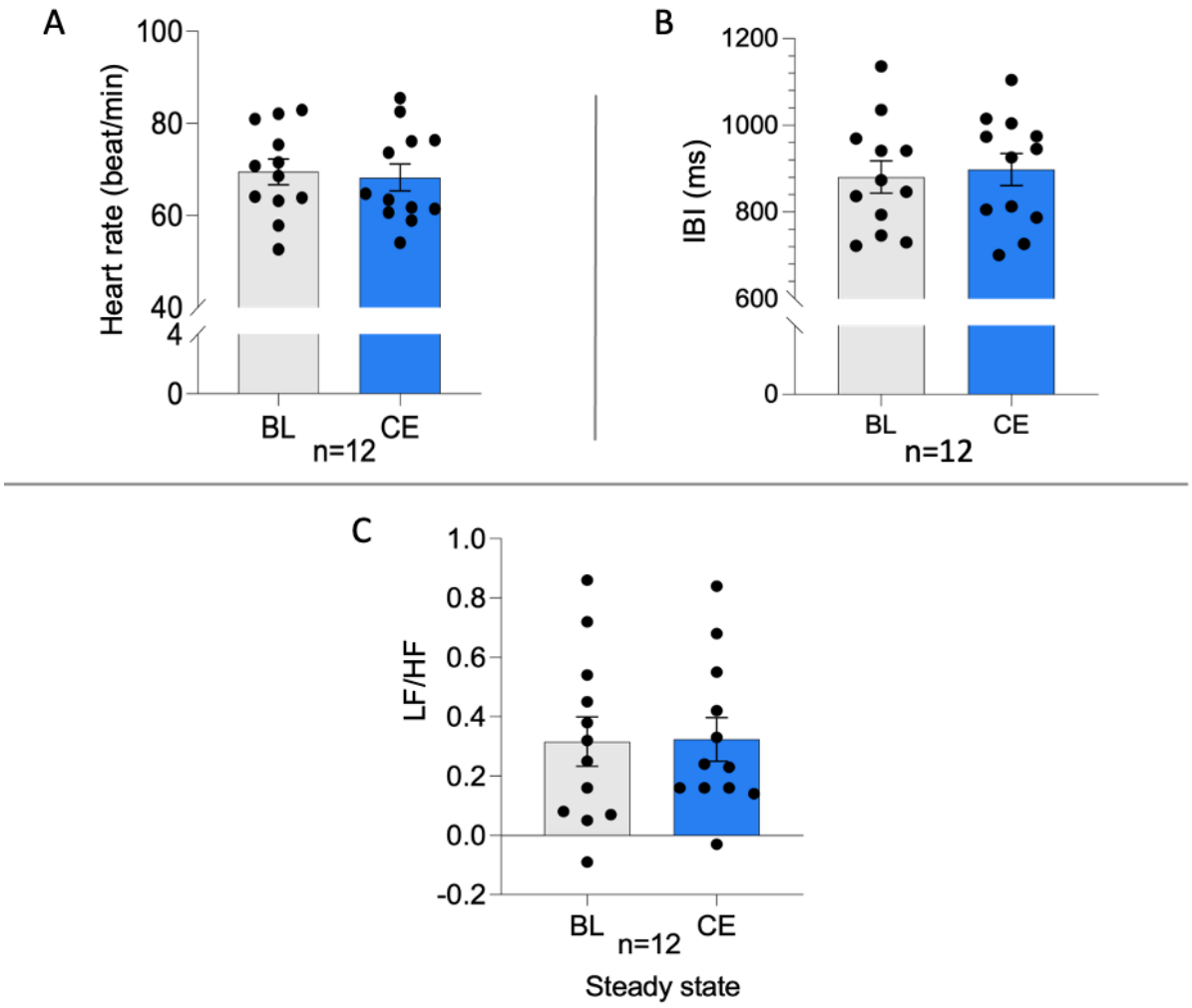

Figure 27. HRV across the experimental sessions.
The panels represent the analysis of the 10 minutes of HRV during steady state A) average of heart rate; B) average of IBI; and C) $\log_{10}$ HF/LF ratio after sub-chronic CE compared to BL. Paired t-test. Data from only 12 participants are available and readable.
Abbreviations: Heart rate variability (HRV); interbeat interval (IBI); low frequency (LF); high frequency (HF); baseline (BL); cold exposure (CE).

3.10 Subjective feelings of appetite increased significantly after sub-chronic cold exposure

Analyzing the VAS questionnaire revealed that the sensation of appetite in the early morning exhibited a significant increase after sub-chronic CE compared to the BL (23.78±5.06 vs. 31.67±4.75, respectively; $p = 0.04$) (Figure 28).

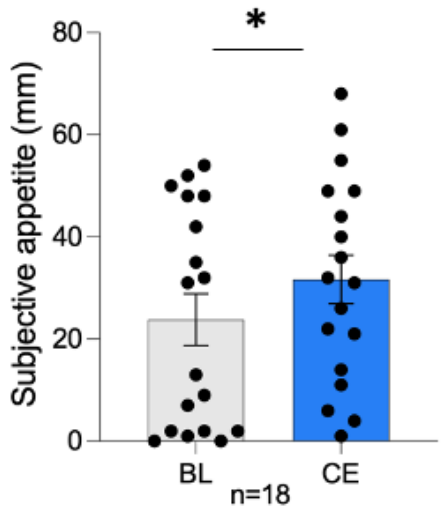

Figure 28. Subjective feeling of appetite across experimental sessions.
The figure shows the subjective feeling upon arrival in the lab unit after sub-chronic CE compared to BL. Wilcoxon paired test. *$p < 0.05$.
Abbreviations: Baseline (BL); cold exposure (CE).

3.11 Physical and mental competence remained unchanged after sub-chronic cold exposure

Analysis of the SF-36 questionnaire revealed, that no changes in the log_{10} Physical component score (PCS) after sub-chronic CE compared to BL (p = 0.51) were observed, whereas the log_{10} Mental component score (MCS) was higher after sub-chronic CE (1.699 ± 0.007 vs. 1.710 ± 0.010, respectively; p = 0.08), yet it failed to reach the level significance between conditions (Figure 29A & B).

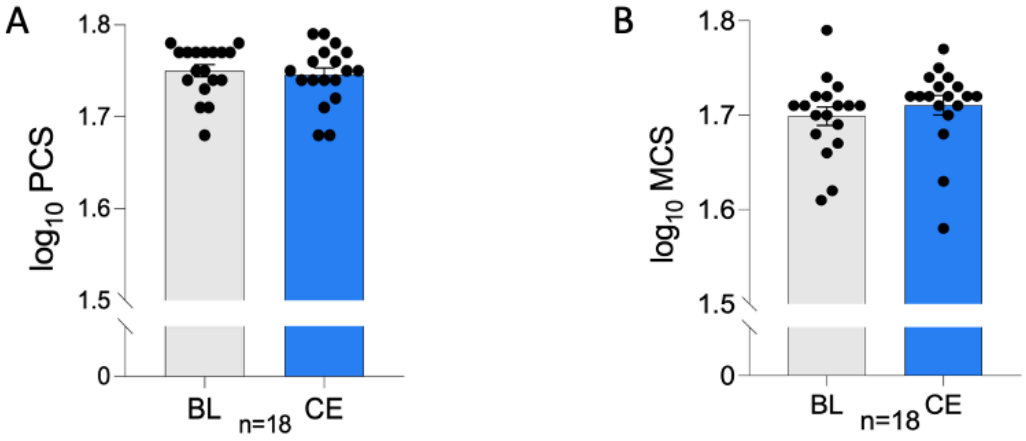

Figure 29. Physical and mental components over experimental sessions.
The figures show A) log_{10} PCS and B) log_{10} MCS after sub-chronic CE compared to BL. Paired t-test.
Abbreviations: Physical component score (PCS); mental component score (MCS); baseline (BL); cold exposure (CE).

3.12 Motivation and pleasure for food remained unchanged after sub-chronic cold exposure

The analysis of any changes in wanting or liking for high-caloric-sweet, high-caloric-savory, and low-caloric showed no differences following four weeks of chronic CE compared to BL. The results of the analysis are given in Table 3.

Table 3. Food desire over the experimental sessions.

Parameter	BL	Post-CE	*p*-value
Liking			
High calorie sweet	3.15 ± 0.17	3.43 ± 0.21	0.26
High calorie savory	3.38 ± 0.13	3.69 ± 0.17	0.11
Low calorie	3.69 ± 0.17	3.53 ± 0.14	0.18
Wanting			
High calorie sweet	2.77 ± 0.22	2.89 ± 0.21	0.51
High calorie savory	3.39 ± 0.23	3.41 ± 0.22	0.56
Low calorie	3.56 ± 0.16	3.49 ± 0.18	0.61

N=18; Data are given in mean ± SEM; Paired t-test.

Abbreviations: Baseline (BL); cold exposure (CE).

3.13 Subjective feeling of cold sensation and perception

To evaluate the applied cooling protocol, the cold sensation and cold perception of the individuals are compared.

The results reported that despite only 29.4% of participants reporting generally higher than average sensitivity to cold temperatures (Figure 30A), almost 80% of individuals reported a close to average or higher perception of cold while wearing the activated vest (Figure 30B).

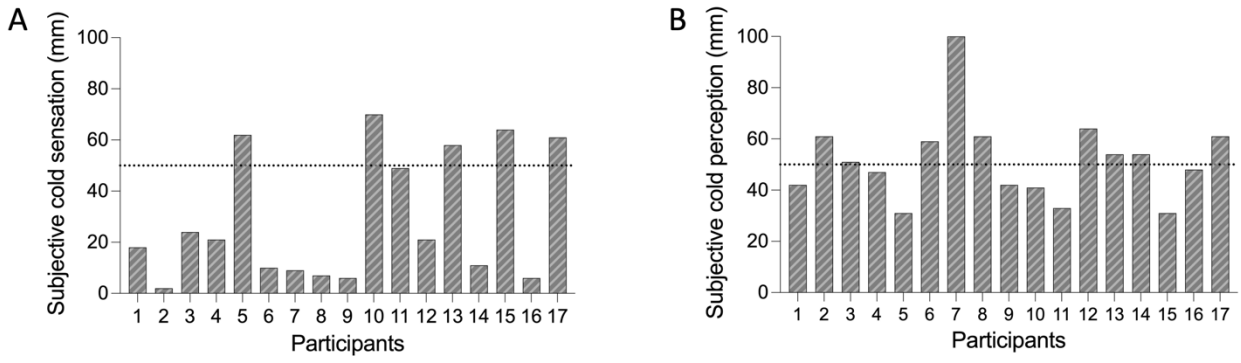

Figure 30. Schematic overview of the self-reported perception of cooling protocols.
The participants marked on a 100 mm line to answer A) On a scale of general cold sensitivity, how would you rate yourself? and B) How would you describe the cooling effectiveness of the activated vest? Data of one participant is missing therefore, n=17.

Hypothesis II: Shotgun metagenomic analyses

3.14 Characteristics of the sub-cohort

Among the 18 participants involved in the present study, eleven individuals contributed stool samples both at BL and after four weeks of chronic daily CE, enabling a comprehensive analysis of the Shotgun metagenomic of gut microbiota. The anthropometric characteristics of the sub-cohort are summarized in Table 4.

Table 4. Characteristics of sub-cohort of metagenomic analysis.

Parameter	Value
Gender (f/m)	3/8
Age (years)	34.1 ± 2.5
Weight (kg)	88.5 ± 4.0
Fat mass (%)	30.9 ± 2.5
BMI (kg/m^2)	28.3 ± 1.1
HbA1c (%)	5.2 ± 0.1
TSH (µE/ml)	1.7 ± 0.2

N=11; Data are mean ± SEM except for gender (absolute values).
Abbreviations: Body mass index (BMI); hemoglobin A1c (HbA1C); thyroid-stimulating hormone (TSH).

In this sub-cohort, a consistent improvement in glucose metabolism and β-cell function was evident, mirroring the findings of the main cohort (see Chapter 3.7). In this subset, the analysis revealed a significant decrease in the $\log_{10}$ AUC of plasma glucose during the IVGTT (p = 0.02) and an increased FPIR (p = 0.06) following CE compared to BL, however, it failed to reach the level of significance (Figure 31A & B).

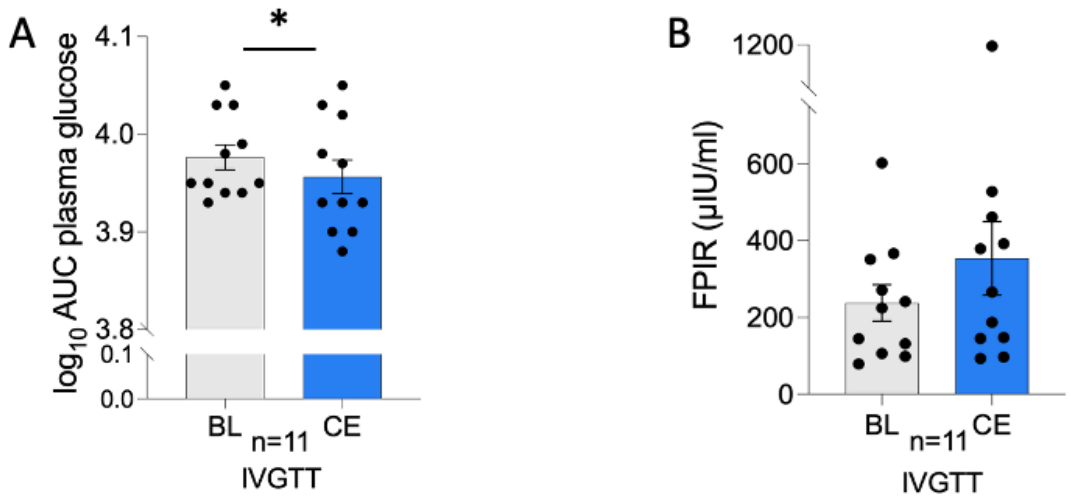

Figure 31. Glucose metabolism of sub-cohort with stool samples across the experimental sessions.

The figures show A) $\log_{10}$ AUC of plasma glucose; and B) FPIR during IVGTT after sub-chronic CE compared to BL. Paired t-test. * $p < 0.05$.

Abbreviations: Area under the curve (AUC); first phase insulin response (FPIR); intravenous glucose tolerance test (IVGTT); baseline (BL) cold exposure (CE).

3.15 Gut microbiota composition changed after sub-chronic cold exposure

This section presents the results of the Shotgun metagenomic analyses of gut microbiota.

3.15.1 Abundance of microbiota at the phylum level changed after sub-chronic cold exposure

Chronic CE induced substantial alterations in gut microbiota composition at the phylum level compared to BL (Figure 32A). Specifically, there was a significant decrease in the relative abundance of Firmicutes and an increase in the relative abundance of Bacteroidetes ($p = 0.007$; $p = 0.02$, respectively) (Figure 32B &C). These findings were consistently replicated following the application of the Benjamini-Hochberg procedure to control for false positive discoveries (pBH = 0.075; pBH = 0.1, respectively) (Figure 32B & C).

Furthermore, upon analyzing the Firmicutes/Bacteroidetes ratio, a decrease following chronic CE compared to BL was observed.

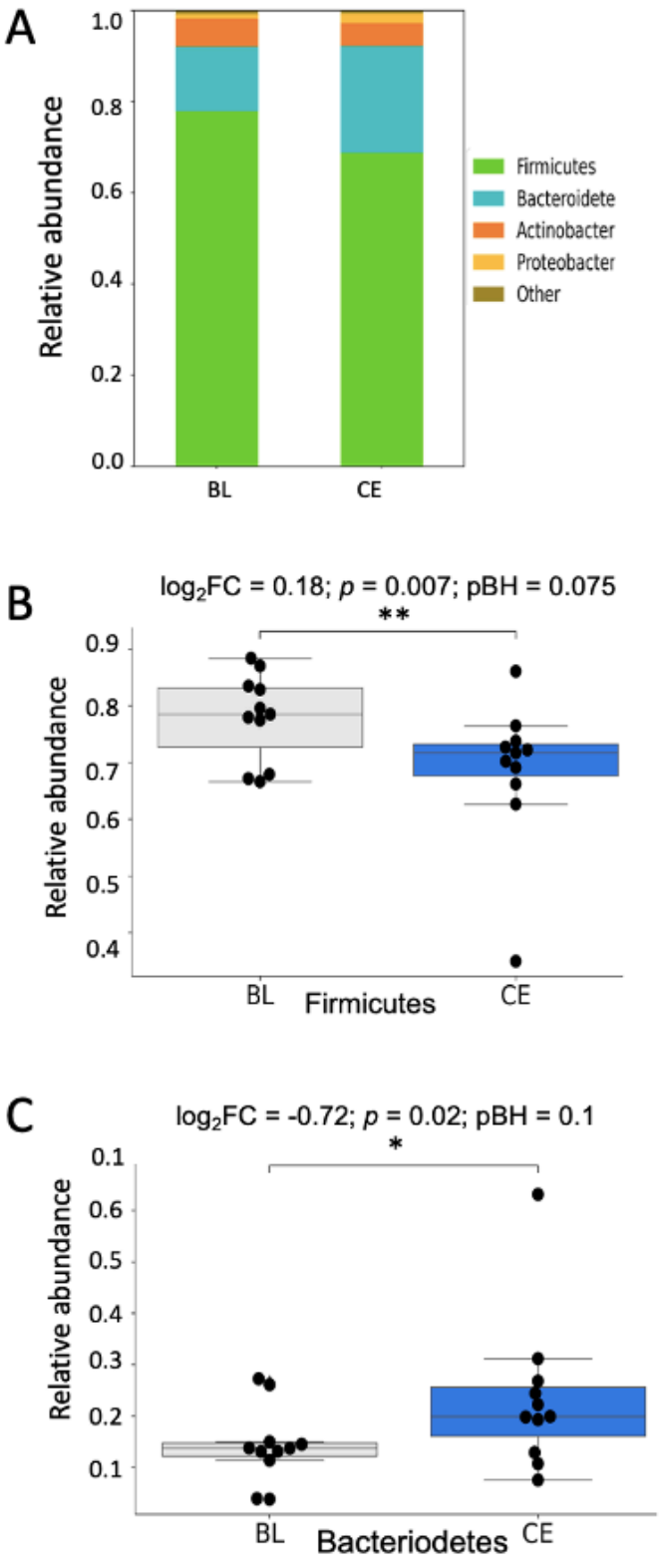

Figure 32. Gut microbiota composition at phylum level over experimental sessions.
The figures show A) at the phylum level the relative abundance of the cohort; B) the relative abundance of Firmicutes; and C) the relative abundance of Bacteroidetes following sub-chronic CE compared to BL. Paired t-test. *$p < 0.05$; **$p < 0.01$.
Abbreviation: Benjamini-Hochberg correction (pBH); baseline (BL); cold exposure (CE).

3.15.2 Abundance of *Bacteroides uniformis* increased after sub-chronic cold exposure

Further Shotgun metagenomic analysis revealed changes in the abundance of gut microbiota at the species level following chronic CE compared to BL. The summary of the species is presented in the following Table 5 (all $p < 0.05$).

Table 5. Overview of the changes at the species level across experimental sessions.

Species	*p*-value	CE vs. BL	pBH	Butyrate producer
Bacteroides uniformis	0.002	Increased	0.39	Yes
Eubacterium ramulus	0.01	Increased	0.67	Yes
GGB51441_SGB71759	0.02	Decreased	0.67	No
Ruminococcus_sp_AF41_9	0.02	Increased	0.67	Yes
Bacteroides thetaiotaomicron	0.02	Increased	0.67	Yes
Streptococcus parasanguinis	0.03	Increased	0.72	No
Clostridium_sp_AF34_10BH	0.03	Decreased	0.72	Yes
Clostridium_sp_AM49_4BH	0.04	Decreased	0.72	Yes
Streptococcus thermophilus	0.04	Increased	0.72	No
Clostridia_unclassified_SGB4121	0.05	Increased	0.72	Yes

N=11; Wilcoxon paired test was used to compare the centered $\log_2$ ratio of the species between conditions.

Abbreviations: Benjamini-Hochberg correction (pBH); baseline (BL); cold exposure (CE).

Upon examining the analysis at the species level, it becomes evident that the centered $\log_2$ ratio (Clr) of *Bacteroides uniformis*, among other species, exhibited a significant increase following CE compared to BL ($p = 0.002$, uncorrected) (Figure 33).

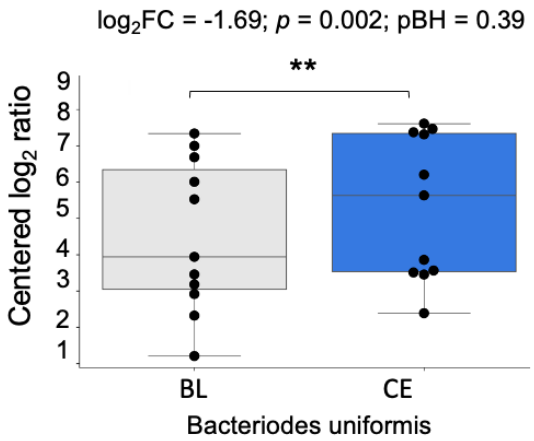

Figure 33. Abundance of *Bacteroides uniformis* over experimental sessions.
The figure represents changes in Clr of *Bacteroides uniformis* following sub-chronic CE compared to BL. Wilcoxon paired test. $^{**}p < 0.01$.
Abbreviation: Centered log₂ ratio (Clr); baseline (BL); cold exposure (CE).

3.15.3 Abundance of butyrate-producing species increased after sub-chronic cold exposure

A closer examination of the alterations in microbiota at the species level reveals a significant increase in certain butyrate-producing species following chronic CE compared to BL. These species include *Bacteroides uniformis*, *Ruminococcus_sp_AF41_9*, *Bacteroides thetaiotaomicron* (Figure 34A & B), and *Clostridia_unclassified_SGB4121* (all with $p < 0.05$, uncorrected). On the other hand, *Clostridium_sp_AF34_10BH* and *Clostridium_sp_AM49_4BH* exhibited a decrease post-CE when compared to the BL ($p < 0.05$) (Table 5).

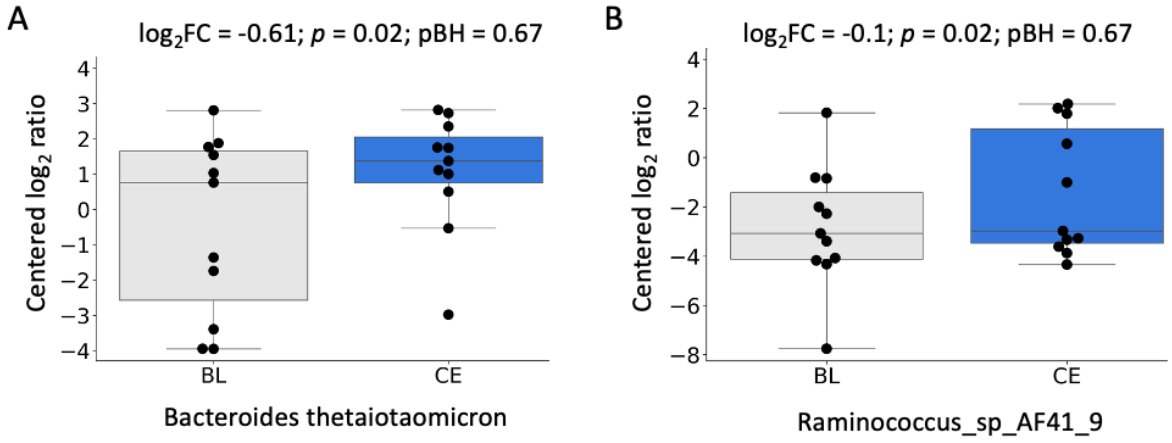

Figure 34. Abundance of butyrate producers over experimental sessions.
The figure represents the changes in Clr of A) *Bacteroides thetaiotaomicron* and B) *Raminococcus_sp_AF41_9* after sub-chronic CE compared to BL.
Abbreviations: Centered log₂ ratio (Clr); baseline (BL); cold exposure (CE).

3.15.4 Abundance of glucose metabolism-related functional profiling changed after sub-chronic cold exposure

Concomitantly, upon closer examination of the 179 pathways indicated in this study by having a look at the first 10 pathways, each indicating a significant change following CE compared to BL (uncorrected *p*-values), seven of them directly or indirectly influence glucose metabolism and/or insulin secretion (Table S1 3 & Table S1 4).

Upon delving deeper into pathways and functional profiling, it becomes evident that the Glycolysis I and II pathways, among others, exhibited a significant increase following CE in comparison to BL ($p = 0.045$; $p = 0.043$ uncorrected, respectively) (Figure 35A & B).

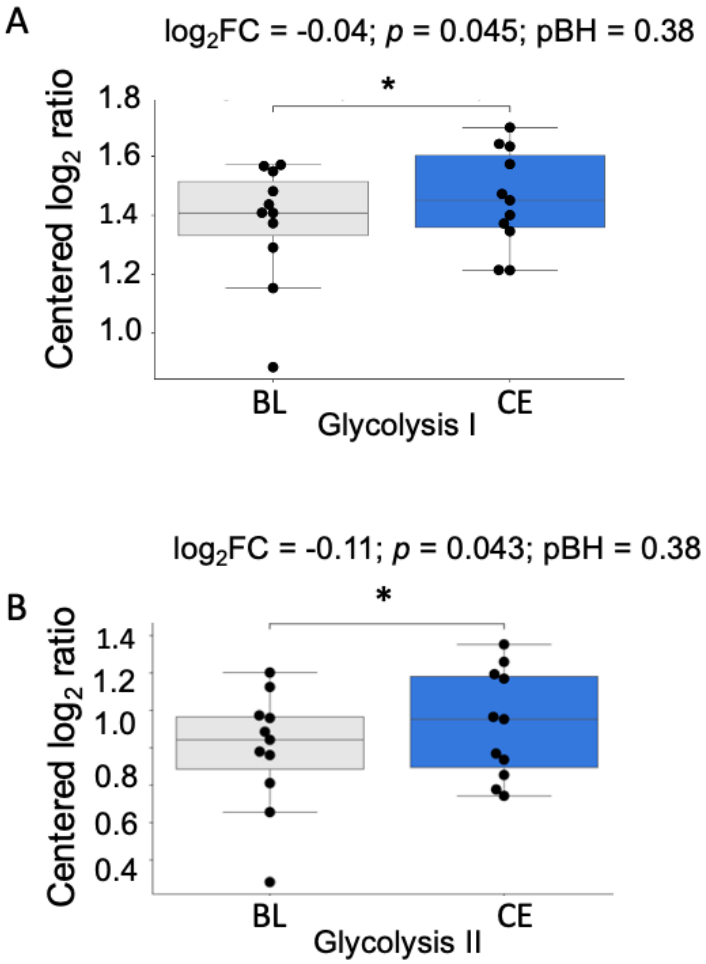

Figure 35. Glycolysis pathways over experimental sessions.
The figures show the Clr of A) Glycolysis I; and B) Glycolysis II after sub-chronic CE compared to BL. Wilcoxon paired test. *$p < 0.05$.
Abbreviations: Centered log$_2$ ratio (Clr); Benjamini-Hochberg (pBH); baseline (BL); cold exposure (CE).

Upon gaining a more profound understanding of the relative abundance of the species within these pathways, it became apparent that *Bacteroides uniformis* is present in these pathways (Figure 36A & B), which presented a significant increase of that in this study following sub-chronic CE compared to BL.

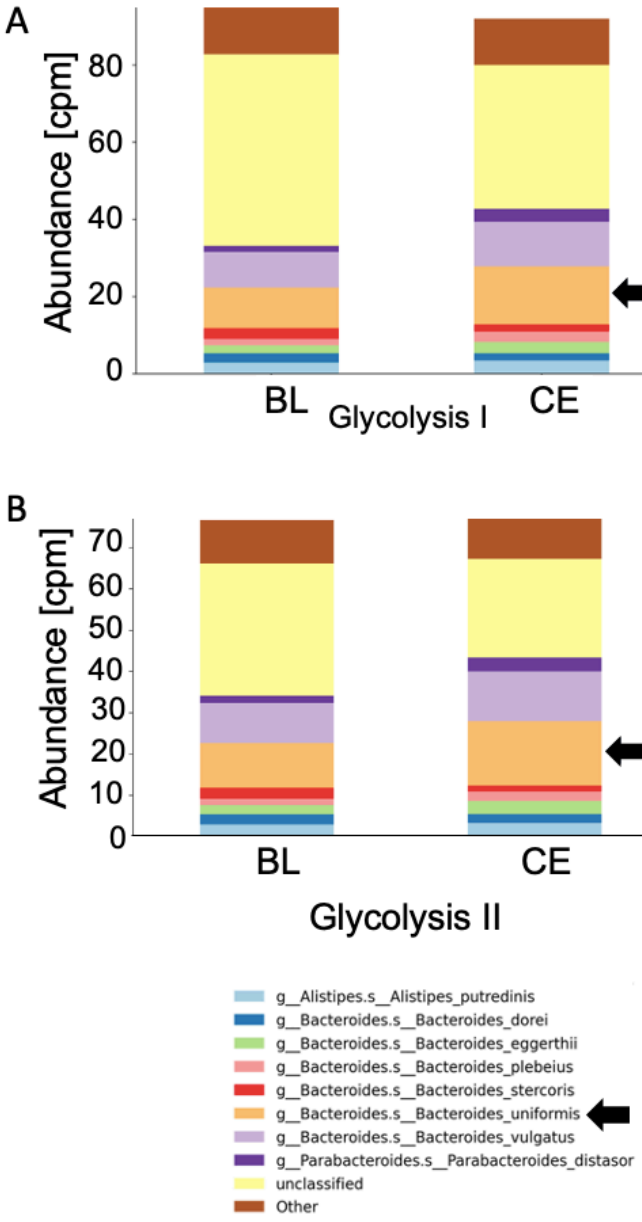

Figure 36. Abundance of present species in Glycolysis pathways over experimental sessions. The figures show an abundance of species that are present in A) Glycolysis I; and B) Glycolysis II after sub-chronic CE compared to BL.
The black arrow depicted the *Bacteroides uniformis* in the pathways.
Abbreviations: Count per million (cpm); baseline (BL); cold exposure (CE).

3.16 Metagenomic results correlate with metabolic outcomes related to glucose metabolism

To investigate the influence of gut microbiota composition on enhanced glucose metabolism including improved β-cell function, increased insulin secretion, and a tendency of improved glucose tolerance following chronic CE compared to BL, a rmcorr analysis was conducted.

A correlation between the AUC of plasma glucose during IVGTT and the increased relative abundance of *Bacteroides uniformis* showed a negative correlation, however it failed to reach the level of significance ($R^2 = 0.30$; $p = 0.066$) (Figure 37A). Concomitantly, the upregulation of Glycolysis I pathways ($R^2 = 0.39$; $p = 0.031$) correlated inversely with the AUC of plasma glucose (Figure 37B).

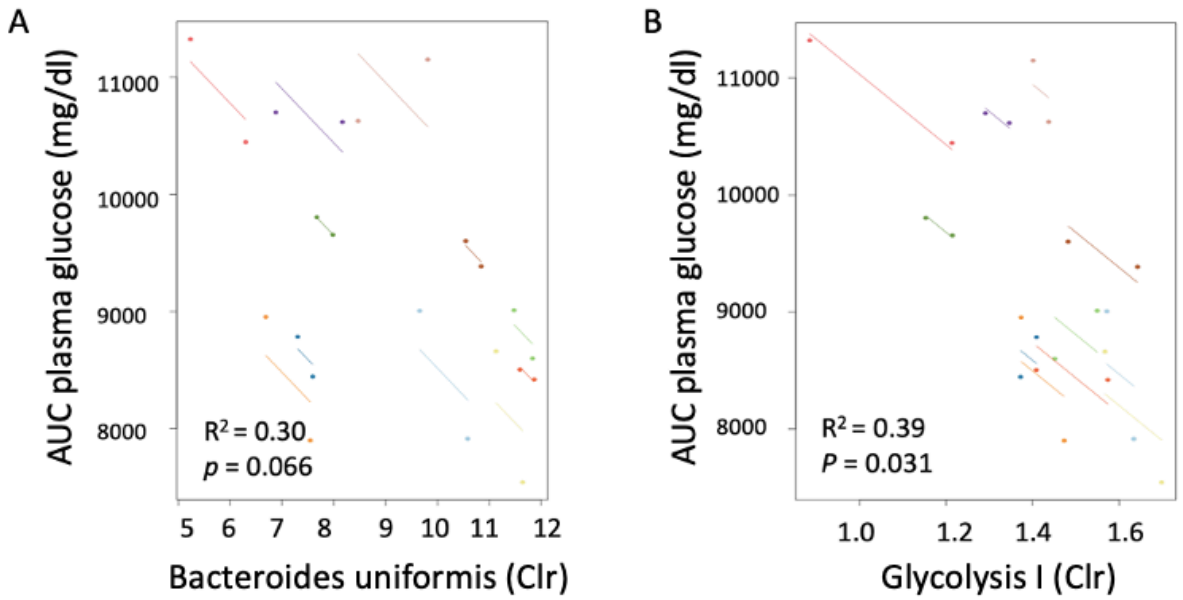

Figure 37. Correlation between metagenomic and metabolic outcomes regarding glucose metabolism.

The repeated measures correlation figures show the correlation between AUC of plasma glucose during IVGTT with A) abundance of *Bacteroides uniformis*; and B) abundance of Glycolysis I following sub-chronic CE compared to BL. Repeated measures correlation (rmcorr). N=11.

Each participant's two measurements are graphically depicted using the same color, and they are connected by a line for visual representation.

Abbreviations: Area under the curve (AUC); intravenous glucose tolerant test (IVGTT); baseline (BL); cold exposure (CE).

Upon further investigation, a positive correlation was uncovered between the elevation of butyrate producers *Ruminococcus_sp_AF41_9*, and an increased Disposition Index (R^2 = 0.82, p = 0.004) (Figure 38A). Additionally, a positive association was observed between an increased abundance of the butyrate-producing bacteria *Bacteroides thetaiotaomicron* and an enhanced FPIR (R^2 = 0.52, p = 0.011) following CE compared to BL (Figure 38B).

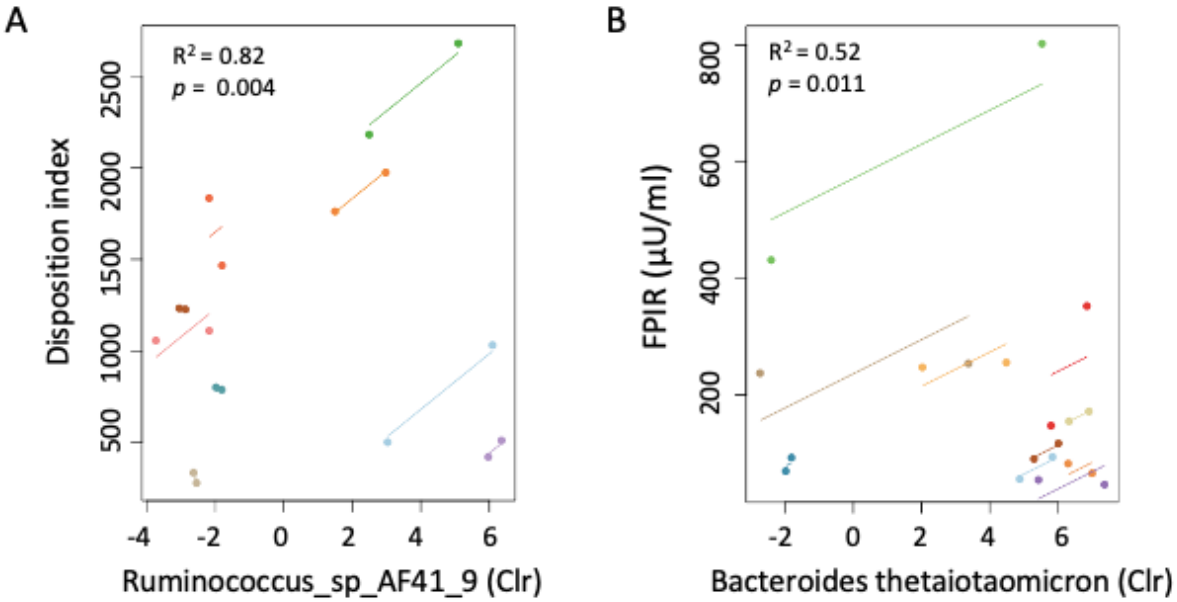

Figure 38. Correlation between metabolic and metagenomic outcomes related to glucose metabolism.

The figures represent the rmcorr between A) Disposition index and a butyrate producer *Raminococcus_sp_AF41_9*; and B) FPIR and a butyrate producer *Bacteroides thetaiotaomicron* following sub-chronic CE compared to BL. Data of one participant is excluded because of an error during insulin assessment, therefore N=10.

Each participant's two measurements are graphically depicted using the same color, and they are connected by a line for visual representation.

Abbreviations: Repeated measures correlation (rmcorr); first phase insulin response (FPIR); baseline (BL); cold exposure (CE).

4 Discussion

Hypothesis I: Metabolic analyses

The present study for the first time aims to explore the metabolic and metagenomic impact of chronic CE for four weeks/daily 10 hours in a cohort of individuals with overweight or mild obesity, without any comorbidities, by using a cooling vest as a novel local cooling protocol under free-living conditions compared to BL. This project expands our preceding study demonstrating improved glucose tolerance in individuals with obesity and increased insulin sensitivity in lean and healthy subjects after an acute CE for two hours by using a whole-body cooling garment under a controlled laboratory setting [1].

4.1 No evidence of the impact of possible confounding factors on outcomes

In the initial phase of our research on the effects of chronic daily CE on BAT activity and various metabolic indicators such as glucose homeostasis, specifically insulin sensitivity, as well as gut microbiota diversity, we were mindful of numerous factors that may influence the results such as outside temperature, experimental room temperature, and humidity [217]. Through comprehensive data collection and analyses of these factors, we found that the aforementioned parameters remained statistically unchanged between and over the time course of experimental sessions.

Additionally, throughout this study, we remained mindful of other factors that could potentially influence BAT activity and glucose homeostasis, especially the participants' physical activity and habitual sleep duration, as our group investigated previously [164,165].

Vigorous physical activity significantly influences body metabolism due to various factors beyond simply muscle contraction. Therefore, in this study, participants were involved, among other inclusion and exclusion factors, based on the predefined vigorous physical activity hours per week, i.e., less than 5 hours per week.

Sleep is another factor that plays an important role in the psychological and physiological functions of our body. We, along with others, have reported the adverse effects of short sleep on glucose homeostasis in humans. Specifically, sleep deprivation reduces glucose tolerance and insulin sensitivity as measured by IVGTT and HEC [165,218,219]. Additionally, irregular sleep-awake rhythm and disrupted circadian cycle are associated with perturbed metabolic

health such as higher postprandial glucose concentration [220,221]. Based on these observations, we added shift working as an additional predefined exclusion criterion.

Taking the above into consideration, we proactively instructed participants to maintain consistent sleep duration and physical activity. We meticulously collected sleep duration and physical activity a week preceding each experimental session. Importantly, participants were advised to prioritize adequate sleep and refrain from engaging in strenuous physical activity the day before each experimental session. In this regard, the analysis of assumed and actual sleep duration as well as total and vigorous physical activity data revealed no differences between conditions. Notably, if sleep deprivation (< 7 hours of actual sleep a night before the experiment) was reported in the experimental sessions, which happened for only one of our participants, we postponed the experiments for the next two days to ensure optimal conditions before the experimental session. As a result, we reasonably assume that these factors did not have a discernible impact on the observed metabolic outcomes.

Throughout our study, we took into account an additional parameter that could potentially introduce bias when analyzing our data between conditions, i.e., the impact of beverages and certain food components on BAT activity. Specifically, substances containing caffeine such as coffee have been observed to stimulate the SNS, leading to increased BAT activity [128]. As a result, participants in our study were explicitly instructed to avoid consuming caffeinated drinks for 24 hours before each experimental session. Furthermore, participants were asked to abstain from consuming spicy foods containing capsaicin the day before the experimental sessions, as capsaicin is known to elevate thermogenesis and BAT activity [222]. All these points were asked in a questionnaire, at both the experimental sessions and before starting the measurements. Furthermore, study participants were asked to avoid using the sauna or any activities with a very low or high temperature for a full day preceding the experimental sessions. Overall, stable environmental factors, controlled sleep habits, and physical activity as well as avoiding specific food ingredients reaffirm well-controlled and comparable conditions during our repeated analysis with minimal evidence of a bias effect on the discussed results in the following sections.

4.2 Indirect assessment of brown adipose tissue activity measured the decreased skin temperature

In our study, the exclusive use of IRT to indirectly assess BAT activity surprisingly revealed a 0.2°C decrease in the mean and 95th percentile of SCV temperature following four weeks of daily CE compared to BL in individuals with overweight and mild obesity.

These findings contradict the expected effect of CE on BAT activity based on existing literature, which suggests that acute CE typically activates BAT, leading to increased NST and dissipating heat from the SCV region [105].

A notable observation was the consistent temperature of a reference point beneath the sternal apex following extended daily CE. Typically, this reference point serves as a control parameter, expected to exhibit no alterations in BAT activity when analyzing IRT images.

This confirms the reliability of our analysis. In our measurements, the reference point was not covered underneath the vest due to the “V” cut around the neck and unchanged temperature provided the important results that the chronic cold did not affect the whole skin temperature and as well as body core temperature remained stable.

Consistent with our results, the team of scientists from the University of Nottingham similarly documented a reduction in SCV temperature by analyzing the IRT images [223].

To examine if two hours of acute CE can impact BAT activity, I designed a pilot study. In this investigative approach, eleven healthy lean men were included. BAT activity was evaluated, implementing the same cooling protocol for a two-hour acute CE within a laboratory setting, followed by the application of the identical IRT technique (unpublished data). Interestingly, we observed the same pattern of significant reduction in SCV temperature following acute CE and unchanged reference point. In this pilot study, these results could be attributed to the timing of the IRT images, captured shortly after the removal of the cooling vest.

The decreased temperature of the exposed area to cold can be explained due to vasoconstriction. The induced vasoconstriction and less blood flow led to a decrease in the SCV temperature. These results indicated that the cooling protocol was sufficient to cool the exposed area; however, no evidence of increased BAT activity could be detected. Consequently, it directs attention towards discussing the nuances of the applied IRT technique as a crucial point for consideration. Although the IRT technique in some studies has been defined as an accurate and non-invasive alternative method to assess BAT activity and positive correlation with FDG uptake in PET/CT images was already reported [105,224,225], its analysis

should be interpreted with caution [217]. First, this method directly assesses the skin temperature and indirectly the BAT activity, thus also integrating the effects of vascularization and blood flow. As this technique is very sensitive, the measurement of SCV temperature can be easily confounded by different factors. Ismael Fernandez-Cuevas and co-authors classified those parameters into environmental, technical, and individual parameters in a review [217]. Considering the stable environmental factors mentioned previously, our IRT analysis utilized a standard SOP and software commonly employed in our lab for other studies, which is described in the methodology section of this work. Moreover, over 80% of participants rated the cooling sensation of the activated vest as average or higher, validating the effectiveness of our mild cooling protocol. The individual parameters in this study differ due to the differences in BMI between overweight and individuals with obesity and therefore higher FM. However, although previous studies suggested the insulation effect of FM in obesity, Alexander Fischer and colleagues recently reported no evidence of subcutaneous fat depot insulation in obesity [226].

To note, one-third of the cohort comprised women, who are known to possess higher ScAT in the chest compared to men [227]. Generally, it is feasible to compare ScAT in humans through skinfold thickness measurements on the arms. An alternative method for experimental comparison of whole-body ScAT thickness involves utilizing Computed Tomography/Magnetic Resonance (CT/MRI). Nevertheless, this approach comes with inherent limitations, notably high costs and limited accessibility.

These limitations aside, the absence of evidence for BAT activity in the present study is in line with our previous observations that whole-body cooling increased FDG uptake in SCV BAT in only three out of 15 normal-weight participants as shown through PET/CT imaging, and even no changes were observed in the sub-cohort with obesity [1]. The latter finding is consistent with established reports indicating a negative correlation between BMI and BAT activity [82].

Although our analysis is valid and reliable, additional gold-standard techniques could be added to confirm these findings. PET/CT remains the gold standard for examining FDG uptake in cold-induced BAT; however, its use is restricted by ethical considerations in Germany for research involving healthy individuals due to its invasive nature and exposure to ionizing radiation. Furthermore, it is noteworthy that insulin-resistant participants showed diminished FDG uptake in BAT despite displaying normal BAT FA uptake [228]. Hence, to delve deeper into the assessment of cold-activated BAT and either confirm or exclude it, it has been suggested to

utilize alternative methods e.g., ^{11}C-acetate PET imaging and ^{18}F-fluroheptadonic acid to assess circulating FFA consumption due to cold-induced BAT [228–230].

Taken together, in this study due to the experimental effect, using local cooling and IRT technique and assessment of BAT activity at the same spot, we could not detect BAT activation after chronic CE compared to BL. However, it is important to mention, that IRT remains a low-cost, easy-to-use, and effective tool to detect the first signs of BAT activation in interventional studies.

4.3 Chronic cold exposure did not impact the hormonal stress axis and heart rate variability

The association between long-term cold temperature and cardiovascular complications, for example, increased mortality or blood pressure in rodents and humans [231,232], and triggering the stress axis is already established [142].

In the present study, to evaluate the impact of chronic CE as a stress parameter the hormonal stress axis including cortisol, and ACTH was investigated. Our results following chronic daily CE for four weeks showed no changes in comparison to BL.

In another study, the effect of winter swimming in ice-cold water for 12 weeks, three times a week for 20 seconds, were studied. The analysis reported no increase in circulating stress hormones, whereas a significantly lower amount was found in weeks 4-12, possibly due to habituation.

Additionally, cold-induced BAT in the previous study in our group did not affect cortisol levels after acute CE in lean individuals or participants with obesity [1]. Another study reported a significant increase in circulating norepinephrine concentration observed after chronic CEs; however, they didn't report either cortisol or ACTH concentration [142]. In contrast, induced cortisol levels following moderate to severe cold have been already reported [233]. These studies indicate that Hypothalamic-Pituitary-Adrenal (HPA) axis activation in cold seems to depend heavily on the chosen paradigm. In our case, as we expected only mild CE did not trigger the stress axis.

In the present study, we did not directly measure the concentration of norepinephrine. However, we conducted an indirect assessment of the activation of SNS by ECG monitoring as

a part of the Actiheart system. The assessment of HRV including the ratio of the LF/HF, inter-beat interval, and heartbeat per minute post-CE, reported no changes between conditions.
In another study, by using acute cooling at 10°C and warming at 45°C the LF/HF ratio and investigating the temperature impact on arterial baroreflex after CE remained unchanged, whereas increased significantly during the heating process [234].
In contrast, 15 students underwent electrocardiogram recording during two lecture sessions at 16-18°C and 20-22°C and there has been a lower LF/HF ratio during cold compared to TN, which reflects the activation of the SNS during cold. The LF/HF ratio stands as a crucial clinical parameter, reflecting cardiovascular health through SNS activity [211]. The contentious outcomes observed in both our study and theirs may be attributed to variations in experimental setups. While their assessments were conducted during acute CE, our experiments transpired at room temperature and under TN conditions. This underscores the notion that changes in HRV, for instance, induced by cold, may be readily acute and reversible. Additionally, further investigation was conducted to evaluate the potential impact of daily chronic exposure to cold on well-being. Analysis of the self-reported SF-36 questionnaire, a well-established tool for evaluating health-related quality of life, revealed no adverse impact of chronic CE on the overall health of individuals. Specifically, there were no differences observed in the physical component following chronic CE, whereas the mental component showed a tendency towards improvement although it failed to reach the level of significance.

Considering these findings collectively, we reported no modulation and absence of negative impact of chronic CE on the stress axis, SNS, and parasympathetic nervous system activity, which was supported by no changes in general well-being as assessed by a questionnaire following a daily cooling vest for four weeks compared to BL. In summary, our findings imply that chronic CE did not act as a major stressor for our cohort, as we found unchanged HPA axis function and HRV. This consistent state of stress hormones also hints at habituation and adaptation, resembling patterns observed in individuals accustomed to CE, such as winter swimmers. The fact of the relation between cold and habituation will be discussed in Chapter 4.6.

4.4 Chronic cold exposure did not impact the body composition, despite increased appetite

In this study, chronic daily exposure to mild cold for four weeks revealed no changes in body weight and composition e.g., FM, or BMI of individuals with overweight and mild obesity.
In the literature, the inverse relationship observed between lower BMI and VisAT, along with increased BAT volume and activity, suggests that obesity and its associated conditions like T2D and hyperlipidemia can be treated through activating BAT. Despite evidence of a negative correlation between obesity and active BAT in humans [82,90,91,235], alterations in body composition resulting from CE and activated BAT are not the primary metabolic effects observed initially. This might elucidate the challenges in altering body composition due to mild CE. Along with our findings, a systematic review regarding cold and BAT activity including 47 clinical trials, considering the heterogeneity of cooling protocols, reported the activation of BAT but with no impact on body weight and is unlikely as an effective therapy to combat obesity [154]. There are estimations that a fully activated BAT can only expand approximately 40 kcal of energy per day [77].
It is essential to note that among human studies, Yoneshiro and colleagues are the only group to observe a reduction in FM in 12 participants following a six-week intervention involving daily two hours CE at 17°C [109]. Concomitantly, rodents housed at cold robustly exhibited increased BAT thermogenesis and reduced FM [236].
Taken together, four weeks of daily CE did not alter the body composition in this study. Habituation and the intricate human physiology, aiming to maintain higher body weight and FM as a protective measure, might elucidate the challenges in altering body composition due to mild CE.

4.5 Chronic cold exposure did not impact food preferences but stimulated the subjective feeling of appetite

The examination of the self-reported VAS questionnaire aimed to explore the influence of CE on subjective feelings of appetite. As anticipated, our findings revealed a significant increase in appetite sensations following chronic CE compared to BL.

Generally, it is well established that exposure to cold increases appetite and ghrelin levels in humans [238]. Additionally, the impact of CE on increased energy expenditure in humans is unsurprising [2,239,240].

In addition to CE, various other factors can influence appetite. For instance, sleep deprivation plays a significant role in increasing appetite and developing obesity and T2D [206]. In our laboratory, my colleagues confirmed this and specifically demonstrated that late sleep loss, and not early sleep loss, leads to heightened appetite in lean, healthy individuals [164]. Moreover, exercise and physical activity represent additional variables that stimulate appetite [241].

In this doctoral study, given the consistent habitual sleep and physical activity over the experimental sessions, which have been previously discussed, we can attribute the observed increase in appetite to chronic CE. We did not directly measure the orexigenic and anorexigenic hormones, such as leptin and ghrelin, which regulate appetite and hunger. This prevented a direct assessment of the impact of chronic CE on these appetite hormones. Additionally, due to COVID-19 hygiene restrictions, we could not measure energy expenditure using indirect calorimetry.

Despite the increased subjective appetite observed following CE, there were no discernible changes in body composition or FM throughout the experimental period. However, as we lack data on potential alterations in calorie and food intake within our cohort, it remains unanswered whether this hints at a potential rise in energy expenditure following chronic CE compared to BL.

Furthermore, to explore the influence of chronic CE on hedonic and homeostatic food preferences, we conducted an analysis using the 'wanting liking' questionnaire [237]. As expected, our findings indicate that the liking for specific foods with pleasurable attributes remained unchanged following chronic CE. Additionally, our analysis revealed consistent preferences across experimental sessions, showing no notable changes in the desire for savory-high-calorie, sweet-high-calorie, or low-calorie foods. Our result aligns with previous findings from our colleagues, affirming that acute CE, when compared to TN, did not induce alterations in food preferences. However, in the existing literature, there is a dearth of investigations exploring food preferences following CE, specifically focusing on hedonic and homeostatic aspects.

Taken together, our data demonstrated an increased self-reported appetite feeling after chronic CE without changes in body composition. However, the data on calorie intake and energy expenditure are not available. In a follow-up study, additionally utilizing a diary for calorie intake calculation, exploring the impact of chronic CE on energy expenditure would be highly intriguing. The innovative cooling protocol employed in free-living conditions might pave the way for additional research into combatting obesity and related metabolic syndromes like hyperglycemia and hyperlipidemia.

4.6 Chronic cold exposure improved β-cell function, whereas insulin sensitivity remained unchanged

To our knowledge, this study stands among the pioneering RCTs involving non-diabetic individuals with overweight or mild obesity that delves into the effects of chronic CE under free-living conditions on glucose homeostasis. This comprehensive approach was designed to evaluate both β-cell function and insulin sensitivity using a Botnia clamp approach.

Our analysis revealed that following chronic exposure to cold, no significant alterations were observed in the concentration of fasting glucose, insulin, and C-peptide when compared to BL. Similar outcomes were previously documented in our lab after acute CE for two hours in a controlled laboratory setting [1]. Consistent with these results, others also reported no marked changes in fasting plasma glucose or basal plasma insulin concentration following CE in comparison to TN [151,152,242–244].
Collectively, these findings underscore the limitation of relying solely on fasting parameters to elucidate the impact of CE on glucose metabolism comprehensively. The absence of notable alterations in these parameters across various studies emphasizes the need for a more nuanced approach to capture the intricate impact of CE on glucose homeostasis.

Upon a more intricate examination of glucose metabolism during the IVGTT, our findings hinted at a potential improved glucose tolerance and decreased AUC of plasma glucose concentration following CE compared to BL, however, it did not reach the level of significance. Although these observations did not reach statistical significance, they underscore the relevance of considering the promising physiological impact of chronic CE on enhancing glucose tolerance among individuals with overweight and mild obesity in this study. This

potential avenue for future research could shed further light on the positive physiological effects of chronic CE on glucose tolerance in individuals with obesity and T2D.

Aligning with our findings, pioneering research by Vallerand and colleagues demonstrated enhanced glucose tolerance and reduced AUC of plasma glucose following a three-hour CE at 10°C accompanied by shivering experiences in healthy lean individuals. Similarly, an animal study observed a diminished AUC of plasma glucose in male mice subjected to intermittent CE at 5°C under an HFD for two weeks compared to control conditions [245]. However, in these studies, the significantly lower cold temperature, and the presence of shivering in comparison to our study, is important to notice, as shivering activates muscles, and it is entirely another mechanism. Furthermore aligning our findings, Iwen and colleagues [1] showcased improved glucose tolerance among a sub-cohort with obesity following a two-hour acute mild CE compared to TN in a laboratory setting.

Our analysis in this doctoral study unveiled noteworthy alterations in plasma insulin and C-peptide concentrations during the Botnia clamp following chronic CE. Our findings showcased a 45% increase in the FPIR after sub-chronic CE in comparison to BL. The concurrent elevation in C-peptide levels, consistent with insulin secretion within the initial six minutes of the IVGTT, substantiated the robustness of our assessments. Generally, the FPIR emerges as a sensitive marker delineating the β-cell response to an acute glucose bolus. Its significance extends to the diagnostic domain, serving as a pivotal tool in identifying impaired insulin secretion and β-cell dysfunction [246]. Notably, this response is commonly compromised in individuals with T2D [247], further underscoring the clinical relevance and implications of our observed enhancements in FPIR following chronic CE. This nuanced understanding reinforces the potential role of chronic CE in modulating β-cell function and insulin secretion dynamics, holding potential suggestions for further exploration in the context of combating obesity and T2D.

Regrettably, the existing literature lacks studies that have directly compared the effects of CE on FPIR compared to BL. Therefore, irrespective of cold intervention, a study by Christoffer Martinussen reported an increased FPIR following IVGTT in patients with T2D post-RYGB and the remission phase of diabetes [247]. Additionally, an 8-week regimen of high-intensity interval training resulted in enhanced pancreatic β-cell function among individuals diagnosed with T2D. These separate findings underscore the importance of investigating FPIR and improving β-cell function to evaluate the impact of an intervention on glucose homeostasis.

Furthermore, while the AUC of plasma insulin and C-peptide remained unchanged between conditions during IVGTT, we observed a significant increase in C-peptide concentration over time and following chronic CE compared to BL, although insulin concentration showed no changes. The discrepancies between plasma insulin and C-peptide concentrations can be explained by the molecular physiology differences between these hormones. The shorter half-life of insulin compared to C-peptide makes it a more reliable alternative parameter in clinical settings [161].

In the literature, the impact of CE on plasma insulin concentration remains contentious. In addition to reports with no alterations, as mentioned at the beginning of this chapter, decreased plasma insulin levels following acute CE have been reported in humans [156]. Furthermore, winter swimmers exhibited lower insulin levels compared to controls, whereas their glucose levels remained unchanged [248]. Generally, this phenomenon's underlying mechanism involves activation of the SNS and subsequent norepinephrine release, which leads to inhibiting insulin secretion [249–251].

To search for what could cause the increased insulin secretion after CE in the present study, the literature search indicated that activation of the parasympathetic nervous system is recognized for its role in stimulating insulin release [115]. In line with this established principle, Mckie and colleagues observed a rise in both insulin and C-peptide concentrations following intermittent CE in male mice under both HFD and LFD conditions, contrasting with TN [245]. Their findings provide additional support for the intricate relationship between CE and increased insulin secretion. However, our study did not reveal evidence of sympathetic and parasympathetic activation, hinting at the presence of an alternative mechanism driving the observed increase in β-cell function.

The next chapter “Metagenomic Analyses” presents our findings and the alternative mechanism behind increased insulin secretion in this study.

Furthermore, one of our main findings is an increase in the Disposition index and a tendency towards improved pancreatic β-cell function, quantified as HOMA-Beta, following chronic CE, albeit falling short of statistical significance. Importantly, these findings suggest that chronic CE prompted a more rapid β-cell response to the substantial glucose bolus, evident in improved pancreatic and hepatic function.

Conversely, HOMA-IR showed no discernible alterations in diabetes status between conditions, reflecting that increased insulin secretion did not impact the insulin resistance of

the cohort. As we expected, only the mild CE did not necessarily change the glucose homeostasis towards marked improvement in healthy non-diabetic participants.

Generally, HOMA-Beta and HOMA-IR are usually used in epidemiological studies to compare the insulin resistance and diabetes status of the community [252]. Nevertheless, there are a few studies that compare the impact of CE on these parameters. Along with our findings, after 10 days of mild CE (6h/day) in healthy lean individuals the HOMA-IR remained unchanged [253]. Conversely, it has been shown a reduced HOMA-IR after CE in rats [254]. Additionally, a study in fat-tailed dwarf lemurs showed that HOMA-IR decreases during hibernation and in the cold season [255]. These discrepancies emphasize the importance of applied cooling protocols and the physiological differences between human and animal models (see Chapter 4.8).

While the AUC of the C-peptide concentration during the steady state of HEC (intervention x time) remained unchanged, the escalating C-peptide concentration over time was observed during the steady state of the HEC. This underscores a crucial physiological state during HEC. As a matter of fact, despite the continual infusion of exogenous insulin, this phase prompts β-cells to secrete insulin in response to the heightened exogenous glucose infusion over time (see Chapter 1.6). Notably, during the analysis of HEC, the consideration of insulin concentration becomes intricate as it encompasses both endogenous and exogenous insulin contribution. Besides, due to the short halftime of insulin, its changes over time failed to reach the level of significance. Furthermore, our findings reported that insulin and C-peptide concentrations were not affected by chronic CE and remained unchanged between conditions. The same results have been also reported after acute CE in the previous study within our lab [1].

In this present work, the four-week daily CE did not yield alterations in insulin sensitivity, as assessed through *M*-value and AUC of GIR during the steady state of the HEC in healthy individuals with overweight and mild obesity when compared to BL. While we did note a significant change in GIR during the steady state, a thorough analysis failed to reveal a distinct pattern. Instead, the changes fluctuated between conditions, showcasing higher rates at BL at the beginning and end of HEC, while displaying higher rates at CE in the middle. This variance observed in our study remains unexplained. Future studies could be designed to investigate if it is a physiological pattern when CE is compared to BL.

Over the past decade, evidence has shown that cold-induced BAT improves glucose regulation in both rodents and humans. In 2014, Chondronikola and colleagues compared the impact of prolonged CE (5-8 hours) using cooling garments at 20°C in subgroups with and without BAT. They observed enhanced insulin sensitivity and improved whole-body glucose regulation specifically in BAT-positive men [92]. In rodents, cold-induced BAT transplantation increased insulin sensitivity and energy expenditure in recipient mice under HFD [256]. When rats were exposed to chronic cold for 10 days at 4°C, it led to an increase in BAT glucose utilization which reflects increased NST. The reason for that could be explained by increased GLUT4 expression in the insulin-sensitive tissues [257]. Generally, the study reported increased insulin sensitivity post-CE, specifically attributed to shivering-induced muscle contractions [258,259]. These divergent outcomes underline the potential impact of shivering and associated muscle contractions in influencing insulin sensitivity during CE protocols.

Consistent with our findings and in the absence of shivering, Remie et al. similarly observed no changes in GIR among their cohort comprising obese individuals with T2D following 10 days of CE at 16-17°C [260].

However, the absence of improved insulin sensitivity following chronic CE in individuals with overweight and mild obesity raises the question: why did this study not reveal any impact on total GIR and insulin sensitivity?

Our previous study within our group showcased a dichotomy: while no changes in insulin sensitivity were noted in the subgroup with obesity, an increase in insulin sensitivity and heightened BAT activity emerged after two hours of acute CE among lean participants in a laboratory setting [1]. Along with our findings, they reported improved glucose tolerance after acute and chronic CE was observed in individuals with obesity. This disparity underscores the divergence in their underlying physiological pathways between improved glucose tolerance and insulin sensitivity. As a suggestion, exploring insulin sensitivity among lean participants through the application of the same chronic cooling protocol under free-living conditions stands as a promising direction for future inquiries, offering insights that could address this query.

Additionally, in this study, the absence of evidence for BAT activity and non-shivering cooling protocol led to unchanged glucose utilization and the absence of uptake glucose in BAT and muscles.

Moreover, the role of adaptation and habituation to prolonged cold assumes significance in understanding these distinct metabolic responses. Prolonged exposure to cold might prompt the body to adapt over time, potentially leading to diminished responses in insulin sensitivity and BAT activity. Habitation, akin to a learning or memory process, is observed across organisms as a protective mechanism against repeated stimuli, such as prolonged CE, serving as a safeguard against physiological strain [261,262]. Concomitantly, localized prolonged CE, such as experienced by fishermen immersing their hands in cold water, leads to adaptation, as evidenced by reduced cold sensation and altered skin temperatures [262]. This insulative adaptation typically involves reduced peripheral heat loss and decreased catecholamine release. Finally, the specific cooling protocol utilized significantly influences BAT research. Therefore, the next Chapter discusses this point.

Collectively, our results indicate enhanced β-cell function following four weeks of sub-chronic mild CE under free-living conditions. We observed an improved glucose tolerance, however it did not reach statistical significance. These findings introduce our applied novel cooling protocol under free-living conditions, as a new cooling method to stimulate insulin secretion, shedding light on research avenues to combat obesity and T2D. The absence of alteration in SNS, HRV and HPA axis hints at another alternative mechanism contributing to the increased insulin secretion and a tendency towards decreased AUC after chronic CE. One of these alternative mechanisms will be explored in further detail in the section “Metagenomic Analyses” of this present work.

Hypothesis II: Metagenomic analyses

4.7 Metabolic and metagenomic outcomes related to glucose metabolism are associated

In the past twenty years, research has progressively highlighted the substantial influence of gut microbiota on human metabolic health. Notably, the gut microbiota can affect glucose regulation in various ways, including producing metabolites like SCFAs that trigger the secretion of GLP-1 and PYY, culminating in increased insulin release from β-cells [216].
Comparative studies have already investigated the diversity of microbiota in both healthy individuals and patients with T2D, revealing a significant distinction in the microbiota composition between these two groups [172]. To investigate the impact of microbiota on observed improved glucose metabolism in this present work we analyzed the metagenomic data.

Recent metagenomic studies have expanded beyond quantifying microbiota diversity, composition, and abundance analyses. There is now a growing interest in integrating metabolic and metabolomic data, broadening the scope of insights gleaned from these investigations [174]. In this doctoral project, following the latest methodology and to delve deeper into the potential influence of chronic CE on the intestinal microbiota at the phylum, species, and functional profiling levels associated with glucose homeostasis and to investigate the correlation between metagenomic and metabolic outcomes, advanced Shotgun metagenomic analyses were employed.
In the present study, the analysis at the phylum level revealed notable changes after chronic CE, including a significant decrease in the abundance of Firmicutes and a marked increase in Bacteroidetes compared to BL.
Typically, Firmicutes maintain a higher abundance than Bacteroidetes under normal physiological conditions [186] and are only altered under severe conditions such as antibiotic use, diabetes, inflammatory diseases, and malnutrition [263].
As expected in this present study on mild chronic CE, while there were alterations in phyla abundances, the proportion of Firmicutes remained higher than Bacteroidetes.
Previously, Chevalier et al., our collaborator lab at the University of Geneva, reported that transplantation of chronic cold microbiota in germ-free mice resulted in increased gut size,

alteration in microbiome composition, and improved insulin sensitivity after four weeks of daily CE at 6°C compared to TN as control [184]. In contrast to our research outcomes, their investigation demonstrated an opposing outcome at the phylum level. They observed an increase in the abundance of Firmicutes alongside a decrease in Bacteroidetes following chronic CE. Discrepancies between our findings and theirs may be attributed to significant variances in human and rodent physiology, variations in controlled environmental conditions, and significant differences in the cooling protocols and temperature, and metagenomic methods (Shotguns vs. 16S) applied.

Nonetheless, it is noteworthy to mention that their study revealed a notable rise in proportion of Firmicutes abundance post-chronic daily CE, contrasting with a lower abundance observed at the TN. These marked distinctions at the BL level emphasize substantial physiological differences between humans and rodents. This evidence underscores the limitation of rodent models in microbiota studies, highlighting their inadequacy as accurate representations of the human model.

In evaluating the composition and equilibrium of the gut microbiome, the Firmicutes/Bacteroidetes ratio stands as a relevant marker [220]. Frequently utilized, it serves as a potential indicator for obesity and associated metabolic syndromes [221,222].

In the present study, upon analyzing the Firmicutes/Bacteroidetes ratio, a decreased ratio following chronic CE compared to BL was observed. In contrast, Chevalier et al. observed a higher Firmicutes/Bacteroidetes ratio after the chronic CE in rodents [184].

When comparing the aforementioned ratio between healthy individuals and those with T2D, conflicting findings emerge. Some studies indicate a reduction in the abundance of Firmicutes in T2D patients [185], whereas others note an elevation in Firmicutes alongside a decrease in Bacteroidetes [189,196]. This disparity suggests that relying solely on phylum-level outcomes might not provide conclusive insights into microbiota composition and function, therefore further scrutiny of the species and strain levels becomes essential. Here, a crucial strength of the present work is the inclusion of untargeted shotgun sequencing, which in comparison to more commonly used 16S rRNA sequencing, allows annotation at species levels. This allowed us to conduct a more detailed analysis in species and functional profiling levels to explore the potential involvement of microbiota in enhancing glucose metabolism and β-cell function.

Generally, no universally agreed-upon “standard” exists for the optimal or ideal composition of human microbiota [174]. Nonetheless, a key indicator of a resilient gut profile frequently centers on the role of butyrate-producing genera by fermenting complex polysaccharides and producing SCFAs including butyrate, propionate, and acetate.

At the species level, this study identified a rise in butyrate producers following chronic CE in comparison to BL. Notably, an increase was observed in *Bacteroides uniformis*, a well-established species known for its influence on glucose metabolism. Previously, the gavage of adult wild-type mice on a HFD for seven weeks with *Bacteroides uniformis*, as opposed to the control group on the same diet, resulted in lower plasma glucose and insulin levels, accompanied by reduced weight gain [190].

Our further examination of the top 10 species with changed abundance following chronic daily CE compared to BL ($p < 0.05$) revealed an increase in *Eubacterium ramulus, Raminucoccous subspecies*, *and Bacteroidetes thetaiotaomicron*, which are all described as butyrate producers. Contrary, the abundance of *Clostridium subspecies*, another butyrate producer showed a decrease following CE compared to BL.

The existing literature consistently highlights a depletion of butyrate producing bacteria, including *Eubacterium rectale, Roseburia intestinali,* and *Faecalibacterium prausnitzii*, in individuals with impaired glucose metabolism to their healthy counterparts [187, 189, 229, 230]. In our study, all these aforementioned species were identified in the metagenomic analysis. However, their abundance remained unchanged following chronic CE. This observation aligns with the metabolic outcome of an unchanged diabetes status (HOMA-IR) after chronic CE compared to BL.

In the present study, a more in-depth exploration into functional profiling revealed notable changes following CE compared to BL, with the top 10 pathways displaying significant alterations. Interestingly, more than half of these pathways were directly or indirectly related to glucose metabolism or insulin secretion. Particularly striking was the observed increase in Glycolysis I and Glycolysis II pathways signatures post chronic CE. Glycolysis, the fundamental process of breaking down glucose into simpler compounds within cellular metabolism, occurs anaerobically in the cytoplasm and aerobically within the mitochondria. Moreover, our analysis highlighted the presence of *Bacteroides uniformis* in both pathways, consistent with its significant increase after chronic CE. This discovery suggests a potential role of this species in enhancing glucose metabolism following chronic CE compared to BL.

In this study, among other observations, the PWY-3001 pathway responsible for L-isoleucine biosynthesis I, exhibited a decrease post CE. This pathway governs the production of isoleucine, a branched-chain amino acid (BCAA) linked to insulin resistance, which supports the impact of this pathway after chronic CE on observed metabolic outcomes, although the insulin resistance and sensitivity with the small number of participants in this study did not show any changes. Conversely, the COBALSYN-PWY pathway, governing adenosylcobalamin salvage from cobinamide I and essential in T2D as it produces cobalamin, displayed a decrease after chronic CE. Cobalamin indirectly affects glucose homeostasis by stimulating β-cell function.

In our exploration of the relationship between metagenomic profiles and metabolic outcomes related to glucose homeostasis, we observed a negative correlation between a lower AUC of plasma glucose levels during IVGTT and increased *Bacteroides uniformis*, although this correlation did not reach statistical significance. Conversely, we noted a positive correlation between the lower AUC of plasma glucose parameter and increased activity in Glycolysis I.

Additionally, a positive correlation between butyrate producers and increased Disposition index and FPIR further suggested the importance of gut microbiota in glucose metabolism.

Taken together, in this doctoral study the collective evidence, spanning heightened populations of butyrate-producers, functional profiling tied to glucose metabolism, and established correlations between metabolic changes and metagenomic outcomes, substantiates our hypothesis regarding the microbiota's influence on glucose metabolism after sub-chronic CE compared to BL.

However, it is important to note a key distinction, that metagenomic analysis significantly differs from the actual composition of the microbiota. First, the DNA of the bacteria is quantified and not the quantity of the live bacteria. Second, the focus of this metagenomic analysis was to investigate the butyrate producers. It is crucial to note that while butyrate production and polysaccharide fermentation predominantly occur within the intestinal lumen, the stool samples collected in this research represent the distal segment of the colon. This distinction highlights a potential limitation that led to finding less robust results, for example after multiple testing, and further correlations. To strengthen the evidence in studying butyrate producers, collecting stool samples directly from the intestinal lumen could yield more robust results. However, this will not be feasible for healthy individuals.

4.8 Importance of using standard cooling protocol and methods to assess metabolic impact and BAT activity in future studies

It is widely recognized that CE impacts the whole-body metabolism, triggers the SNS and among others, activates BAT. Nevertheless, the varied cooling protocols employed across studies complicate direct comparisons of the results. When delving into investigations on cold-induced BAT activity, alongside considering the characteristics of the cohort, e.g., age, sex, and BMI, the primary and pivotal determinant is the conducted cooling protocol itself.

Huttunen and colleagues reported that one minute of acute immersion in cold water activates the SNS and regular immersion increases this effect [264]. Van der Lans et al., showed an increased BAT activity using PET/CT following chronic CE (15-16°C) for 10 consecutive days: two hours on the first day, four hours on the second day, and six hours on the remaining days [144]. Along with these findings, Saito and colleagues showed an increased BAT activity after six weeks of daily two hours of acute CE (17°C) in subjects with low or undetectable BAT [109] It has been proposed that reaching the temperature of cold-induced BAT activity requires mild shivering intensity. Blondin et al., showed six healthy lean men exposed to 18 acclimation sessions (five consecutive days/2 hours per day for four weeks) by using the liquid-containing suit at 10°C could increase 45% in the volume of cold-induced BAT using PET/CT, and a trend of increased glucose FDG uptake as well as a 2.2-fold increase in oxidative capacity. It is important to mention that shivering capacity has been reported in this study, however, it remained unchanged before and after acclimation to cold [240].

In human studies, a spectrum of protocols has been employed, ranging from acute to chronic CE, lasting from mere hours to consecutive or intermittent cooling spanning days to weeks. These methodologies encompass the use of garments, T-shirts, and vests, primarily in controlled laboratory settings, and techniques such as immersing feet or hands on the ice or in cold water, utilizing cooling chambers, and implementing personalized cooling protocols above the shivering point or by mild shivering.

When comparing the acute and chronic cooling protocols between the previous and the present study respectively, some differences are noticeable. The prior study utilized an acute and meticulously controlled cooling protocol conducted in a laboratory setting [1]. Participants were positioned in hospital beds, restricted in physical activity, and wore standardized clothing. At the experimental session, individuals were exposed to mild cold

(18°C) for two hours, deliberately kept above their shivering point, achieved by wearing a specialized whole-body garment, while HEC was conducted as a glucose metabolism test. In the present study, the applied cooling protocol was focused on a localized cooling approach that only exposed the chest and back region of the body up to the abdomen and kidneys, respectively, thus omitting whole-body coverage. During chronic CE for four weeks/10 hours a day under free-living conditions, participants were tasked with activating a cooling vest at home based on practical instructions at the end of the first experimental session. A video link was also provided as a guideline on how to activate the vests as well as an SOP to ensure their correct activation. Additionally, a follow-up email from myself two days after commencing the CE ensured the correct application of the vest activation. It should be acknowledged, that the participants were encouraged to wear the activated vest indoors to maintain a controlled temperature. However, they retained the freedom to continue their daily routines, whether at work, school, outdoors, or engaging in activities like gym workouts. This flexibility allowed for a more realistic representation of their usual activities during the study. The constant body activity while exposed to cold might have led to a dissipation of the cooling effect over time by elevating energy expenditure, potentially reducing the cooling effect. However, the analysis of the cooling perception of the activated vest revealed that more than 60% of the participants rated the cooling perception as average or higher, and the analysis of the IRT images which showed the decreased skin temperature following chronic CE, confirmed the effectiveness of the mild cooling protocol.

Taken together, the multitude of these diverse and non-standardized protocols presents a significant challenge when attempting to compare findings across different studies. Contrarily, in rodent studies, the housing conditions significantly vary. Cooling procedures often involve subjecting rodents to severe low temperatures at around 4°C for days and weeks, leading to heightened BAT and skeletal muscle activity. Therefore, it is crucial to note that directly translating these results obtained from severe cooling protocols in rodents to human studies is unfeasible. The observable physiological differences between humans and rodents, as highlighted by Warner and Mittag [77], pose a notable barrier in this translation process.

5 Limitations

The present work has some limitations, which need to be mentioned. The progress of this study started in March 2020 and was significantly disrupted by the COVID-19 pandemic and lockdown in Germany, which led to significant delays in recruitment and a smaller than expected cohort size. Additionally, challenges in reaching "healthy" patients with T2D, initially intended as part of the study's target group per the protocol, necessitated their exclusion from the study.

Due to hygiene and COVID-19 restrictions, we had to exclude indirect calorimetry, the gold-standard technique used to evaluate energy expenditure and BAT activity in cooling studies. Furthermore, complications arising from the insertion of a cannula in some participants necessitated the exclusion of this data at the end of our analysis. The protocol originally planned to include healthy women and men (each 50%); however, due to the difficulties in recruitment, the gender ratio reached 1:3 of women to men. These gender differences need to be considered in both metabolic and metagenomics analyses.

Furthermore, participants were only instructed to wear a thin T-shirt under the vest during the four weeks of CE, lacking standardized clothing. Also, while participants were advised to avoid certain foods and drinks the day before the experiment, the absence of a food diary across the study and standardized meals prior to experimental sessions in this study is evident. Using a cooling vest for the first time under free-living conditions posed a challenge in interpreting the project's outcomes. Additionally, focusing on the impact of CE on BAT activity and distinguishing between the “BAT+” and “BAT-” subgroups stand as a crucial initial phase in investigating BAT activation. Regrettably, limitations associated with nuclear imaging techniques prevented us from employing this method to categorize our participants and more precisely evaluate the BAT activity after chronic CE compared to BL.

The limitation of our Shotgun metagenomic analyses is also the small sample size, as only approximately 60% of the cohort provided the stool samples both at BL and after sub-chronic CE. The small sample size made the statistical power insufficient to detect small changes and affected the Benjamini-Hochberg correction values, therefore we addressed the uncorrected *p*-values in the results and discussion of this study.

Additionally, the shallow sequencing did not provide the information to analyze the microbiota at the strain level. However, it is important to mention that in comparison to the 16S method, which does not provide the data at the species level, our metagenomics analysis provided important data on the microbiome composition.

It is noteworthy that singular modification within a specific species or phylum seldom wields a dominant influence on shaping phenotypic outcomes [228] and it typically emerges from an interaction of different physiological and environmental factors.

6 Conclusion

The present study introduces a novel approach, employing chronic daily CE under free-living conditions and utilizing a local cooling vest in an RCT setting among healthy individuals but overweight or with mild obesity. The metabolic evaluation specifically involved the Botnia clamp approach, serving as the gold standard for assessing glucose homeostasis, complemented by advanced Shotgun metagenomic analysis to explore microbiota diversity following chronic daily CE compared to BL.

Intriguingly, post-chronic CE, we observed an increased FPIR and Disposition index, which reflect the improved β-cell function in individuals with overweight or mild obesity. An improved glucose tolerance compared to BL has been observed, although it did not reach the level of significance. As expected, we also observed an increase in subjective appetite feelings in our cohort after sub-chronic CE.

Furthermore, our results revealed no changes in fasting-level glucose metabolism hormones and metabolites, i.e., plasma glucose and insulin and C-peptide, between conditions, reflecting the importance of using the “gold standard” technique to evaluate the metabolic outcomes following interventions. Other metabolic conditions such as insulin sensitivity, BAT activity, and body composition remained unaltered, which was in accordance with our previous findings in sub-cohort with obesity after acute CE in the laboratory setting.

Comparison with our earlier study following acute CE, demonstrating improved glucose tolerance in obesity and enhanced insulin sensitivity in lean individuals, suggests independent mechanisms underlying glucose tolerance and insulin sensitivity.

The highlight of our investigations is the findings of the mechanism behind the increased insulin secretion following chronic CE and the importance of gut microbiota by using Shotgun metagenomic analysis. This analysis indicated a potential interplay between glucose metabolism and gut microbiota, notably identifying an increase in butyrate-producing species like *Bacteroides uniformis* after sub-chronic CE. *Bacteroides uniformis* is recognized for its impact on glucose metabolism, notably present in the 'Glycolysis I' pathway. The observed negative association between AUC of plasma glucose and Glycolysis I, suggests a potential role for butyrate producers in the metabolic changes after four weeks of chronic daily CE compared to BL. Alongside repeated measures correlation with *Bacteroides uniformis* and AUC of plasma glucose showed a positive correlation, yet it failed to reach the level of significance.

Moreover, the positive correlation observed between the elevated Disposition Index and FPIR with the increased abundance of butyrate producers further underscores the significant role of the microbiota in glucose metabolism.

All these findings suggest that chronic daily CE using a local cooling vest under free-living conditions is a new avenue to improve increase insulin secretion to combat obesity and related metabolic syndromes such as T2D.

7 Outlook

The gut microbiota produces a diverse array of metabolites, some of which enter the bloodstream and circulatory system [177]. Following the observed increase in butyrate-producers and glucose metabolism-related functional profiling pathways after chronic CE, there is a growing interest in understanding the mechanisms involving various metabolites like SCFAs, including butyrate, that play a role in the stimulation of GLP1, β-cell, and insulin secretion.

In the subsequent phase of this study, mass spectrometry will be utilized to assess a wide range of metabolites, including butyrate and bile acids. This pivotal step aims to uncover new connections between metagenomics, metabolites, and metabolic traits. Such an approach promises deeper insights into their potential interactions and crosstalk, advancing our understanding of these complex relationships.

Furthermore, for a comprehensive examination of the impact of CE on insulin sensitivity and BAT activity, I suggest incorporating lean participants into future studies, as they are exposed to have higher volume of active BAT. Additionally, for the chronic CE aspect, consider commencing exposure at 4 hours in the first week and progressively extending it to 6, 8, and 10 hours in subsequent weeks to minimize the potential possibility for adaptation to prolonged CE.

8 References

1. Iwen KA, Backhaus J, Cassens M, Waltl M, Hedesan OC, Merkel M, et al. Cold-Induced Brown Adipose Tissue Activity Alters Plasma Fatty Acids and Improves Glucose Metabolism in Men. The Journal of Clinical Endocrinology & Metabolism. November 1, 2017;102(11):4226–34.
2. Hanssen MJW, Hoeks J, Brans B, van der Lans AAJJ, Schaart G, van den Driessche JJ, et al. Short-term cold acclimation improves insulin sensitivity in patients with type 2 diabetes mellitus. Nat Med. August 2015;21(8):863–5.
3. Chevalier C, Stojanović O, Colin DJ, Suarez-Zamorano N, Tarallo V, Veyrat-Durebex C, et al. Gut Microbiota Orchestrates Energy Homeostasis during Cold. Cell. December 2015;163(6):1360–74.
4. Ichikawa N, Sasaki H, Lyu Y, Furuhashi S, Watabe A, Imamura M, et al. Cold Exposure during the Active Phase Affects the Short-Chain Fatty Acid Production of Mice in a Time-Specific Manner. Metabolites. December 27, 2021;12(1):20.
5. Zhu LB, Zhang YC, Huang HH, Lin J. Prospects for clinical applications of butyrate-producing bacteria. World Journal of Clinical Pediatrics. September 9, 2021;10(5):84.
6. WHO. WHO European Regional Obesity: Report 2022. Copenhagen: World Health Organization, Regional Office for Europe; 2022.
7. Spiegelman BM, Flier JS. Obesity and the Regulation of Energy Balance. Cell. February 2001;104(4):531–43.
8. Torres-Carot V, Suárez-González A, Lobato-Foulques C. The energy balance hypothesis of obesity: do the laws of thermodynamics explain excessive adiposity? Eur J Clin Nutr. October 2022;76(10):1374–9.
9. Franssens BT, Hoogduin H, Leiner T, van der Graaf Y, Visseren FLJ. Relation between brown adipose tissue and measures of obesity and metabolic dysfunction in patients with cardiovascular disease. Journal of Magnetic Resonance Imaging. 2017;46(2):497–504.
10. Ng TP, Jin A, Chow KY, Feng L, Nyunt MSZ, Yap KB. Age-dependent relationships between body mass index and mortality: Singapore longitudinal ageing study. Vinciguerra M, Herausgeber. PLoS ONE. July 24, 2017;12(7):e0180818.
11. Stevens J, Cai J, Pamuk ER, Williamson DF, Thun MJ, Wood JL. The effect of age on the association between body-mass index and mortality. N Engl J Med. January 1, 1998;338(1):1–7.
12. Abdelaal M, le Roux CW, Docherty NG. Morbidity and mortality associated with obesity. Ann Transl Med. April 2017;5(7):161.
13. Blüher M. Metabolically Healthy Obesity. Endocrine Reviews. June 1, 2020;41(3):bnaa004.
14. Blüher M. Obesity: global epidemiology and pathogenesis. Nat Rev Endocrinol. May 2019;15(5):288–98.
15. Farooqi IS, Matarese G, Lord GM, Keogh JM, Lawrence E, Agwu C, et al. Beneficial effects of leptin on obesity, T cell hyporesponsiveness, and neuroendocrine/metabolic dysfunction of human congenital leptin deficiency. J Clin Invest. October 2002;110(8):1093–103.
16. Farooqi IS, O'Rahilly S. 20 YEARS OF LEPTIN: Human disorders of leptin action. Journal of Endocrinology. October 2014;223(1):T63–70.
17. Knowler WC, Pettitt DJ, Bennett PH, Williams RC. Diabetes mellitus in the Pima Indians: Genetic and evolutionary considerations. Am J Phys Anthropol. September

1983;62(1):107- 14.
18. Schulz LO, Chaudhari LS. High-Risk Populations: The Pimas of Arizona and Mexico. Curr Obes Rep. March 2015;4(1):92–8.
19. Khan MAB, Hashim MJ, King JK, Govender RD, Mustafa H, Al Kaabi J. Epidemiology of Type 2 Diabetes – Global Burden of Disease and Forecasted Trends. J Epidemiol Glob Health. March 2020;10(1):107–11.
20. Marín-Peñalver JJ, Martín-Timón I, Sevillano-Collantes C, del Cañizo-Gómez FJ. Update on the treatment of type 2 diabetes mellitus. World J Diabetes. September 15, 2016;7(17):354–95.
21. Amanat S, Ghahri S, Dianatinasab A, Fararouei M, Dianatinasab M. Exercise and Type 2 Diabetes. Adv Exp Med Biol. 2020:1228:91–105.
22. Mahindru A, Patil P, Agrawal V. Role of Physical Activity on Mental Health and Well-Being: A Review. Curses. January 7, 2023;15(1):e33475.
23. Zahalka SJ, Abushamat LA, Scalzo RL, Reusch JEB, Feingold KR, Anawalt B, Blackman MR, Boyce A, Chrousos G, Corpas E, et al. The Role of Exercise in Diabetes. Endocrinology book. January 6, 2023.
24. Piercy KL, Troiano RP. Physical Activity Guidelines for Americans From the US Department of Health and Human Services: Cardiovascular Benefits and Recommendations. Circ: Cardiovascular Quality and Outcomes. November 2018;11(11):e005263.
25. Clemente-Suárez VJ, Beltrán-Velasco AI, Redondo-Flórez L, Martín-Rodríguez A, Tornero-Aguilera JF. Global Impacts of Western Diet and Its Effects on Metabolism and Health: A Narrative Review. Nutrients. June 14, 2023;15(12):2749.
26. Zinöcker MK, Lindseth IA. The Western Diet-Microbiome-Host Interaction and Its Role in Metabolic Disease. Nutrients. March 17, 2018;10(3):365.
27. Muscogiuri G, Verde L, Sulu C, Katsiki N, Hassapidou M, Frias-Toral E, et al. Mediterranean Diet and Obesity-related Disorders: What is the Evidence? Curr Obes Rep. 30. September 2022;11(4):287–304.
28. Shai I, Schwarzfuchs D, Henkin Y, Shahar DR, Witkow S, Greenberg I, et al. Weight loss with a low-carbohydrate, Mediterranean, or low-fat diet. N Engl J Med. July 17, 2008;359(3):229–41.
29. Martini D. Health Benefits of Mediterranean Diet. Nutrients. August 5, 2019;11(8):1802.
30. Arciero PJ, Poe M, Mohr AE, Ives SJ, Arciero A, Sweazea KL, etl al. Intermittent fasting and protein pacing are superior to caloric restriction for weight and visceral fat loss. Obesity (Silver Spring, Md). February 2023;31(Suppl 1):139.
31. Welton S, Minty R, O'Driscoll T, Willms H, Poirier D, Madden S, et al. Intermittent fasting and weight loss: Systematic review. Canadian Family Physician. February 2020;66(2):117.
32. van Baak MA, Mariman ECM. Dietary Strategies for Weight Loss Maintenance. Nutrients. August 15, 2019;11(8):1916.
33. Blomain ES, Dirhan DA, Valentino MA, Kim GW, Waldman SA. Mechanisms of Weight Regain following Weight Loss. ISRN Obes. 2013;2013:210524.
34. Srivastava G, Apovian CM. Current pharmacotherapy for obesity. Nat Rev Endocrinol. January 2018;14(1):12–24.
35. Apostolova N, Iannantuoni F, Gruevska A, Muntane J, Rocha M, Victor VM. Mechanisms of action of metformin in type 2 diabetes: Effects on mitochondria and leukocyte-endothelium interactions. Redox Biology. July 2020;34:101517.
36. Yerevanian A, Soukas AA. Metformin: Mechanisms in Human Obesity and Weight Loss.

Curr Obes Rep. June 2019;8(2):156–64.
37. Davies MJ, Aroda VR, Collins BS, Gabbay RA, Green J, Maruthur NM, et al. Management of Hyperglycemia in Type 2 Diabetes, 2022. A Consensus Report by the American Diabetes Association (ADA) and the European Association for the Study of Diabetes (EASD). Diabetes Care. 1. November 2022;45(11):2753–86.
38. Rehfeld JF. The Origin and Understanding of the Incretin Concept. Front Endocrinol. 16. July 2018;9:387.
39. Müller TD, Finan B, Bloom SR, D'Alessio D, Drucker DJ, Flatt PR, et al. Glucagon-like peptide 1 (GLP-1). Molecular Metabolism. December 2019;30:72–130.
40. Nadkarni P, Chepurny OG, Holz GG. Regulation of Glucose Homeostasis by GLP-1. Progress in Molecular Biology and Translational Science. 2014:121:23-65.
41. Almarshad F. Short-term monotherapy with Liraglutide for weight management: A case study. J Family Med Prim Care. 2019;8(5):1804.
42. Bonora E, Frias JP, Tinahones FJ, Van J, Malik RE, Yu Z, et al. Effect of dulaglutide 3.0 and 4.5 mg on weight in patients with type 2 diabetes: Exploratory analyses of AWARD -11. Diabetes Obesity Metabolism. October 2021;23(10):2242–50.
43. Wilding JPH, Batterham RL, Calanna S, Davies M, Van Gaal LF, Lingvay I, et al. Once-Weekly Semaglutide in Adults with Overweight or Obesity. N Engl J Med. March 18, 2021;384(11):989–1002.
44. Müller TD, Blüher M, Tschöp MH, DiMarchi RD. Anti-obesity drug discovery: advances and challenges. Nat Rev Drug Discov. March 2022;21(3):201–23.
45. Jastreboff AM, Aronne LJ, Ahmad NN, Wharton S, Connery L, Alves B, et al. Tirzepatide Once Weekly for the Treatment of Obesity. N Engl J Med. July 21, 2022;387(3):205–16.
46. Daneschvar HL, Aronson MD, Smetana GW. FDA-Approved Anti-Obesity Drugs in the United States. The American Journal of Medicine. August 2016;129(8):879.e1-879.e6.
47. Tak YJ, Lee SY. Long-Term Efficacy and Safety of Anti-Obesity Treatment: Where Do We Stand? Curr Obes Rep. March 2021;10(1):14–30.
48. Chumakova-Orin M, Vanetta C, Moris DP, Guerron AD. Diabetes remission after bariatric surgery. WJD. July 15, 2021;12(7):1093–101.
49. Moradi M, Kabir A, Khalili D, Lakeh MM, Dodaran MS, Pazouki A, et al. Type 2 diabetes remission after Roux-en-Y gastric bypass (RYGB), sleeve gastrectomy (SG), and one anastomosis gastric bypass (OAGB): results of the longitudinal assessment of bariatric surgery study. BMC Endocr Disord. October 26, 2022;22(1):260.
50. Arterburn DE, Telem DA, Kushner RF, Courcoulas AP. Benefits and Risks of Bariatric Surgery in Adults: A Review. JAMA. September 1, 2020;324(9):879.
51. Weiss D. Long-term Complications of Bariatric Surgery. JAMA. January 12, 2021;325(2):186.
52. Han TS, Lean ME. A clinical perspective of obesity, metabolic syndrome and cardiovascular disease. JRSM Cardiovascular Disease. January 1, 2016;5:204800401663337.
53. Jehan S, Zizi F, Pandi-Perumal SR, McFarlane SI, Jean-Louis G, Myers AK. Energy imbalance: obesity, associated comorbidities, prevention, management and public health implications. Adv Obes Weight Manag Control. 2020;10(5):146–61.
54. Arner P, Rydén M. Human white adipose tissue: A highly dynamic metabolic organ. J Intern Med. May 2022;291(5):611–21.
55. Cypess AM. Reassessing Human Adipose Tissue. Ingelfinger JR, Herausgeber. N Engl J Med. February 24, 2022;386(8):768–79.
56. Park A. Distinction of white, beige and brown adipocytes derived from mesenchymal stem cells. WJSC. 2014;6(1):33.

57. Lee MK, Lee B, Kim CY. Natural Extracts That Stimulate Adipocyte Browning and Their Underlying Mechanisms. Antioxidants. February 17, 2021;10(2):308.
58. Tabei S. Charakterisierung von Adipozytengröße und Makrophageninfiltration in verschiedenen humanen Fettgeweben. 2019;
59. Bjørndal B, Burri L, Staalesen V, Skorve J, Berge RK. Different Adipose Depots: Their Role in the Development of Metabolic Syndrome and Mitochondrial Response to Hypolipidemic Agents. Journal of Obesity. 2011;2011:1–15.
60. Chait A, Den Hartigh LJ. Adipose Tissue Distribution, Inflammation and Its Metabolic Consequences, Including Diabetes and Cardiovascular Disease. Front Cardiovasc Med. February 25, 2020;7:22.
61. Henry SL, Bensley JG, Wood-Bradley RJ, Cullen-McEwen LA, Bertram JF, Armitage JA. White adipocytes: More than just fat depots. The International Journal of Biochemistry & Cell Biology. March 2012;44(3):435–40.
62. Wronska A, Kmiec Z. Structural and biochemical characteristics of various white adipose tissue depots. Acta Physiol. June 2012;205(2):194–208.
63. Marketou ME, Buechler NS, Fragkiadakis K, Plevritaki A, Zervakis S, Maragkoudakis S, et al. Visceral fat and cardiometabolic future in children and adolescents: a critical update. Pediatr Res. July 4, 2023;94(5):1639-1647.
64. Massier L, Chakaroun R, Tabei S, Crane A, Didt KD, Fallmann J, et al. Adipose tissue derived bacteria are associated with inflammation in obesity and type 2 diabetes. Gut. October 2020;69(10):1796–806.
65. Raheem J, Sliz E, Shin J, Holmes MV, Pike GB, Richer L, et al. Visceral adiposity is associated with metabolic profiles predictive of type 2 diabetes and myocardial infarction. Commun Med. July 1, 2022;2(1):81.
66. Recinella L, Orlando G, Ferrante C, Chiavaroli A, Brunetti L, Leone S. Adipokines: New Potential Therapeutic Target for Obesity and Metabolic, Rheumatic, and Cardiovascular Diseases. Front Physiol. October 30, 2020;11:578966.
67. Kim JE, Kim JS, Jo MJ, Cho E, Ahn SY, Kwon YJ, et al. The Roles and Associated Mechanisms of Adipokines in Development of Metabolic Syndrome. Molecules. January 6, 2022;27(2):334.
68. Pilkington AC, Paz HA, Wankhade UD. Beige Adipose Tissue Identification and Marker Specificity—Overview. Front Endocrinol. March 12, 2021;12:599134.
69. Sharp LZ, Shinoda K, Ohno H, Scheel DW, Tomoda E, Ruiz L, et al. Human BAT Possesses Molecular Signatures That Resemble Beige/Brite Cells. Waki H, Herausgeber. PLoS ONE. November 16, 2012;7(11):e49452.
70. Bartelt A, Heeren J. Adipose tissue browning and metabolic health. Nature Reviews Endocrinology. January 1, 2014;10(1):24–36.
71. Thyagarajan B, Foster MT. Beiging of white adipose tissue as a therapeutic strategy for weight loss in humans. Hormone Molecular Biology and Clinical Investigation. Jun 23, 2017;31(2).
72. Finlin BS, Memetimin H, Confides AL, Kasza I, Zhu B, Vekaria HJ, et al. Human adipose beiging in response to cold and mirabegron. JCI Insight. August 9, 2018;3(15):e121510.
73. Giralt M, Villarroya F. White, Brown, Beige/Brite: Different Adipose Cells for Different Functions? Endocrinology. September 1, 2013;154(9):2992–3000.
74. Kiefer FW. Browning and thermogenic programing of adipose tissue. Best Practice & Research Clinical Endocrinology & Metabolism. August 2016;30(4):479–85.
75. Okamatsu-Ogura Y, Tsubota A, Ohyama K, Nogusa Y, Saito M, Kimura K. Capsinoids suppress diet-induced obesity through uncoupling protein 1-dependent mechanism in mice.

Journal of Functional Foods. December 2015;19:1–9.
76. Harb E, Kheder O, Poopalasingam G, Rashid R, Srinivasan A, Izzi-Engbeaya C. Brown adipose tissue and regulation of human body weight. Diabetes Metabolism Res. January 2023;39(1):e3594.
77. Warner A, Mittag J. Breaking BAT: can browning create a better white? Journal of Endocrinology. January 2016;228(1):R19–29.
78. Haman F, Blondin DP. Shivering thermogenesis in humans: Origin, contribution and metabolic requirement. Temperature. July 3, 2017;4(3):217–26.
79. Pan R, Chen Y. Management of Oxidative Stress: Crosstalk Between Brown/Beige Adipose Tissues and Skeletal Muscles. Front Physiol. September 16, 2021;12:712372.
80. Sahu B, Tikoo O, Pati B, Senapati U, Bal NC. Role of Distinct Fat Depots in Metabolic Regulation and Pathological Implications. Reviews of Physiology, Biochemistry and Pharmacology. 2023:186:135-176.
81. Scheele C, Wolfrum C. Brown Adipose Crosstalk in Tissue Plasticity and Human Metabolism. Endocr Rev. October 15, 2019;41(1):53–65.
82. Cypess AM, Lehman S, Williams G, Tal I, Rodman D, Goldfine AB, et al. Identification and Importance of Brown Adipose Tissue in Adult Humans. N Engl J Med. April 9, 2009;360(15):1509–17.
83. Scheel AK, Espelage L, Chadt A. Many Ways to Rome: Exercise, Cold Exposure and Diet—Do They All Affect BAT Activation and WAT Browning in the Same Manner? IJMS. 26. April 2022;23(9):4759.
84. Zhang Z, Yang D, Xiang J, Zhou J, Cao H, Che Q, et al. Non-shivering Thermogenesis Signalling Regulation and Potential Therapeutic Applications of Brown Adipose Tissue. Int J Biol Sci. 2021;17(11):2853–70.
85. Trayhurn P. Brown Adipose Tissue: A Short Historical Perspective. Methods Mol Biol. 2022:2448:1-18.
86. Smith RE, Hock RJ. Brown Fat: Thermogenic Effector of Arousal in Hibernators. Science. April 12, 1963;140(3563):199–200.
87. Lowell BB, S-Susulic V, Hamann A, Lawitts JA, Himms-Hagen J, Boyer BB, et al. Development of obesity in transgenic mice after genetic ablation of brown adipose tissue. Nature. 23. December 1993;366(6457):740–2.
88. Lidell ME. Brown Adipose Tissue in Human Infants. Handb Exp Pharmacol. 2019:251:107-123.
89. Saely CH, Geiger K, Drexel H. Brown versus white adipose tissue: a mini-review. Gerontology. 2012;58(1):15–23.
90. Van Marken Lichtenbelt WD, Vanhommerig JW, Smulders NM, Drossaerts JMAFL, Kemerink GJ, Bouvy ND, et al. Cold-Activated Brown Adipose Tissue in Healthy Men. N Engl J Med. April 9, 2009;360(15):1500–8.
91. Virtanen KA, Lidell ME, Orava J, Heglind M, Westergren R, Niemi T, et al. Functional Brown Adipose Tissue in Healthy Adults. N Engl J Med. April 9, 2009;360(15):1518–25.
92. Chondronikola M, Volpi E, Børsheim E, Porter C, Annamalai P, Enerbäck S, et al. Brown adipose tissue improves whole-body glucose homeostasis and insulin sensitivity in humans. Diabetes. December 2014;63(12):4089–99.
93. Porter C. Quantification of UCP1 function in human brown adipose tissue. Adipocyte. April 3, 2017;6(2):167–74.
94. Townsend K, Tseng YH. Brown adipose tissue: Recent insights into development, metabolic function and therapeutic potential. Adipocyte. January 2012;1(1):13–24.
95. Hoeke G, Kooijman S, Boon MR, Rensen PCN, Berbée JFP. Role of Brown Fat in

Lipoprotein Metabolism and Atherosclerosis. Circ Res. January 8, 2016;118(1):173–82.
96. Gaspar RC, Pauli JR, Shulman GI, Muñoz VR. An update on brown adipose tissue biology: a discussion of recent findings. American Journal of Physiology-Endocrinology and Metabolism. March 1, 2021;320(3):E488–95.
97. Deshmukh AS, Peijs L, Beaudry JL, Jespersen NZ, Nielsen CH, Ma T, et al. Proteomics-Based Comparative Mapping of the Secretomes of Human Brown and White Adipocytes Reveals EPDR1 as a Novel Batokine. Cell Metabolism. November 2019;30(5):963-975.e7.
98. Stanford KI, Middelbeek RJW, Townsend KL, An D, Nygaard EB, Hitchcox KM, et al. Brown adipose tissue regulates glucose homeostasis and insulin sensitivity. J Clin Invest. January 2013;123(1):215–23.
99. Dodangeh M, Dodangeh M. Metabolic regulation and the anti-obesity perspectives of brown adipose tissue (BAT); a systematic review. Obesity Medicine. March 2020;17:100163.
100. Martins FF, Souza-Mello V, Aguila MB, Mandarim-de-Lacerda CA. Brown adipose tissue as an endocrine organ: updates on the emerging role of batokines. Hormone Molecular Biology and Clinical Investigation. Jun3 30, 2023;44(2):219–27.
101. Ussar S, Lee KY, Dankel SN, Boucher J, Haering MF, Kleinridders A, et al. Asc-1, PAT2 and P2RX5 are novel cell surface markers for white, beige and brown adipocytes. Sci Transl Med. July 30, 2014;6(247):247ra103.
102. Fraum TJ, Crandall JP, Ludwig DR, Chen S, Fowler KJ, Laforest RA, et al. Repeatability of Quantitative Brown Adipose Tissue Imaging Metrics on Positron Emission Tomography with 18F-Fluorodeoxyglucose in Humans. Cell Metabolism. July 2019;30(1):212-224.e4.
103. Sun L, Camps SG, Goh HJ, Govindharajulu P, Schaefferkoetter JD, Townsend DW, et al. Capsinoids activate brown adipose tissue (BAT) with increased energy expenditure associated with subthreshold 18-fluorine fluorodeoxyglucose uptake in BAT-positive humans confirmed by positron emission tomography scan. Am J Clin Nutr. January 1, 2018;107(1):62–70.
104. Tay S, Goh H, Govindharajulu P, Cheng J, Camps S, Haldar S, et al. Brown Fat Activity Determined by Infrared Thermography and Thermogenesis Measurement Using Whole Body Calorimetry (BRIGHT Study). Physiol Res. February 18, 2020;85–97.
105. Law J, Chalmers J, Morris DE, Robinson L, Budge H, Symonds ME. The use of infrared thermography in the measurement and characterization of brown adipose tissue activation. Temperature. April 3, 2018;5(2):147–61.
106. Au-Yong ITH, Thorn N, Ganatra R, Perkins AC, Symonds ME. Brown Adipose Tissue and Seasonal Variation in Humans. Diabetes. November 1, 2009;58(11):2583–7.
107. Senn JR, Maushart CI, Gashi G, Michel R, Lalive d'Epinay M, Vogt R, et al. Outdoor Temperature Influences Cold Induced Thermogenesis in Humans. Front Physiol. August 23, 2018;9:1184.
108. Vijgen GHEJ, Bouvy ND, Teule GJJ, Brans B, Schrauwen P, Van Marken Lichtenbelt WD. Brown Adipose Tissue in Morbidly Obese Subjects. Fadini GP, Herausgeber. PLoS ONE. February 24, 2011;6(2):e17247.
109. Yoneshiro T, Aita S, Matsushita M, Kayahara T, Kameya T, Kawai Y, et al. Recruited brown adipose tissue as an antiobesity agent in humans. J Clin Invest. August1, 2013;123(8):3404–8.
110. Levy SB. Brown adipose tissue and type 2 diabetes. Evolution, Medicine, and Public Health. January 1, 2020;2020(1):70–1.
111. Hoffman JM, Valencak TG. Sex differences and aging: Is there a role of brown adipose tissue? Molecular and Cellular Endocrinology. July 2021;531:111310.
112. Pfannenberg C, Werner MK, Ripkens S, Stef I, Deckert A, Schmadl M, et al. Impact of Age on the Relationships of Brown Adipose Tissue With Sex and Adiposity in Humans.

Diabetes. July 1, 2010;59(7):1789–93.
113. Bartness TJ, Vaughan CH, Song CK. Sympathetic and sensory innervation of brown adipose tissue. Int J Obes. October 2010;34(S1):S36–42.
114. Nonogaki K. New insights into sympathetic regulation of glucose and fat metabolism. Diabetologia. May 2000;43(5):533–49.
115. Moullé VS, Tremblay C, Castell AL, Vivot K, Ethier M, Fergusson G, et al. The autonomic nervous system regulates pancreatic β-cell proliferation in adult male rats. Am J Physiol Endocrinol Metab. August 1, 2019;317(2):E234–43.
116. Collins S. β-Adrenergic Receptors and Adipose Tissue Metabolism: Evolution of an Old Story. Annu Rev Physiol. February 10, 2022;84(1):1–16.
117. O'Mara AE, Johnson JW, Linderman JD, Brychta RJ, McGehee S, Fletcher LA, et al. Chronic mirabegron treatment increases human brown fat, HDL cholesterol, and insulin sensitivity. Journal of Clinical Investigation. March 23, 2020;130(5):2209–19.
118. Bel JS, Tai TC, Khaper N, Lees SJ. Mirabegron: The most promising adipose tissue beiging agent. Physiol Rep. March 2021;9(5).
119. Blondin DP, Nielsen S, Kuipers EN, Severinsen MC, Jensen VH, Miard S, et al. Human Brown Adipocyte Thermogenesis Is Driven by β2-AR Stimulation. Cell Metabolism. August 4, 2020;32(2):287-300.e7.
120. Hibi M, Oishi S, Matsushita M, Yoneshiro T, Yamaguchi T, Usui C, et al. Brown adipose tissue is involved in diet-induced thermogenesis and whole-body fat utilization in healthy humans. Int J Obes (Lond). November 2016;40(11):1655–61.
121. Rothwell NJ, Stock MJ. A Role for Brown Adipose Tissue in Diet-Induced Thermogenesis. Obesity Research. November 1997;5(6):650–6.
122. Saito M, Matsushita M, Yoneshiro T, Okamatsu-Ogura Y. Brown Adipose Tissue, Diet-Induced Thermogenesis, and Thermogenic Food Ingredients: From Mice to Men. Front Endocrinol. April 21, 2020;11:222.
123. Vosselman MJ, Brans B, van der Lans AA, Wierts R, van Baak MA, Mottaghy FM, et al. Brown adipose tissue activity after a high-calorie meal in humans. The American Journal of Clinical Nutrition. July 1, 2013;98(1):57–64.
124. Von Essen G, Lindsund E, Cannon B, Nedergaard J. Adaptive facultative diet-induced thermogenesis in wild-type but not in UCP1-ablated mice. American Journal of Physiology-Endocrinology and Metabolism. November 1, 2017;313(5):E515–27.
125. Ang QY, Goh HJ, Cao Y, Li Y, Chan SP, Swain JL, et al. A new method of infrared thermography for quantification of brown adipose tissue activation in healthy adults (TACTICAL): a randomized trial. J Physiol Sci. May 2017;67(3):395–406.
126. Yoneshiro T, Aita S, Kawai Y, Iwanaga T, Saito M. Nonpungent capsaicin analogs (capsinoids) increase energy expenditure through the activation of brown adipose tissue in humans. Am J Clin Nutr. April 2012;95(4):845–50.
127. Van Schaik L, Kettle C, Green R, Sievers W, Hale MW, Irving HR, et al. Stimulatory, but not anxiogenic, doses of caffeine act centrally to activate interscapular brown adipose tissue thermogenesis in anesthetized male rats. Sci Rep. January 8, 2021;11(1):113.
128. Velickovic K, Wayne D, Leija HAL, Bloor I, Morris DE, Law J, et al. Caffeine exposure induces browning features in adipose tissue in vitro and in vivo. Sci Rep. June 24, 2019;9(1):9104.
129. Stallknecht B, Vinten J, Ploug T, Galbo H. Increased activities of mitochondrial enzymes in white adipose tissue in trained rats. American Journal of Physiology-Endocrinology and Metabolism. September 1, 1991;261(3):E410–4.
130. Maliszewska K, Kretowski A. Brown Adipose Tissue and Its Role in Insulin and Glucose

Homeostasis. IJMS. February 3, 2021;22(4):1530.
131. Bonfante ILP, Monfort-Pires M, Duft RG, Da Silva Mateus KC, De Lima Júnior JC, Dos Santos Trombeta JC, et al. Combined training increases thermogenic fat activity in patients with overweight and type 2 diabetes. Int J Obes. June 2022;46(6):1145–54.
132. Vidal P, Stanford KI. Exercise-Induced Adaptations to Adipose Tissue Thermogenesis. Front Endocrinol. April 29, 2020;11:270.
133. Dittner C, Lindsund E, Cannon B, Nedergaard J. At thermoneutrality, acute thyroxine-induced thermogenesis and pyrexia are independent of UCP1. Molecular Metabolism. July 2019;25:20–34.
134. Oelkrug R, Harder L, Pedaran M, Hoffmann A, Kolms B, Inderhees J, et al. Maternal thyroid hormone receptor β activation in mice sparks brown fat thermogenesis in the offspring. Nat Commun. October 24, 2023;14(1):6742.
135. Sentis SC, Oelkrug R, Mittag J. Thyroid hormones in the regulation of brown adipose tissue thermogenesis. Endocr Connect. January 20, 2021;10(2):R106–15.
136. Sinha RA, Singh BK, Yen PM. Direct effects of thyroid hormones on hepatic lipid metabolism. Nat Rev Endocrinol. May 2018;14(5):259–69.
137. Weiner J, Kranz M, Klöting N, Kunath A, Steinhoff K, Rijntjes E, et al. Thyroid hormone status defines brown adipose tissue activity and browning of white adipose tissues in mice. Sci Rep. December 12, 2016;6(1):38124.
138. Chartoumpekis DV, Habeos IG, Ziros PG, Psyrogiannis AI, Kyriazopoulou VE, Papavassiliou AG. Brown Adipose Tissue Responds to Cold and Adrenergic Stimulation by Induction of FGF21. Mol Med. July 2011;17(7–8):736–40.
139. Westerlund T, Uusitalo A, Smolander J, Mikkelsson M. Heart rate variability in women exposed to very cold air (−110°C) during whole-body cryotherapy. Journal of Thermal Biology. May 2006;31(4):342–6.
140. Shida A, Ikeda T, Tani N, Morioka F, Aoki Y, Ikeda K, et al. Cortisol levels after cold exposure are independent of adrenocorticotropic hormone stimulation. Bonaz B, Herausgeber. PLoS ONE. February 18, 2020;15(2):e0218910.
141. Tsibul'nikov SYu, Maslov LN, Naryzhnaya NV, Ivanov VV, Lishmanov YuB. Specific features of adaptation of rats to chronic cold treatment. Dokl Biol Sci. September 2016;470(1):214–6.
142. Leppäluoto J, Westerlund T, Huttunen P, Oksa J, Smolander J, Dugué B, et al. Effects of long-term whole-body cold exposures on plasma concentrations of ACTH, beta-endorphin, cortisol, catecholamines and cytokines in healthy females. Scandinavian Journal of Clinical and Laboratory Investigation. January 2008;68(2):145–53.
143. Ravussin Y, Xiao C, Gavrilova O, Reitman ML. Effect of Intermittent Cold Exposure on Brown Fat Activation, Obesity, and Energy Homeostasis in Mice. Aguila MB, Herausgeber. PLoS ONE. 17. January 2014;9(1):e85876.
144. van der Lans AAJJ, Hoeks J, Brans B, Vijgen GHEJ, Visser MGW, Vosselman MJ, et al. Cold acclimation recruits human brown fat and increases nonshivering thermogenesis. J Clin Invest. August 1, 2013;123(8):3395–403.
145. Van Marken Lichtenbelt WD, Schrauwen P. Implications of nonshivering thermogenesis for energy balance regulation in humans. American Journal of Physiology-Regulatory, Integrative and Comparative Physiology. August 2011;301(2):R285–96.
146. Van Marken Lichtenbelt WD, Schrauwen P, Van De Kerckhove S, Westerterp-Plantenga MS. Individual variation in body temperature and energy expenditure in response to mild cold. American Journal of Physiology-Endocrinology and Metabolism. May 1, 2002;282(5):E1077–83.

147. Horn DB, Almandoz JP, Look M. What is clinically relevant weight loss for your patients and how can it be achieved? A narrative review. Postgraduate Medicine. May 19, 2022;134(4):359–75.
148. Heeren J, Scheja L. Brown adipose tissue and lipid metabolism. Current Opinion in Lipidology. June 2018;29(3):180–5.
149. Bartelt A, Bruns OT, Reimer R, Hohenberg H, Ittrich H, Peldschus K, et al. Brown adipose tissue activity controls triglyceride clearance. Nat Med. February 2011;17(2):200–5.
150. Chondronikola M, Volpi E, Børsheim E, Porter C, Saraf MK, Annamalai P, et al. Brown Adipose Tissue Activation Is Linked to Distinct Systemic Effects on Lipid Metabolism in Humans. Cell Metab. June 14, 2016;23(6):1200–6.
151. Vosselman MJ, van der Lans AAJJ, Brans B, Wierts R, van Baak MA, Schrauwen P, et al. Systemic β-Adrenergic Stimulation of Thermogenesis Is Not Accompanied by Brown Adipose Tissue Activity in Humans. Diabetes. December 2012;61(12):3106–13.
152. Vosselman MJ, Hoeks J, Brans B, Pallubinsky H, Nascimento EBM, van der Lans AAJJ, et al. Low brown adipose tissue activity in endurance-trained compared with lean sedentary men. Int J Obes. December 2015;39(12):1696–702.
153. U Din M, Raiko J, Saari T, Kudomi N, Tolvanen T, Oikonen V, et al. Human brown adipose tissue [15O]O2 PET imaging in the presence and absence of cold stimulus. Eur J Nucl Med Mol Imaging. September 2016;43(10):1878–86.
154. Peres Valgas Da Silva C, Hernández-Saavedra D, White J, Stanford K. Cold and Exercise: Therapeutic Tools to Activate Brown Adipose Tissue and Combat Obesity. Biology. February 12, 2019;8(1):9.
155. Cannon B, Nedergaard J. Brown Adipose Tissue: Function and Physiological Significance. Physiological Reviews. January 2004;84(1):277–359.
156. Orava J, Nuutila P, Lidell ME, Oikonen V, Noponen T, Viljanen T, et al. Different Metabolic Responses of Human Brown Adipose Tissue to Activation by Cold and Insulin. Cell Metabolism. August 3, 2011;14(2):272–9.
157. Aronoff SL, Berkowitz K, Shreiner B, Want L. Glucose Metabolism and Regulation: Beyond Insulin and Glucagon. Diabetes Spectrum. July 1, 2004;17(3):183–90.
158. Ahmed B, Sultana R, Greene MW. Adipose tissue and insulin resistance in obese. Biomedicine & Pharmacotherapy. May 2021;137:111315.
159. Röder PV, Wu B, Liu Y, Han W. Pancreatic regulation of glucose homeostasis. Exp Mol Med. March 11, 2016;48(3):e219–e219.
160. Bano G. Glucose homeostasis, obesity and diabetes. Best Practice & Research Clinical Obstetrics & Gynaecology. October 2013;27(5):715–26.
161. Brandenburg D. History and Diagnostic Significance of C-Peptide. Experimental Diabetes Research. 2008;2008:1–7.
162. Polonsky KS, Rubenstein AH. C-Peptide as a Measure of the Secretion and Hepatic Extraction of Insulin: Pitfalls and Limitations. Diabetes. May 1, 1984;33(5):486–94.
163. Lam CKL, Chari M, Lam TKT. CNS Regulation of Glucose Homeostasis. Physiology. June 2009;24(3):159–70.
164. Meyhöfer S, Dembinski K, Schultes B, Born J, Wilms B, Lehnert H, et al. Sleep deprivation prevents counterregulatory adaptation to recurrent hypoglycaemia. Diabetologia. July 2022;65(7):1212–21.
165. Wilms B, Leineweber EM, Mölle M, Chamorro R, Pommerenke C, Salinas-Riester G, et al. Sleep Loss Disrupts Morning-to-Evening Differences in Human White Adipose Tissue Transcriptome. The Journal of Clinical Endocrinology & Metabolism. May 1, 2019;104(5):1687–96.

166. Norton L, Lewis N, Norton. Exercise training improves fasting glucose control. OAJSM. November 2012;209.
167. Nakamura K, Tajiri E, Hatamoto Y, Ando T, Shimoda S, Yoshimura E. Eating Dinner Early Improves 24-h Blood Glucose Levels and Boosts Lipid Metabolism after Breakfast the Next Day: A Randomized Cross-Over Trial. Nutrients. July 15, 2021;13(7):2424.
168. Echouffo-Tcheugui JB, Perreault L, Ji L, Dagogo-Jack S. Diagnosis and Management of Prediabetes: A Review. JAMA. April 11, 2023;329(14):1206.
169. Harreiter J, Roden M. Diabetes mellitus – Definition, Klassifikation, Diagnose, Screening und Prävention (Update 2023). Wien Klin Wochenschr. Januar 2023;135(S1):7–17.
170. Tripathy D, Wessman Y, Gullström M, Tuomi T, Groop L. Importance of Obtaining Independent Measures of Insulin Secretion and Insulin Sensitivity During the Same Test. Diabetes Care. May 1, 2003;26(5):1395–401.
171. DeFronzo RA, Tobin JD, Andres R. Glucose clamp technique: a method for quantifying insulin secretion and resistance. American Journal of Physiology-Endocrinology and Metabolism. September 1, 1979;237(3):E214.
172. Turnbaugh PJ, Ley RE, Hamady M, Fraser-Liggett CM, Knight R, Gordon JI. The Human Microbiome Project. Nature. October 2007;449(7164):804–10.
173. Deschasaux M, Bouter KE, Prodan A, Levin E, Groen AK, Herrema H, et al. Depicting the composition of gut microbiota in a population with varied ethnic origins but shared geography. Nat Med. October 2018;24(10):1526–31.
174. Coelho GDP, Ayres LFA, Barreto DS, Henriques BD, Prado MRMC, Passos CMD. Acquisition of microbiota according to the type of birth: an integrative review. Rev Latino-Am Enfermagem. 2021;29:e3446.
175. Jandhyala SM. Role of the normal gut microbiota. WJG. 2015;21(29):8787.
176. Rinninella E, Raoul P, Cintoni M, Franceschi F, Miggiano G, Gasbarrini A, et al. What is the Healthy Gut Microbiota Composition? A Changing Ecosystem across Age, Environment, Diet, and Diseases. Microorganisms. January 10, 2019;7(1):14.
177. Fan Y, Pedersen O. Gut microbiota in human metabolic health and disease. Nat Rev Microbiol. January 2021;19(1):55–71.
178. Thomas T, Gilbert J, Meyer F. Metagenomics - a guide from sampling to data analysis. Microb Informatics Exp. December 2012;2(1):3.
179. Zheng D, Liwinski T, Elinav E. Interaction between microbiota and immunity in health and disease. Cell Res. June 2020;30(6):492–506.
180. Tang WHW, Kitai T, Hazen SL. Gut Microbiota in Cardiovascular Health and Disease. Circ Res. 31. March 2017;120(7):1183–96.
181. Turnbaugh PJ, Gordon JI. The core gut microbiome, energy balance and obesity. The Journal of Physiology. September 2009;587(17):4153–8.
182. Arora T, Bäckhed F. The gut microbiota and metabolic disease: current understanding and future perspectives. J Intern Med. October 2016;280(4):339–49.
183. Kootte RS, Vrieze A, Holleman F, Dallinga-Thie GM, Zoetendal EG, De Vos WM, et al. The therapeutic potential of manipulating gut microbiota in obesity and type 2 diabetes mellitus. Diabetes, Obesity and Metabolism. February 2012;14(2):112–20.
184. Wells JM, Brummer RJ, Derrien M, MacDonald TT, Troost F, Cani PD, et al. Homeostasis of the gut barrier and potential biomarkers. Am J Physiol Gastrointest Liver Physiol. March 1, 2017;312(3):G171–93.
185. Karl JP, Hatch AM, Arcidiacono SM, Pearce SC, Pantoja-Feliciano IG, Doherty LA, et al. Effects of Psychological, Environmental and Physical Stressors on the Gut Microbiota. Front Microbiol. 11. September 2018;9:2013.

186. Li B, Li L, Li M, Lam SM, Wang G, Wu Y, et al. Microbiota Depletion Impairs Thermogenesis of Brown Adipose Tissue and Browning of White Adipose Tissue. Cell Reports. March 2019;26(10):2720-2737.e5.
187. Larsen N, Vogensen FK, Van Den Berg FWJ, Nielsen DS, Andreasen AS, Pedersen BK, et al. Gut Microbiota in Human Adults with Type 2 Diabetes Differs from Non-Diabetic Adults. Bereswill S, Herausgeber. PLoS ONE. February 5, 2010;5(2):e9085.
188. Cunningham AL, Stephens JW, Harris DA. Gut microbiota influence in type 2 diabetes mellitus (T2DM). Gut Pathog. December 2021;13(1):50.
189. Furet JP, Kong LC, Tap J, Poitou C, Basdevant A, Bouillot JL, et al. Differential Adaptation of Human Gut Microbiota to Bariatric Surgery–Induced Weight Loss. Diabetes. December 1, 2010;59(12):3049–57.
190. Li Y, Yun K, Mu R. A review on the biology and properties of adipose tissue macrophages involved in adipose tissue physiological and pathophysiological processes. Lipids Health Dis. December 2020;19(1):164.
191. Sedighi M, Razavi S, Navab-Moghadam F, Khamseh M, Alaei Shahmiri F, Mehrtash A, et al. Comparison of gut microbiota in adult patients with type 2 diabetes and healthy individuals. Microbial Pathogenesis. September 1, 2017;111.
192. Gauffin Cano P, Santacruz A, Moya Á, Sanz Y. Bacteroides uniformis CECT 7771 Ameliorates Metabolic and Immunological Dysfunction in Mice with High-Fat-Diet Induced Obesity. Bereswill S, Herausgeber. PLoS ONE. July 26, 2012;7(7):e41079.
193. R L, J H, X X, Q F, D Z, Y G, et al. Gut microbiome and serum metabolome alterations in obesity and after weight-loss intervention. Nature medicine. July 2017;23(7):859-868.
194. Vanhoutvin SALW, Troost FJ, Hamer HM, Lindsey PJ, Koek GH, Jonkers DMAE, et al. Butyrate-Induced Transcriptional Changes in Human Colonic Mucosa. Bereswill S, Herausgeber. PLoS ONE. 25. August 2009;4(8):e6759.
195. Sanna S, Van Zuydam NR, Mahajan A, Kurilshikov A, Vich Vila A, Võsa U, et al. Causal relationships among the gut microbiome, short-chain fatty acids and metabolic diseases. Nat Genet. April 2019;51(4):600–5.
196. Perry RJ, Peng L, Barry NA, Cline GW, Zhang D, Cardone RL, et al. Acetate mediates a microbiome–brain–β-cell axis to promote metabolic syndrome. Nature. June 9, 2016;534(7606):213–7.
197. Liu JL, Segovia I, Yuan XL, Gao Z hua. Controversial Roles of Gut Microbiota-Derived Short-Chain Fatty Acids (SCFAs) on Pancreatic β-Cell Growth and Insulin Secretion. International Journal of Molecular Sciences. February 2020;21(3).
198. Zhao L, Zhang F, Ding X, Wu G, Lam YY, Wang X, et al. Gut bacteria selectively promoted by dietary fibers alleviate type 2 diabetes. Science. March 9, 2018;359(6380):1151–6.
199. Portincasa P, Bonfrate L, Vacca M, De Angelis M, Farella I, Lanza E, et al. Gut Microbiota and Short Chain Fatty Acids: Implications in Glucose Homeostasis. International Journal of Molecular Sciences. January 2022;23(3):1105.
200. Li Z, Yi CX, Katiraei S, Kooijman S, Zhou E, Chung CK, et al. Butyrate reduces appetite and activates brown adipose tissue via the gut-brain neural circuit. Gut. July 2018;67(7):1269–79.
201. May KS, Den Hartigh LJ. Gut Microbial-Derived Short Chain Fatty Acids: Impact on Adipose Tissue Physiology. Nutrients. January 5, 2023;15(2):272.
202. Lim S, Honek J, Xue Y, Seki T, Cao Z, Andersson P, et al. Cold-induced activation of brown adipose tissue and adipose angiogenesis in mice. Nat Protoc. March 2012;7(3):606–15.
203. Chen JQ, Zhang LW, Zhao RM, Wu HX, Lin LH, Li P, et al. Gut microbiota differs between two cold-climate lizards distributed in thermally different regions. BMC Ecol Evo. December

2022;22(1):1–13.
204. Santisteban JA, Brown TG, Gruber R. Association between the Munich Chronotype Questionnaire and Wrist Actigraphy. Sleep Disorders. May 9, 2018:5646848.
205. Rs F, Gj L, K B, T LA. Measuring Physical Activity in Older Adults Using MotionWatch 8 Actigraphy: How Many Days are Needed? Journal of aging and physical activity. January 2017;25(1).
206. Bosy-Westphal A, Mast M, Eichhorn C, Becker C, Kutzner D, Heller M, et al. Validation of air-displacement plethysmography for estimation of body fat mass in healthy elderly subjects. European Journal of Nutrition. August 1, 2003;42(4):207–16.
207. Ware JE, Sherbourne CD. The MOS 36-item short-form health survey (SF-36). I. Conceptual framework and item selection. Med Care. June 1992;30(6):473–83.
208. I H, M UD. Brown Adipose Tissue: Activation and Metabolism in Humans. Endocrinology and metabolism. April 2023;38(2):214-222.
209. Berridge KC, Robinson TE, Aldridge JW. Dissecting components of reward: 'liking', 'wanting', and learning. Current opinion in pharmacology. February 2009;9(1):65.
210. Finlayson G, Dalton M. Hedonics of Food Consumption: Are Food 'Liking' and 'Wanting' Viable Targets for Appetite Control in the Obese? Curr Obes Rep. March 2012;1(1):42–9.
211. Goldberger JJ. Sympathovagal balance: how should we measure it? American Journal of Physiology-Heart and Circulatory Physiology. April 1999;276(4):H1273–80.
212. Malik M. Heart Rate Variability. Annals of Noninvasive Electrocardiology. April 1, 1996;1(2):151–81.
213. Khalili D, Khayamzadeh M, Kohansal K, Ahanchi NS, Hasheminia M, Hadaegh F, et al. Are HOMA-IR and HOMA-B good predictors for diabetes and pre-diabetes subtypes? BMC Endocr Disord. February 14, 2023;23(1):39.
214. Kieser S, Brown J, Zdobnov EM, Trajkovski M, McCue LA. ATLAS: a Snakemake workflow for assembly, annotation, and genomic binning of metagenome sequence data. BMC Bioinformatics. December 2020;21(1):1–8.
215. Blanco-Míguez A, Beghini F, Cumbo F, McIver LJ, Thompson KN, Zolfo M, et al. Extending and improving metagenomic taxonomic profiling with uncharacterized species using MetaPhlAn 4. Nat Biotechnol. November 2023;41(11):1633–44.
216. Beghini F, McIver LJ, Blanco-Míguez A, Dubois L, Asnicar F, Maharjan S, et al. Integrating taxonomic, functional, and strain-level profiling of diverse microbial communities with bioBakery 3. ELife. May 4, 2021:10:e65088.
217. Fernández-Cuevas I, Bouzas Marins JC, Arnáiz Lastras J, Gómez Carmona PM, Piñonosa Cano S, García-Concepción MÁ, et al. Classification of factors influencing the use of infrared thermography in humans: A review. Infrared Physics & Technology. July 2015;71:28–55.
218. Schmid SM, Hallschmid M, Schultes B. The metabolic burden of sleep loss. The Lancet Diabetes & Endocrinology. January 2015;3(1):52–62.
219. Sondrup N, Termannsen AD, Eriksen JN, Hjorth MF, Færch K, Klingenberg L, et al. Effects of sleep manipulation on markers of insulin sensitivity: A systematic review and meta-analysis of randomized controlled trials. Sleep Medicine Reviews. April 2022;62:101594.
220. Puttonen S, Viitasalo K, Härmä M. The relationship between current and former shift work and the metabolic syndrome. Scand J Work Environ Health. July 2012;38(4):343–8.
221. Sharma A, Laurenti MC, Dalla Man C, Varghese RT, Cobelli C, Rizza RA, et al. Glucose metabolism during rotational shift-work in healthcare workers. Diabetologia. August 2017;60(8):1483–90.
222. Saito M. Capsaicin and Related Food Ingredients Reducing Body Fat Through the Activation of TRP and Brown Fat Thermogenesis. Advances in Food and Nutrition Research.

2015:76:1–28.
223. Lazaridi A. Identification of factors that stimulate the brown adipose tissue in healthy adults and patients. University of Nottingham; 2020.
224. Me S, K H, L E, C B, D S, Ac P, et al. Thermal imaging to assess age-related changes of skin temperature within the supraclavicular region co-locating with brown adipose tissue in healthy children. The Journal of pediatrics. November 2012;161(5).
225. P L, Kk H, P L, Jr G, Kk H, Jr G. Hot fat in a cool man: infrared thermography and brown adipose tissue. Diabetes, obesity & metabolism. January 2011;13(1).
226. Aw F, Ri C, G von E, B C, J N. No insulating effect of obesity. American journal of physiology Endocrinology and metabolism. January 7, 2016;311(1).
227. Ma B. Sex Differences in Body Composition. Advances in experimental medicine and biology. 2017;1043.
228. Hankir MK, Klingenspor M. Brown adipocyte glucose metabolism: a heated subject. EMBO Reports. September 2018;19(9). /
229. M B, Dr M, Be S, Sr B. Delineation of myocardial oxygen utilization with carbon-11-labeled acetate. Circulation. September 1987;76(3).
230. Tr D, Hh C, G S. 14(R,S)-[18F]fluoro-6-thia-heptadecanoic acid (FTHA): evaluation in mouse of a new probe of myocardial utilization of long chain fatty acids. Journal of nuclear medicine. October 1991;32(10):1888-96.
231. B A, H K, D R, Am VC, Y G, Si P, et al. Associations Between Extreme Temperatures and Cardiovascular Cause-Specific Mortality: Results From 27 Countries. Circulation. Jan 3, 2023;147(1).
232. Cold weather-related cardiorespiratory symptoms predict higher morbidity and mortality. Environmental Research. December 1, 2020;191:110108.
233. Pääkkönen T, Leppäluoto J. Cold exposure and hormonal secretion: A review. International Journal of Circumpolar Health. September 1, 2002
234. F Y, R S. Modulation of arterial baroreflex control of heart rate by skin cooling and heating in humans. Journal of applied physiology. February 2000;88(2):393-400.
235. Saito M, Okamatsu-Ogura Y, Matsushita M, Watanabe K, Yoneshiro T, Nio-Kobayashi J, et al. High Incidence of Metabolically Active Brown Adipose Tissue in Healthy Adult Humans: Effects of Cold Exposure and Adiposity. Diabetes. July 1, 2009;58(7):1526–31.
236. Aj Kowaltowski. Cold Exposure and the Metabolism of Mice, Men, and Other Wonderful Creatures. Physiology (Bethesda). September 1, 2022;37(5).
237. Tibboel H, De Houwer J, Van Bockstaele B. Implicit measures of “wanting” and “liking” in humans. Neuroscience & Biobehavioral Reviews. October 2015;57:350–64.
238. Langeveld M, Tan CY, Soeters MR, Virtue S, Ambler GK, Watson LPE, et al. Mild cold effects on hunger, food intake, satiety and skin temperature in humans. Endocrine Connections. March 2016;5(2):65–73.
239. Blondin DP, Daoud A, Taylor T, Tingelstad HC, Bézaire V, Richard D, et al. Four-week cold acclimation in adult humans shifts uncoupling thermogenesis from skeletal muscles to brown adipose tissue. J Physiol. March 15, 2017;595(6):2099–113.
240. Blondin DP, Labbé SM, Tingelstad HC, Noll C, Kunach M, Phoenix S, et al. Increased Brown Adipose Tissue Oxidative Capacity in Cold-Acclimated Humans. J Clin Endocrinol Metab. March 2014;99(3):E438–46.
241. Thackray AE, Stensel D. The impact of acute exercise on appetite control: Current insights and future perspectives. Appetite. July 1, 2023;186:106557.
242. Chondronikola M, Porter C, Malagaris I, Nella AA, Sidossis LS. Brown Adipose Tissue is Associated with Systemic Concentrations of Peptides Secreted from the Gastrointestinal

System and Involved in Appetite Regulation. Eur J Endocrinol. July 2017;177(1):33–40.
243. u Din M, Raiko J, Saari T, Kudomi N, Tolvanen T, Oikonen V, . Human brown adipose tissue [15O]O2 PET imaging in the presence and absence of cold stimulus. Eur J Nucl Med Mol Imaging. September 1, 2016;43(10):1878–86.
244. Wijers SLJ, Schrauwen P, van Baak MA, Saris WHM, van Marken Lichtenbelt WD. β-Adrenergic Receptor Blockade Does Not Inhibit Cold-Induced Thermogenesis in Humans: Possible Involvement of Brown Adipose Tissue. The Journal of Clinical Endocrinology & Metabolism. April 1, 2011;96(4):E598–605.
245. McKie GL, Shamshoum H, Hunt KL, Thorpe HHA, Dibe HA, Khokhar JY, et al. Intermittent cold exposure improves glucose homeostasis despite exacerbating diet-induced obesity in mice housed at thermoneutrality. The Journal of Physiology. February 2022;600(4):829–45.
246. Lin JD. Levels of the first-phase insulin secretion deficiency as a predictor for type 2 diabetes onset by using clinical-metabolic models. Annals of Saudi Medicine. April 2015;35(2):138.
247. C M, Kn BM, C D, Sh J, Nb J, Vb K, et al. Immediate enhancement of first-phase insulin secretion and unchanged glucose effectiveness in patients with type 2 diabetes after Roux-en-Y gastric bypass. American journal of physiology Endocrinology and metabolism. March 15, 2015;308(6).
248. Søberg S, Löfgren J, Philipsen FE, Jensen M, Hansen AE, Ahrens E, et al. Altered brown fat thermoregulation and enhanced cold-induced thermogenesis in young, healthy, winter-swimming men. Cell Reports Medicine. October 2021;2(10):100408.
249. Gasparetti AL, Souza CT, Pereira-da-Silva M, Oliveira RLGS, Saad MJA, Carneiro EM, et al. Cold Exposure Induces Tissue-Specific Modulation of the Insulin-Signalling Pathway in *Rattus Norvegicus*. The Journal of Physiology. October 2003;552(1):149–62.
250. Vallerand AL, Perusse F, Bukowiecki LJ. Stimulatory effects of cold exposure and cold acclimation on glucose uptake in rat peripheral tissues. American Journal of Physiology-Regulatory, Integrative and Comparative Physiology. November 1, 1990;259(5):R1043–9.
251. Wang X, Wahl R. Responses of the Insulin Signaling Pathways in the Brown Adipose Tissue of Rats following Cold Exposure. Randeva HS, Herausgeber. PLoS ONE. June 10, 2014;9(6):e99772.
252. Tm W, Jc L, Dr M. Use and abuse of HOMA modeling. Diabetes. June 2004;27(6).
253. van der Lans AAJJ, Vosselman MJ, Hanssen MJW, Brans B, van Marken Lichtenbelt WD. Supraclavicular skin temperature and BAT activity in lean healthy adults. J Physiol Sci. January 2016;66(1):77–83.
254. X W, C W, Yu Y, Z W, J K, Xu Y, et al. Effect of Cold Exposure and Exercise on Insulin Sensitivity and Serum Free Fatty Acids in Obese Rats. Medicine and science in sports and exercise. January 8, 2023;55(8).
255. Mb B, Lk G, Ln E, Cv W, Ca O, Mm D, et al. Seasonal variation in glucose and insulin is modulated by food and temperature conditions in a hibernating primate. Frontiers in physiology. September 7, 2023;14:1251042.
256. K S, D K, S G, S V, S R, A S, et al. Role of brown adipose tissue in modulating adipose tissue inflammation and insulin resistance in high-fat diet fed mice. European journal of pharmacology. July 5, 2019;854:354-364.
257. Nikami H, Shimizu Y, Endoh D, Yano H, Saito M. Cold exposure increases glucose utilization and glucose transporter expression in brown adipose tissue. Biochemical and Biophysical Research Communications. June 1992;185(3):1078–82.
258. Hanssen MJW, van der Lans AAJJ, Brans B, Hoeks J, Jardon KMC, Schaart G, et al. Short-term Cold Acclimation Recruits Brown Adipose Tissue in Obese Humans. Diabetes. May

2016;65(5):1179–89.
259. Blondin DP, Labbé SM, Noll C, Kunach M, Phoenix S, Guérin B, et al. Selective Impairment of Glucose but Not Fatty Acid or Oxidative Metabolism in Brown Adipose Tissue of Subjects With Type 2 Diabetes. Diabetes. July 2015;64(7):2388–97.
260. Remie CME, Moonen MPB, Roumans KHM, Nascimento EBM, Gemmink A, Havekes B, et al. Metabolic responses to mild cold acclimation in type 2 diabetes patients. Nat Commun. March 9, 2021;12(1):1–10.
261. Ch R, T A, Rj B, S B, Df C, J C, et al. Habituation revisited: an updated and revised description of the behavioral characteristics of habituation. Neurobiology of learning and memory. September 2009; 92(2):135-8.
262. Br Y, Bk A, Ad S, Jw C. Human cold habituation: Physiology, timeline, and modifiers. Temperature. May 25, 2021;9(2):122-157.
263. Maciel-Fiuza MF, Muller GC, Campos DMS, do Socorro Silva Costa P, Peruzzo J, Bonamigo RR, et al. Role of gut microbiota in infectious and inflammatory diseases. Front Microbiol. March 27, 2023;14:1098386.
264. Huttunen P, Rintamäki H, Hirvonen J. Effect of Regular Winter Swimming on the Activity of the Sympathoadrenal System Before and After a Single Cold Water Immersion. International Journal of Circumpolar Health. Int J Circumpolar Health. August 1, 2001;60(3): 400-6.

List of Appendix Tables

Table S1 1. List of materials utilized in the present study. 113
Table S1 2. Mean ± SEM of measured parameters and the statistical tests. 114
Table S1 3. Overview of the top 10 pathways changed over experimental sessions. 116
Table S1 4. Do the top 10 pathways over experimental sessions have an impact on glucose metabolism? 117

Table S1 1. List of materials utilized in the present study.

Medical and chemical solution & product	Company
Cutasept F	Hartmann, Heidenheim, Germany
Dextrose	Dextro Energy GmbH & Co, Krefeld, Germany
Insuman Rapid (Insulin human)	SANOFI, Frankfurt am Main, Germany
Isotonic sodium chloride solution 0.9%	DELTAMEDICA, Reutlingen, Germany
KALINOR (1,56 g Potassium)	Desma GmbH, Wiesbaden, Germany
QIAamp PowerFecal Pro DNA kits	Qiagen GmbH, Gilden, Germany
RNAprotect, Tissue Reagent	Qiagen GmbH, Gilden, Germany
Scandicain 2%	Aspen Pharmcarem, Durban, Southafrica
Sodium (Na 147) & Potassium (K4) solution	DELTAMEDICA, Reutlingen, Germany
Sterile glucose solution 20% (G20)	Fresenius Kabi, Bad Homburg, Germany
Software	**Company**
Actiheart	CamNtech, Fenstanton, UK
Clamp EKF Diagnostic	Barleben, Germany
COSMED	COSMED Germany, Werneck, Germany
FLIR Thermal Studio Pro	FLIR Systems, Oregon, USA
GraphPad PRISM	GraphPad by Dotmatics, Boston, USA
MATLAB	MathWorks, Massachusetts, USA
Motionwatch	CamNtech, Fenstanton, UK
Python	Python, Delaware, USA
RStudio	R Core Team, Massachusetts, USA
SPSS	IBM, New York, USA
Device and objects	**Company**
Actiheart	CamNtech, Fenstanton, UK
Biosen C-line	EKF-diagnostic GmbH, Barleben, Germany
BODPOD	COSMED Germany, Werneck, Germany
Clamp computer	Terra, Hüllhorst, Germany
Cooling vest	E-cooline, Ulm, Germany
Digital scale	Seca, Hamburg, Germany
Ear thermometer	B. BRUAN, Melsungen, Germany
FLIR T530	FLIR-Systems, Oregon, USA
Infusion pump fm	B. BRUAN, Melsungen, Germany
Infusion pump fmS	B. BRUAN, Melsungen, Germany
Laptop 15.6”	Fujitsu, Tokyo, Japan
Laptop 13.3”	Lenovo, Beijing, China
Motionwatch	CamNtech, Fenstanton, UK
Stadiometer	Seca, Hamburg, Germany
Terra computer	Wortmann AG, Hüllhorst,Germany

Table S1 2. Mean ± SEM of measured parameters and the *p*-values of the statistical tests.

Parameter	n	BL	CE	*p*-value (paired t-test)	*p*-value (Wilcoxon)
7 days outside temperature (°C)	18	11.43 ± 1.35	9.10 ± 6.69	0.16	0.21
Log_{10} Room temperature	18	1.35 ± 0.002	1.34 ± 0.002	0.51	
Log_{10} Room humidity	18	1.51 ± 0.01	1.49 ± 0.02	0.29	
SCV temperature (°C)	18	33.81 ± 0.12	32.56 ± 0.14	0.003	
95^{th} SCV temperature (°C)	18	33.85 ± 0.41	33.62 ± 0.45	0.009	
Core body temperature (°C)	16	36.07 ± 0.13	35.89 ± 0.14	0.52	
Reference point (°C)	18	31.66 ± 0.78	31.46 ± 0.84	0.29	
Actual sleep (h)	18	7.36 ± 0.19	7.22 ± 0.20	0.49	
Log_{10} Assumed sleep	18	0.83 ± 0.77	0.88 ± 0.77	0.89	
Total physical activity (h/24h)	18	12.78 ± 0.42	12.50 ± 0.53	0.51	
Log_{10} Vigorous physical activity	18	1.98 ± 1.36	2.78 ± 1.39	0.79	
Body weight (kg)	18	88.31 ± 2.93	89.31 ± 3.12	0.10	
Fat mass (%)	18	31.33 ± 1.92	31.77 ± 2.12	0.34	
Log_{10} BMI	18	1.45 ± 0.05	1.45 ± 0.05	0.26	
Subjective appetite (mm)	18	23.78 ± 5.06	31.67 ± 4.75	*	0.04
Liking food preference					
High calorie sweet	18	3.15 ± 0.17	3.43 ± 0.21	0.26	
High calorie savory	18	3.38 ± 0.13	3.69 ± 0.17	0.11	
Low calorie	18	3.69 ± 0.17	3.53 ± 0.14	0.18	
Wanting food preference					
High calorie sweet	18	2.77 ± 0.22	2.89 ± 0.21	0.51	
High calorie savory	18	3.39 ± 0.23	3.41 ± 0.22	0.56	
Low calorie	18	3.56 ± 0.16	3.49 ± 0.18	0.61	
Heart rate variability during steady state of hyperinsulinemic euglycemic clamp (HEC)					
Heart rate (beat/min)	12	69.47 ± 2.80	68.24 ± 2.92	0.51	
Interbeat interval (ms)	12	880.95 ± 37.01	898.95 ± 36.78	0.49	
Low frequency/high frequency ratio	12	2.57 ± 0.56	2.51 ± 0.51	0.94	
Stress axis					
Fasting cortisol	17	9.15 ± 0.94	9.68 ± 0.89	0.68	
Fasting ACTH	16	12.32 ± 1.67	13.36 ± 1.27	0.43	
Log_{10} AUC cortisol IVGTT	17	2.20 ± 0.04	2.24 ± 0.32	0.41	
AUC ACTH IVGTT	16	719.89 ± 79.19	793.76 ± 68.23	0.41	
AUC cortisol HEC	15	412.87 ± 29.08	353.83 ± 26.03	0.13	
AUC ACTH HEC	14	656.49 ± 70.90	706.78 ± 66.28	0.45	
SF-36 questionnaire					
Log_{10} Physical component score (PCS)	18	1.749 ± 0.006	1.745 ± 0.007	0.51	
Log_{10} Mental component score (MCS)	18	1.699± 0.007	1.710 ± 0.010	0.08	

Abbreviations: Body mass index (BMI); Adrenocorticotropic hormone (ACTH); area under the curve (AUC); intravenous glucose tolerance test (IVGTT); hyperinsulinemic euglycemic clamp (HEC).

Parameter	n	BL	CE	*p*-value (paired t-test)	*p*-value (Wilcoxon)
Plasma fasting…concentration					
Glucose (mg/dl)	18	80.59 ± 1.15	80.07 ± 1.37	0.31	
Log_{10} Insulin	17	0.62 ± 0.70	0.77 ± 0.94	0.12	
Log_{10} C-peptide	17	0.13 ± 0.40	0.17 ± 0.43	0.43	
Cortisol (µg/dl)	17	9.15 ± 0.94	9.68 ± 0.89	0.61	
ACTH (pg/ml)	16	12.32 ± 1.67	13.36 ± 1.27	0.21	
IVGTT					
AUC glucose (mg/dl)	18	9506.50 ± 221.29	9171.92 ± 277.65	0.059	
Log_{10} AUC insulin	17	3.22 ± 0.05	3.30 ± 0.64	0.12	0.12
Log_{10} AUC C-peptide	17	2.42 ± 0.04	2.44 ± 0.03	0.39	0.43
Log_{10} FPIR	17	2.04 ± 0.07	2.17 ± 0.08	0.01	
Disposition index	15	953.87 ± 134.72	1221.15 ± 178.82	0.03	
Log_{10} HOMA-IR	17	-0.09 ± 0.75	0.06 ± 0.10	0.31	
Log_{10} HOMA-Beta	17	1.95 ± 0.77	2.12 ± 0.10	0.06	
Hyperinsulinemic euglycemic clamp					
M-value	16	11.6 ± 7.53	12.92 ± 7.37	0.99	
Total GIR	16	293.34 ± 21.47	292.96 ± 21.96	0.78	
AUC GIR (mg/kg/min)	16	408.23 ± 31.04	409.03 ± 32.96	0.98	
Log_{10} AUC plasma C-peptide	15	2.19 ± 0.05	2.20 ± 0.05	0.73	

Abbreviations: Adrenocorticotropic hormone (ACTH); area under the curve (AUC); intravenous glucose tolerance test (IVGTT); hyperinsulinemic euglycemic clamp (HEC); first phase insulin response (FPIR); glucose infusion rate (GIR); homeostatic model assessment-insulin response (HOMA-IR); homeostatic model assessment-beta (HOMA-Beta); baseline (BL); cold exposure (CE).

Repeated measures ANOVA				
IVGTT	n	Time (60 min)	Intervention (BL vs. CE)	Time*intervention
Plasma glucose (mg/dl)	18	0.001	0.42	0.08
Log_{10} Plasma insulin	17	< 0.001	0.08	0.19
Log_{10} Plasma C-peptide	17	< 0.001	0.24	0.01
Plasma Cortisol	17	0.21	0.45	0.18
Plasma ACTH	16	0.28	0.21	0.78
HEC		Time (60 min steady state)	Intervention	Time*intervention
GIR	16	<0.001	0.96	0.014
Plasma C-peptide	15	0.005	0.58	0.47
Log_{10} plasma insulin	15	0.057	0.058	0.50
Log_{10} Plasma Cortisol	15	0.24	0.14	0.26
Plasma ACTH	14	0.12	0.48	0.39

Abbreviations: Adrenocorticotropic hormone (ACTH); intravenous glucose tolerance test (IVGTT); hyperinsulinemic euglycemic clamp (HEC); glucose infusion rate (GIR); baseline (BL); cold exposure (CE).

Table S1 3. Overview of the top 10 pathways changed over experimental sessions.

Functional profiling	*p*-value	Abundance CE vs. BL	pBH
PYRIDNUCSYN-PWY: NAD de novo biosynthesis I	0.007	Increased	0.38
PWY-7456: & beta;-(1,4)-mannan degradation	0.014		0.38
FASYN-ELONG-PWY: fatty acid elongation -- saturated	0.020		0.38
PWY-5484: glycolysis II	0.043		0.38
GLYCOLYSIS: glycolysis I	0.045		0.38
PWY66-389: phytol degradation	0.004	Decreased	0.38
COBALSYN-PWY: superpathway of adenosylcobalamin salvage from cobinamide I	0.008		0.38
PWY-3001: superpathway of L-isoleucine biosynthesis I	0.014		0.38
ARGSYNBSUB-PWY: L-arginine biosynthesis II	0.017		0.38
ARGSYNBSUB-PWY: L-arginine biosynthesis II	0.018		0.38

Abbreviations: Benjamini-Hochberg (BH); Baseline (BL); cold exposure (CE).

Table S1 4. Do the top 10 pathways over experimental sessions have an impact on glucose metabolism?

Functional profiling	Impact on glucose metabolism?	If yes, shortly explain…
PYRIDNUCSYN-PWY: NAD de novo biosynthesis I	No	------
PWY-7456: & beta;-(1,4)-mannan degradation	Maybe indirectly	Beta;-(1,4)-mannan degradation products can be utilized within glucose metabolism pathways to generate energy and metabolic intermediates.
FASYN-ELONG-PWY: fatty acid elongation -- saturated	No	------
PWY-5484: glycolysis II	Yes	Glucose breakdown, energy production, nicotinamide adenine dinucleotide (NAD) production, pyruvate fate.
GLYCOLYSIS: glycolysis I	Yes	Glucose breakdown, energy production, nicotinamide adenine dinucleotide (NAD) production, pyruvate fate.
PWY66-389: phytol degradation	No	-----
COBALSYN-PWY: superpathway of adenosylcobalamin salvage from cobinamide I	Yes	Cobalamin is essential for patients with T2D. Moen et al. 2014, found that B12 has a causal effect on fasting glucose. The effect could be an impact on β-cell proliferation and increased insulin secretion.
PWY-3001: superpathway of L-isoleucine biosynthesis I	Yes	Higher amount of isoleucine is associated with insulin resistance. Mice fed an isoleucine deprivation diet for one day have improved insulin sensitivity.
ARGSYNBSUB-PWY: L-arginine biosynthesis II	Yes	L-arginine is essential for pancreatic beta-cell functional integrity, metabolism, and defense from inflammatory challenge.
GLYCOLYSIS-E-D: superpathway of glycolysis and the Entner-Doudoroff pathway	Maybe indirectly	It has an impact on glucose metabolism but is not a primary regulator of insulin secretion.

Acknowledgments

First, I would like to express my gratitude to my supervisor, Prof. Sebastian M. Meyhöfer, for allowing me to undertake my thesis under his guidance and join his research team. I am grateful for his continuous support and valuable feedback during this time, as well as for providing the opportunity to learn and conduct research at an international level. Additionally, I would like to thank my co-supervisor, Dr. Britta Wilms, for her support and feedback, both in initiating and finalizing my project and, more generally, throughout my Ph.D. journey. Furthermore, my sincere thanks to Prof. Jens Mittag, head of the Institute of Endocrinology and Diabetes, for his great support.

I owe my heartfelt thanks to Prof. Henriette Kirchner, whose mentorship has been exemplary. Her guidance has been pivotal in providing me with invaluable insights, advice, and encouragement to keep going. I appreciate her continuous support throughout the doctoral phase, whether in joining her Journal Club, having time for valuable discussions, or introducing me to DZD Next and other relevant conferences and workshops to expand my knowledge in the field of diabetes and obesity, which greatly aided me in staying up to date. I will always cherish her contribution to my personal and professional growth.

My great thanks moreover go to Dr. Lucas Massier, who has been my greatest inspiration as a scientist from the first day of my Master's project (also introducing me to the fascinating world of Microbiota) to the last day of my Ph.D. journey. I deeply appreciate his support and friendship for always finding time to discuss, despite his busy schedule. Thank you, Lucas, for providing the best answers to all my questions, and offering valuable feedback, advice, and guidance throughout this journey.

Furthermore, I would like to thank my colleagues who assisted me with the Botnia clamp procedure, namely the study doctors: Dr. Svenja Meyhöfer, Dr. Katarzyna Worobiec, and Dr. Eleni Papa, as well as the study nurses and Hiwis. I extend special thanks to my dear colleagues Susanne Behling, Dr. Rodrigo Chamorro, and Binja Tams for their continuous support. In addition, I want to thank all the participants for their willingness to take part in this scientific endeavor and doctoral study.

I appreciate the support of GRK members: Professors, Ph.D. students, and especially Chaoqun Chiang, for making this research training a successful experience.

I am grateful to Prof. Trajkovski and Matija Trickovic from the University of Geneva for their supervision of the Shotgun metagenomic analysis. Working alongside them and other team members in a friendly and professional environment was a truly enriching experience.
I owe a big thanks to Prof. Michael Symonds, Dr. James Law, and Dr. Lindsay Robinson from the University of Nottingham for providing the IRT software, re-analysis, and helpful discussions. Additionally, I am grateful to Prof. Matthias Blüher and Prof. Peter Kovacs for their invaluable guidance and support in preparing me for my future endeavors.

How can I thank my dear friend, Dr. Mehdi Pedaran? His support has been a constant source of encouragement from day one to the completion of this journey. Th
I also wish to acknowledge the support of my dear colleague and friend, Andrea Schulze, for helping to start up the project during the COVID-19 pandemic. Even after she left, her support has been unwavering. I appreciate the support of Dr. Mohammed Hankir for generously sharing his professional advice and for always having the best papers on hand for discussion.
A special thanks to my best friends, Farnaz, Lika, and Jasmin, who supported me through thick and thin, shared their experiences, and encouraged me.

Last but not least, I would like to express my deepest appreciation to my beloved family: Pari, Roya, Ramin, and especially my nephew Shahin, for their love, support, and patience during these years, which were not always easy.

“In this earth, in this soil, in this pure field,

let's not plant any seed other than seeds of compassion and love.”

Rumi